Assessment of lowering strategies for monopile installation from a dynamically positioned vessel

Christos Charalambous

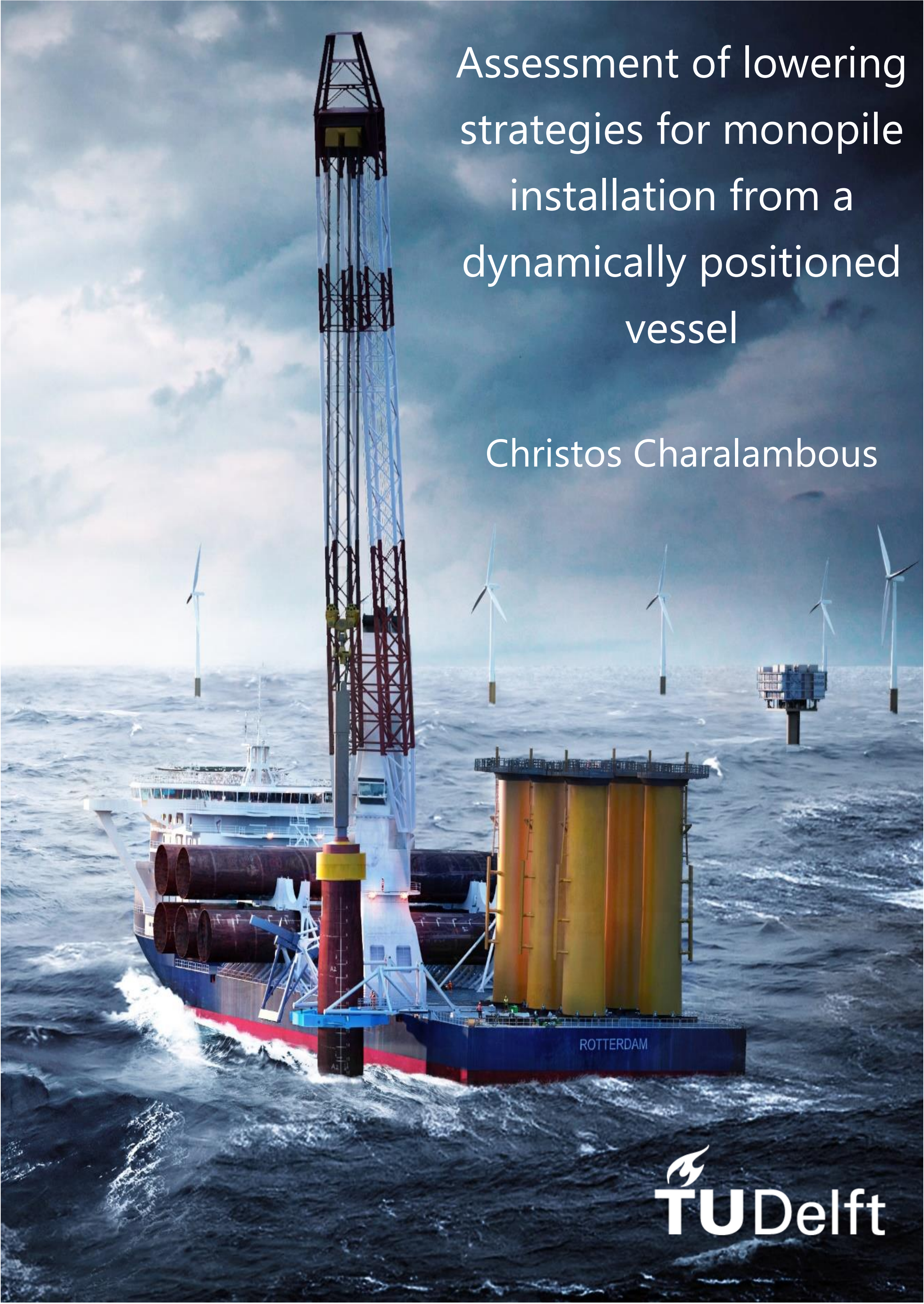

Assessment of lowering strategies for monopile installation from a dynamically positioned vessel

Master of Science Thesis

to obtain the degree of Master of Science
at the Delft University of Technology,
to be defended publicly on Thursday July 6, 2017 at 09:30 AM.

by

Christos Charalambous
MSc in Marine Technology
Faculty Mechanical, Maritime and Materials Engineering
TU Delft, Delft, The Netherlands.

Student number:	4487176	
Thesis number:	SDPO.17.015.m	
Project duration:	October 1, 2016 – July 6, 2017	
Thesis committee:	Ir. K. Visser,	TU Delft, supervisor
	Dr. Ir. M. Godjevac,	TU Delft, daily supervisor
	Dr. Ir. H.J. de Koning Gans,	TU Delft
	Ir. A. de Jager,	TWD BV

As you get older, you realize that no one has all the answers.
It turns out that life is an exercise
in living with the certainty of uncertainty.

Jason Kilar

Contents

List of Figures v

List of Tables ix

Summary xi

Preface xiii

Abbreviation xv

1 Introduction 1
- 1.1 Background and motivation . . . 2
  - 1.1.1 Offshore wind industry . . . 2
  - 1.1.2 OWT foundations and installation procedures . . . 3
  - 1.1.3 Trends and figures . . . 5
- 1.2 Scope and aim . . . 8
- 1.3 Thesis outline . . . 10

2 Functional design and possible design strategies 11
- 2.1 Initialization of functional design . . . 12
  - 2.1.1 Introducing and defining the problem . . . 12
  - 2.1.2 Requirements and criteria . . . 13
- 2.2 Problem and solution formation . . . 14
- 2.3 Possible design strategies . . . 16

3 Environmental Conditions 21
- 3.1 Global and Local Conventions . . . 22
  - 3.1.1 Axes and Motions Definitions . . . 22
  - 3.1.2 Axes Transformation and Euler Rotations . . . 23
- 3.2 Environmental Loads . . . 25
  - 3.2.1 Wind Loads . . . 25
  - 3.2.2 Current Loads . . . 26
  - 3.2.3 Wave Loads . . . 28

4 Monopile model 37
- 4.1 Variable Definition and Naming . . . 38
- 4.2 Monopile Model . . . 39
  - 4.2.1 Lagrangian Mechanics . . . 40
  - 4.2.2 Monopile's Equations of Motion . . . 41
  - 4.2.3 Forces Derivation . . . 42
    - 4.2.3.1 Conservative forces . . . 42
    - 4.2.3.2 Non-conservative forces . . . 42

4.2.4 Monopile simulation. 45
4.2.5 Model Parameters 48

5 Vessel model and Dynamic Positioning 51
5.1 Vessel conventions 52
5.2 Vessel model 53
5.3 Dynamic Positioning 56
5.3.1 Purpose of DP 56
5.3.2 Analysis of DP system 57
5.3.3 Reference systems and sensors. 58
5.3.4 Signal processing 59
5.3.5 Kalman filter 59
5.3.6 Controllers 65
5.3.7 Thrust allocation and actuators 67

6 Monopile control strategies 69
6.1 Free floating monopile 70
6.2 Fixed/Passive gripper 73
6.3 Active gripper 77
6.4 Mooring/Double gripper 83
6.5 Multi-Criteria Analysis 84

7 Conclusions and recommendations 95
7.1 Conclusions. 96
7.2 Recommendations 98

References 101

List of Figures

1.1 Onshore (Left) and Offshore (Right) expenses EWEA et al. [2016] 2
1.2 Progression of wind turbine evolution based on water depth, Source: NREL 3
1.3 OWT foundation variations 4
1.4 OWT installation vessels 5
1.5 2015 share of new renewable power capacity installations (MW). Total 22,267.9 MW EWEA et al. [2016] 6
1.6 Total annual investments in wind energy 2010–2015. Figures include investments in new assets (€ BN) EWEA et al. [2016] 6
1.7 Foundation distribution for the period 2013-2015 7
1.8 Offshore wind farms installation locations. 7
1.9 JUB and floating vessels maximum crane capacity 8

2.1 MP installation process 13
2.2 Design Strategy No.1: Free hanging MP 18
2.3 Design Strategy No.2: Fixed/Passive gripper 18
2.4 Design Strategy No.3: Active compensating gripper (MCPG) 19
2.5 Design Strategy No.4: Mooring/Double gripper 19

3.1 Axes conventions 22
3.2 Euler transformation sequence 24
3.3 Wind and tidal current profiles 27
3.4 Linear and non-linear stretching of current profile up to wave surface . . . 28
3.5 Harmonic wave definitions Journèe and Massie [2001] 29
3.6 Illustration of the difference in the appearance of the sea surface Journèe and Massie [2001] 29
3.7 Regions of applying wave theories 30
3.8 Comparison of horizontal water velocities Journèe and Massie [2001] . . . 32
3.9 Superposition of many regular waves that conclude to an irregular sea . . 32
3.10 Wave record analysis and regeneration Journèe and Massie [2001] 33
3.11 JONSWAP wave spectrum with $H_S = 2.5m$ and $T_P = 7sec$ 35
3.12 Random sea state realization with 300 wave components 35

4.1 General layout 38
4.2 Forces acting on MP during lowering operation 39
4.3 Force components acting on a strip of the MP 43
4.4 MP model overview 46
4.5 MP forces simulation block 47
4.6 Equations of motion block 48

4.7 Translations transformations from local to global axes 48
4.8 Different modes of free-hanging monopile 49

5.1 Vessel Conventions 52
5.2 Motion conventions 53
5.3 Wave loads superposition Journèe and Massie [2001] 54
5.4 Vessel model generated in MATLAB/Simulink 55
5.5 Dynamic Positioning applications 56
5.6 Overview of a control system build for vessels 57
5.7 Low and high frequency components of vessel's motions 60
5.8 Kalman structure of prediction-correction process 63
5.9 Block diagram for Prediction-Correction of Kalman filter 64
5.10 Total, LF and WF motions of the vessel 65
5.11 PID controller block diagram 66
5.12 Control system response 68
5.13 Vessel's COG motions in surge, sway and yaw 68

6.1 Boom tip point translations 70
6.2 Sling connection point translations 71
6.3 Bottom point translations 72
6.4 Monopile rotations 72
6.5 Schematic layout of a fixed passive gripper 73
6.6 Fixed gripper translations due to vessel motions 73
6.7 Monopile translations and rotations at center of gravity 74
6.8 Sling connection point translations 75
6.9 Bottom point translations 75
6.10 DAF, off-lead and side-lead angles 76
6.11 Total forces and moment acting on monopile's center of gravity 77
6.12 Actuation system overview 77
6.13 System layout for active compensating cylinder 78
6.14 Hydraulic actuation system 79
6.15 Double acting, single ended hydraulic cylinder 80
6.16 Simulink implementation of hydraulic actuating system 80
6.17 Translations and rotations at monopile's center of gravity 81
6.18 Sling connection translations 82
6.19 Bottom point translations 82
6.20 Translations and rotations at monopile's center of gravity for a mooring gripper 83
6.21 Translations at sling connection point for a mooring gripper 83
6.22 Translations at bottom point for a mooring gripper 84
6.23 Simulink model for alternative gripper configurations 85
6.24 Criteria and sub-criteria for evaluation of design strategies 86
6.25 Performance of different strategies for horizontal translations of monopile's bottom point regarding significant wave height 88
6.26 Performance analysis for off-lead and side-lead angles regarding significant wave height 89

6.27 Convention of environmental headings 90
6.28 Performance analysis for horizontal translations of monopile's bottom point regarding environmental heading 90
6.29 Performance analysis for off-lead and side-lead angles regarding regarding environmental heading 91
6.30 Performance analysis for off-lead and side-lead angles regarding monopile dimensions 92
6.31 MCA weight factors sensitivity 94

7.1 Model overview in Simulink 96

List of Tables

2.1 Problems and sub problems relevance 15
2.2 Possible solutions for each sub problem 16
2.3 Possible solution combinations 17
2.4 Possible solution combinations-Alternative representation 17

3.1 Shape coefficient, C_s, for perpendicular wind approach angles 25

4.1 Crane variables 48
4.2 Monopile Parameters 49
4.3 Eigenfrequencies and Eigenperiods of free hanging monopile 50

5.1 Modes decomposition 53
5.2 Ziegler-Nichols control tuning method 67

6.1 Trade-off table of possible actuators 78
6.2 Considered monopiles for the assessment 91
6.3 Score for different design concepts 93

SUMMARY

The rapid rate in technological advancements leaves little to none options for our environment to react. The excessive use of "conventional" energy is bringing planet Earth to its knees. However, people started recognizing the value of renewable energy sources. One of the major renewable sources is the wind energy. The wind energy can be divided in two categories; onshore and offshore wind energy. Offshore wind energy has many advantages in comparison with onshore but comes with a major disadvantage, the installation cost. Since installing an offshore wind turbine is far more complex than installing the same wind turbine onshore, different ways needs to be developed to compensate for the excess costs.

Even though the cost is a significant aspect, it is not the most critical one. Since more power is required, bigger offshore wind turbines are needed, thus larger foundation structures and bigger water depths. The conventional Jack-Up Barge that was being used for such operations so far is driving to a saturation on its operability due to limitations on maximum crane capacity and maximum water depth. For the aforementioned reasons, a floating vessel is considered to install bigger foundations but this leads to the loss of fixed ground that the Jack-Up Barge provided. This creates a significant problem that motions are generated and disturb the installation process. For this reason, a compensating strategy should be developed to allow such installations.

Such solution comes from TWD with the Motion Compensating Pile Gripper. In order to reduce the installation costs and to allow installation of wind turbines in higher depths of water, a floating vessel has to be deployed instead of the conventional Jack-Up Barges. The use of a floating vessel though, generates motions that disturb the installation procedure. This is the reason that TWD came up with a compensating gripper. This gripper uses hydraulic cylinders to generate forces for the monopile and vessel in order to counteract unwanted motions and to keep the monopile in the required position.

In this thesis, initially a functional design is conducted. This analysis concludes with the possible design strategies that can restrict the monopile through the lowering operation. After the possible design strategies are established, a simulation model is generated that involves environmental loads, a vessel model, a monopile model and a gripper model.

Through that simulation model, the different alternatives are tested and simulated in order to evaluate the performance of each and observe their responses. Finally, after all the alternatives are simulated, a Multi-Criteria Analysis takes place that evaluates each one of the possible strategies based on various criteria in order to conclude to the winning strategy that is then suggested to be implemented in the lowering operation of the monopile erection process.

PREFACE

This has been a roller coaster ride. The last two years were definitely the most stressful period of my life but they provided knowledge beyond expectations. With this thesis I hopefully conclude my academic years. There are so many people that I have to thank but please bear with me.

Firstly, it would be impossible to achieve even the smallest fraction of my career without my parents, my brother and my grandmother. The things you sacrificed were not apparent to me from the beginning. Now everything is clear. Words cannot describe how thankful I am for your support. Even at my darkest times, you neither stopped believing in me, nor supporting me. I could have never asked for a better family. I owe you everything in my life.

I would like to thank my girlfriend as well for everything that she have done for me. She has been one of the main reasons that I pursued my dream to become an engineer. She stayed by my side through thick and thin for the last 9 years and always supported my decisions, no matter what.

Furthermore, I want to thank my daily supervisor, Dr. Ir. M. Godjevac for all the help that he gave me through this thesis as well as the time that he spent guiding me. I also want to thank my supervisor Ir. K. Visser for all the critical input that he provided and his effort towards me for becoming a better engineer. In addition, I would like to thank Arnold de Jager for supervising my thesis in TWD and helping me whenever I had questions. Also, I would like to thank the entire company for giving me the opportunity to be a part of it and research such a beautiful topic. I am thankful as well to Dr. Ir. H.J. de Koning Gans for the time that he spent on assessing my thesis and giving me valuable feedback. It was an honour working with all of you.

Lastly, I want to thank my friends and $\Pi\alpha\rho\alpha\delta o\chi\acute{\epsilon}\varsigma$ for their support and mental encouragement throughout this period of my life. With all the laughs that we shared, everything had a positive twist in the end. I wish you all the best in your lives and careers.

Christos Charalambous
Delft, July 2017

Abbreviation

BP	Bottom Point
BT	Boom Tip
COB	Center of Buoyancy
COG	Center of Gravity
DAF	Dynamic Amplification Factor
DNV	Det Norske Veritas
DP	Dynamic Positioning
EOM	Equations of Motion
FRA	Fixed Reference Axis
FS	Free Surface
GPS	Global Positioning System
HF	High Frequency
HLV	Heavy Lift Vessel
ILT	Internal Lifting Tool
IMO	International Maritime Organization
JONSWAP	Joint North Sea Wave Project
JUB	Jack-Up Barge
LF	Low Frequency
LSA	Local Structure Axis
MCA	Multi-Criteria Analysis
MCPG	Motion Compensating Pile Gripper
MP	Monopile
OWT	Offshore Wind Turbine
SC	Sling Connection
SWL	Safe Working Load
TWD	Temporary Works Design
WF	Wave Frequency

1

Introduction

The art and science of asking questions
is the source of all knowledge.

Thomas Berger

The first chapter of this thesis will establish the base of the analysis as well as the reasons that led to such research. Initially, the reader will briefly be introduced to the offshore wind industry, present some European trends in the specified energy sector, different installation procedures and types of wind turbine foundations. In addition, a general scope of the thesis will be explained along with the research aim and goals. Finally, the author will present an outline of the work that has been executed throughout the entire research phase.

1

1.1. BACKGROUND AND MOTIVATION

1.1.1. OFFSHORE WIND INDUSTRY

Since 20^{th} century, human race established the urge for excessive amounts of energy that created all the astonishing achievements that today are taken as granted. On the other hand though, nothing comes without a price. The huge demand for energy has led to global warming and other severe impacts on the environment. Thus, the need for alternative energy sources other than coal and petrol, led to renewable and reliable energy technologies such as solar, biomass, hydroelectric and wind power.

Wind power is converted into electricity from wind turbines. Those wind turbines can either be onshore or offshore. The offshore sector has been very popular over the past years, specifically in Europe. In order to generate electricity in the offshore sector, wind turbines are installed in the ocean that can use wind energy and convert it into useful electricity. There are many reasons to install wind turbines - either onshore or offshore - but those are not discussed in this research. However, the advantages and disadvantages that emerge when an Offshore Wind Turbine (OWT) is compared with an onshore are presented below.

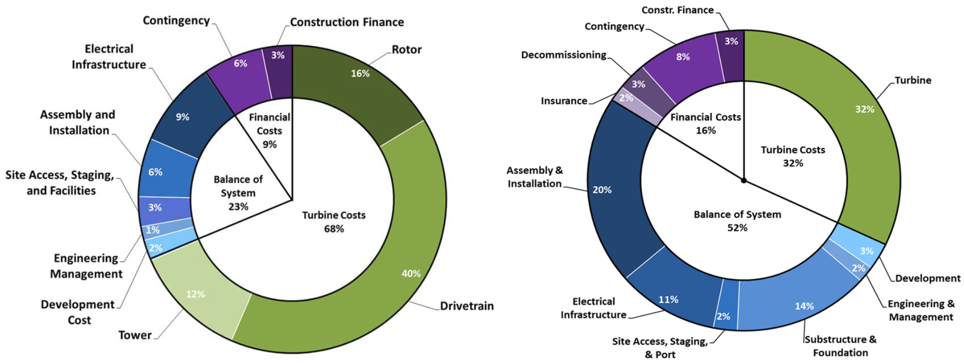

Figure 1.1: Onshore (Left) and Offshore (Right) expenses EWEA et al. [2016]

Throughout several studies on this area, one can find out that offshore wind energy can take advantage of larger continuous areas in the sea rather than the available onshore area for installation of wind turbines. Furthermore, the wind speeds in the offshore sector are higher than the ones onshore resulting in such way in more electricity even when an OWT is used with the same efficiency as an onshore. This results to a bigger profit margin for the stakeholders, thus a more attractive solution. As one progresses from the land to the ocean, lower turbulence of the wind flow is observed as well as lower wind shear resulting in such way to an increased efficiency. Finally, OWTs may be considered more attractive solutions since there is no, or very limited noise and visual pollution. On the other hand, OWTs has a major disadvantage that needs to be addressed.

The capital expenditure for an OWT is considerably bigger than the one for an onshore wind turbine. Given that, in order to make the offshore section for wind turbine installation more alluring to the stakeholders, that disadvantage needs to be addressed. In Figure 1.1, the reader can see the differences in expenses distribution for an onshore and an OWT. Those expenses include turbine costs, financial costs and balance of system costs.

For an onshore wind turbine, it is clear that the turbine costs are the biggest part of the expenses since installation, transportation and in general system's balance is not of big issue in land. In comparison, for an OWT, system's balance costs outweigh the turbine costs. This is only logical since the operation in the ocean is fundamentally more dangerous and complex. Finally, the reader can observe that one of the most critical changes between those two pie charts is the Assembly and installation costs. For the onshore wind turbine it sums up to 6% of the total costs, whereas for the OWT, that cost explodes to 20%. This observation shows that by reducing the cost for assembly and installation and keeping safety, installation time and precision on acceptable levels, the total expenses will significantly drop, thus making the OWT investment more attractive to the potential customer.

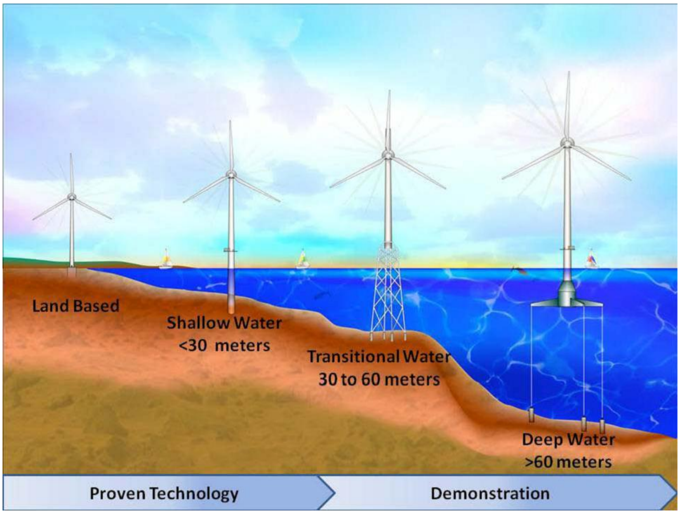

Figure 1.2: Progression of wind turbine evolution based on water depth, Source: NREL

1.1.2. OWT FOUNDATIONS AND INSTALLATION PROCEDURES

There are four different classifications for wind turbines and those are categorized based on the water depth at which they are installed. Firstly, there is the land based wind turbine that one might say is the "conventional" way of converting wind energy to electricity. The next categories are divided as shallow water, transitional water and deep water wind turbines. In Figure 1.2, one can see the different categories and their respective water depths.

In addition, there are many different designs (established or concepts) that serves as foundations for the OWTs. In Figure 1.3, the foundation variations are presented. The monopile (MP) is the most common foundation and this is elaborated further below. It is a single cylindrical steel tube that is hammered into the seabed. Then the transition piece and wind turbine pieces are integrated on the MP. The diameter, length and wall thickness are decided upon the operation profile of the wind turbine and the surrounding environment. The jacket foundation can be designed with three or four legs. There are two different installation methods for jacket foundations. Either pre-piling, where a sub-sea template is installed at first to aid the jacket or post-piling, that the piles are installed through the sleeves that are located on the jacket legs.

The next foundation is the tripod. It is lighter than the other foundations. The piles are hammered into the seabed to support the foundation. The tripod foundation is pre-assembled in land. The gravity based support structure is in principal a concrete structure that might have installed skirts on it. When the gravity based support structure is placed in position, scour protection is required for stability. Finally, the tri-pile consists of three tubular steel piles and a transition piece. Once the tri-pile is placed in position, it connects to a MP above water level.

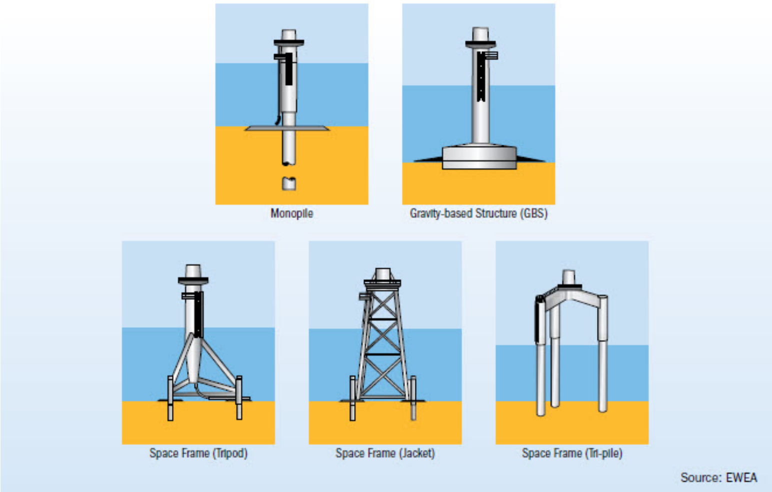

Figure 1.3: OWT foundation variations

Other than various substructures that can be used as foundations, there are many installation vessels for OWTs as well. In Figure 1.4, one can see some of the alternatives that exist for the installation procedure, not only for the foundation but for the transition piece, wind turbine tower, nacelle and blades. The most common vessel for such operations is the Jack-Up vessel. So far, Jack-Ups are the most popular amongst OWTs installation vessels. It can provide the necessary stability for the operation since it is approximately equivalent to working onshore. On the other hand though, Jack-Ups are one of the most expensive solutions and their throughput time is significantly high.

Figure 1.4: OWT installation vessels

One of the most competitive alternative for Jack-Ups are Heavy Lift Vessels (HLV). Those vessels that are equipped with Dynamic Positioning (DP), are cheaper to operate and can transport the parts in less time than what jack-ups require. However, HLVs cannot provide the required stability for the installation procedure. As it was mentioned before, the costs for balance of system and specifically the assembly and installation costs needs to be reduced in order for the OWTs to be more attractive to the potential customers. Thus, the demand for new technologies that can be used for HLVs while in installation operation rise. In a latter stage of the same chapter, this need will be further analysed.

1.1.3. TRENDS AND FIGURES

Offshore wind energy has an increased trend in the 21st century. The reasons vary from capability to profit and from low emissions to high technological maturity of wind turbines. This is illustrated in Figure 1.5, where 57.5% of the total power capacity installation comes from Wind. Solar PV is ranked as second source of power capacity and the rest of the sources (geothermal, ocean, waste, biomass, hydro and CSP) are ranged between 0.01 and 1.7.

As one can see in Figure 1.6, the trend for offshore wind energy is increasing exponentially whereas the OWTs technology is considered within its learning curve yet. After 2012, wind energy investments are rapidly increasing and this increase is even more substantial in the offshore sector where from 2014 to 2015, the investments were nearly doubled. This increase in investments is another reason for further research in the offshore wind energy sector since companies that are involved might benefit from developments in that area.

1

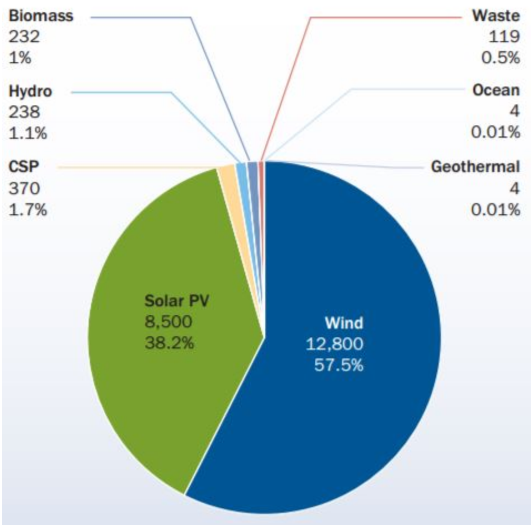

Figure 1.5: 2015 share of new renewable power capacity installations (MW). Total 22,267.9 MW EWEA et al. [2016]

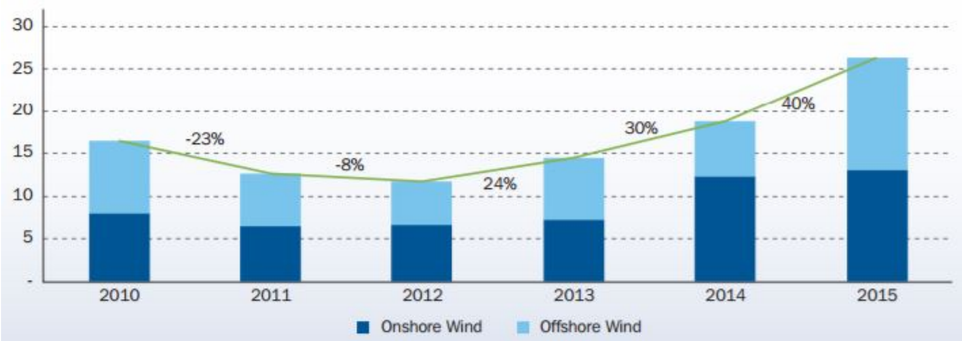

Figure 1.6: Total annual investments in wind energy 2010–2015. Figures include investments in new assets (€ BN) EWEA et al. [2016]

In order to establish the foundation of the OWT that the research will be based on, different foundations were analysed from 2013 until 2015. This is done to consider the possible popular solution for the substructure of an OWT since the most popular foundation is undoubtedly the most preferable for a possible investor. Figure 1.7 shows the percentage of usage of each foundation in the European wind farms. That shows an astonishing difference between MPs and the rest of the foundation alternatives (jacket, tripods and gravity-based substructures). Furthermore, not only MPs are the most favourable choice but one can see that the MP usage itself is growing throughout the years resulting to 97 % for 2015. EWEA et al. [2016]

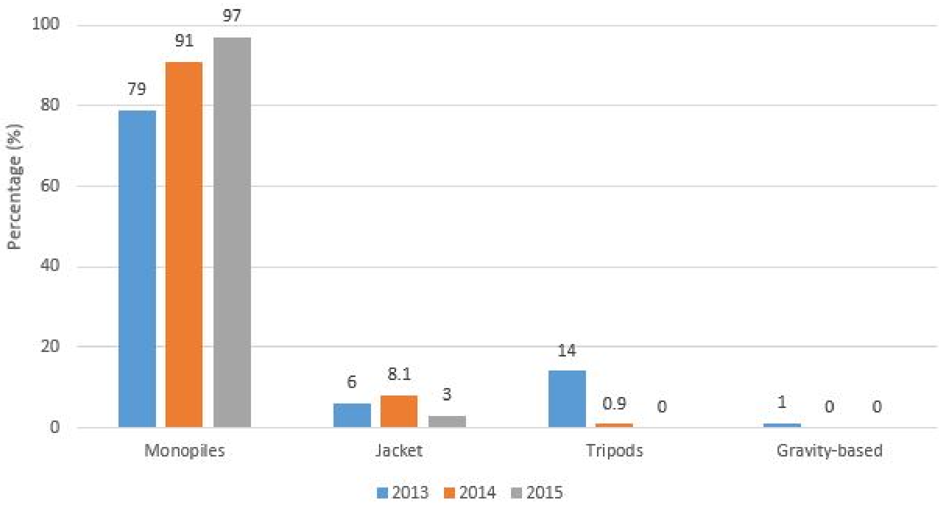

Figure 1.7: Foundation distribution for the period 2013-2015

Furthermore, it is known that the offshore wind energy is constantly increased and for this reason, higher water depths and distance to shore are needed. As one can see in Figure 1.8, the Offshore Wind Farms that are installed through time are shown while considering the distance to shore with respect to water depth. Considering this figure, a clear increasing trend for future projects can be derived. This trend means that in near future, the water depth requirement will be increased as well as the distance to shore. Considering that a JUB has a limitation in water depths that can operate, different types of vessels are required to execute such operations.

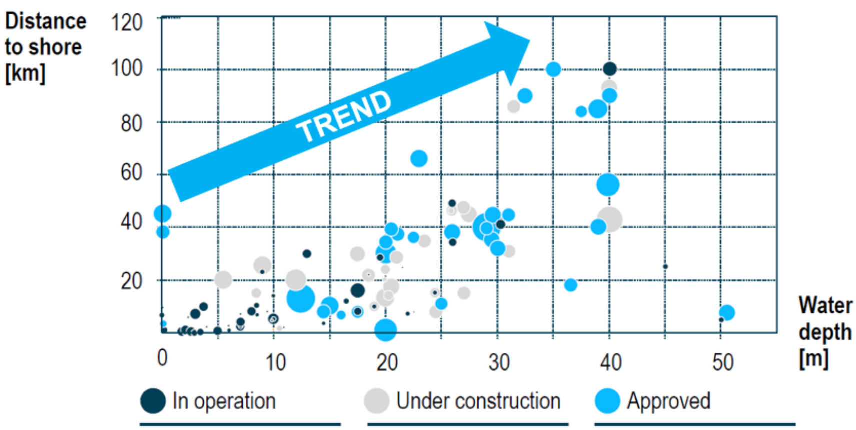

Figure 1.8: Offshore wind farms installation locations.

In addition, it is only logical that since the power requirements of the OWT is increasing, the foundations of the structure will be larger. That means that the MP will become bigger and heavier. Sequentially, the maximum crane capacity of the vessel should be increased. In the bar chart that the reader can see in Figure 1.9, different JUB and floating vessels are shown. It is deemed that for future projects, the crane capacity should be higher than 1300mT. It is clear then that the JUB that exist at the moment are limited in that requirement. This is an additional reason for considering a floating vessel since the crane capacity can be significantly higher.

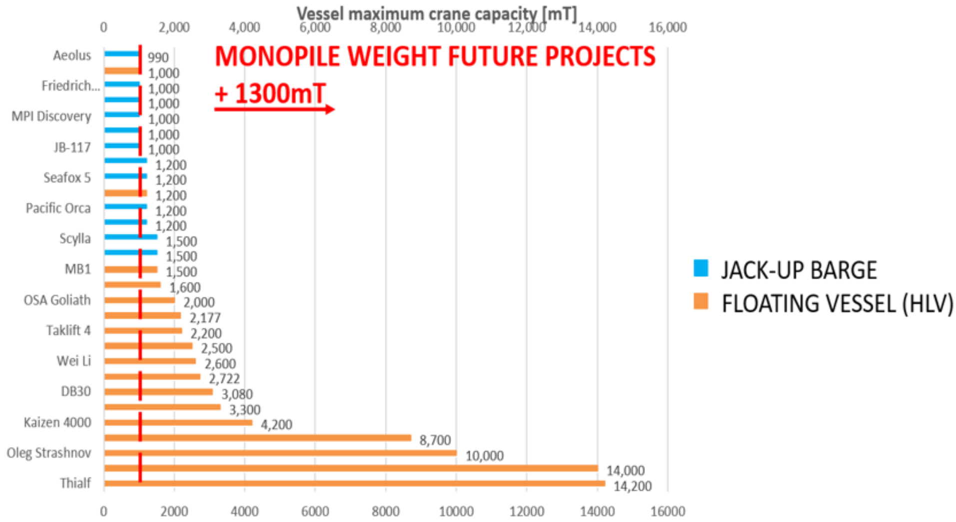

Figure 1.9: JUB and floating vessels maximum crane capacity

1.2. SCOPE AND AIM

The offshore wind farm sector is a fast-growing industry in the renewable energy market. In order to install an OWT, the foundation needs to be installed first. The most common foundation though is the MP. For the installation of MP the most common practice is a Jack-Up Barge (JUB) that can create a fixed working platform thus the installation of the MP will not be influenced by the vessel motions. A JUB nevertheless has high day-rates of leasing and in combination with the small operating window that a company has in order to install MP due to weather limitations, Temporary Works Design (TWD) and Barge Master came up with a revolutionary new concept of a Motion Compensating Pile Gripper (MCPG) that can allow straight piling of a MP from a floating vessel.

The MCPG uses hydraulic cylinders that compensate for the movements based on measurements from motion reference sensors of the MP in the installation phase, keeping the pile vertical in more adverse sea states enhancing the operating window of the foundations installation phase. By doing so, the aforementioned assembly and installation costs will be reduced in a great manner.

An analysis about the lowering phase of a MP with the aid of MCPG does not exist. Such analysis is essential in order to proceed further with the concept design of the MCPG. In this thesis, research will take place about the lowering phase of MP erection process with the use of MCPG and several other design strategies that will be presented in the next chapter. Furthermore, additional research will occur based on which design strategy needs to be followed in the lowering operation of the MP.

The thesis begins with a functional design to define the requirements, problems and solutions for the research question. Based on that, several design strategies will be established that will lead the thesis to the next part. The modeling of the entire system will take place, including environment, MP, gripper(s), vessel and DP. Based on that model, various simulations will take place and the results of it will derived based on critical inputs and outputs that will be presented in the thesis at a latter stage.

Subsequently, all the different generated systems will be integrated together to result in a more realistic representation of the simulation. A sensitivity analysis then will be executed to define a range of vessels and MPs that can be used for the existing models and that the results would still be acceptable when altered inputs are used rather than the prototypes. Finally, a Multi-Criteria Analysis (MCA) will take place in order to find the optimal solution that will be followed by the company. Below, one can find the main objectives of the thesis in headlines:

1. Identify all the different possibilities for design strategies on the MP lowering phase and elaborate on their configuration.

2. Generate environmental conditions that will impact the lowering operation.

3. Create MP, vessel, DP and gripper(s) model based.

4. Perform numerous simulations for all possible design strategies and analyze their response.

5. Perform a MCA, that based on the defined criteria, sub-criteria and weight factors the strategies will be evaluated and result to the suggested wining strategy.

Research Objective:
Assess various design strategies that meet the established requirements and enable a safe lowering operation for MP installation from a dynamically positioned vessel in order to determine the wining strategy.

1

1.3. THESIS OUTLINE

In this section, an outline is presented to the reader regarding each chapter that constitutes the thesis. The chapters are the following:

Chapter 1: The first chapter introduced the reader to the research that has been done so far in this area. The background and motivation is the first topic that is discussed, including the offshore wind energy sector, the installation procedures and foundations of an OWT as well as trends and figures that were the initial motivation for the research. In addition, the general scope and aim of the thesis is presented to the reader including the process that will be followed and the objectives that are established.

Chapter 2: This chapter presents the functional design that took place in the thesis to assess the different possibilities that can be used in such problem concluding in four design strategies that will be considered in further chapters. It includes all the requirements for such operation, the problems that were defined, the solutions, the different criteria and finally the suggested design strategies that will be further modeled, analyzed and assessed.

Chapter 3: In order to have a realistic simulation model, the environmental loads need to be introduced. This takes place in chapter 3 where wind, current and wave loads are analyzed and presented to the reader. General conventions for axes transformations that took place in the research are also presented in the same chapter.

Chapter 4: In this chapter, all the analysis that concluded in the MP model is presented. Initially, the definitions and conventions are shown, followed by forces and Equations of Motion (EOM) derivation and concluding to the generated MP model through MATLAB/Simulink.

Chapter 5: After the MP is modelled, the next step is to include a vessel in the simulation model to recreate a more realistic lowering operation. By using a floating vessel, the need of DP rises. The modelling of the vessel and DP is shown to the reader including filtering and controlling motions in the horizontal plane.

Chapter 6: The final chapter of the thesis considers all the design strategies for controlling the lowering operation of the MP. Each strategy is simulated and analysed, concluding to a MCA that based on various criteria and weight factors, the aforementioned strategies are evaluated and compared to result in the suggested winning strategy.

2

Functional design and possible design strategies

The greatest challenge to any thinker
is stating the problem in a way
that will allow a solution.

Bertrand Russell

This chapter will introduce the analysis that was established for possible design strategies. A functional design took place in order to divide the task in smaller parts based on what the requirements are, what problems occur in such concepts and what solutions can the author define that might be able to fulfill those requirements. Finally, four possible design strategies are the outcome of this analysis that are further explained for the reader.

2

2.1. INITIALIZATION OF FUNCTIONAL DESIGN

2.1.1. INTRODUCING AND DEFINING THE PROBLEM

In order to establish an analysis for the lowering phase of MP installation process, a design strategy has to be defined. The possible design strategies that will be assessed in the thesis have to be able to compensate for all the obstacles that are considered or at the worst case scenario to be able to mitigate the outcomes as much as possible.

The difficulties that such a project expects to face, comes not only from the lowering phase itself but with the interrelation of that phase with different ones (preceding or following phases). Thus, for the ease of reader's understanding, the entire process of MP installation will be briefly explained.

Phase 1-Horizontal MP lifting/ Connecting ILT: After the vessel is positioned in the desired location, the ILT and crane are connected to the MP. Subsequently, the lifting process takes place in order to lift the MP from the currently horizontal position in the vessel.

Phase 2-Upending: The next phase is to upend the MP to a vertical (or approximately vertical) position next to the vessel and attach it to the gripper that will aid the MP to stay in the desired position for the entire process.

Phase 3-Pile lowering: In this phase the MP is lowered from the initial position to the seabed keeping its verticality to the anticipated margins. The pile lowering phase will be examined in the thesis.

Phase 4-Touchdown of MP onto seabed: The MP reaches the seabed and its position is measured in order to verify that it is placed in the specified area with an acceptable inclination.

Phase 5-Adjust DP position to landed MP position: Based on the position of the MP, the vessel undertakes the necessary adjustments in position in order to keep the MP at the most vertical position.

Phase 6-Lowering of MP to full self-penetration: The MP is partially lowered into the seabed due to self-penetration. Here the point of no return is defined, which is as soon as the MP is full self-penetrated. The MP cannot be lifted anymore by the crane.

Phase 7-Release ILT and place hammer: This is the intermediate step between lowering and pilling phases, where the ILT is removed and the hammer is placed above the the MP, integrated to the top point of it.

Phase 8-MP driving: The piling phase takes place while an active compensating gripper compensates for any possible motions that are exerted to the MP.

Phase 9-Release gripper: The installation phase is finished and the gripper is disconnected from the MP.

In Figure 2.1, one can visualize the sequence of the steps that were described before. The circled phase is the lowering of MP that will be examined in the thesis. In order to establish a functional design, the first step is to define the problem.

Problem Definition: *Safe lowering of MP from an approximately vertical position above (or most of MP above) sea level to a specified position on seabed within an acceptable tolerance.*

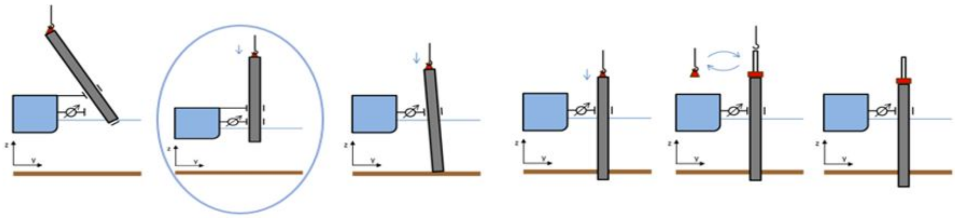

Figure 2.1: MP installation process

2.1.2. REQUIREMENTS AND CRITERIA

In order to proceed to the a design the basic requirements have to be analyzed. Those requirements are divided upon must fulfill and nice to fulfill. The must fulfill requirements are the ones that are necessary for the product and without those requirements fulfilled, a functional design strategy cannot exist. On the other hand, the nice to fulfill requirements are the ones that make the product more attractive. Without those requirements, the operation can still be carried out. The requirements are presented below.

Must fulfil:

1. Perform the lowering operation with the same sea state as the one during the pilling phase.
2. MP's Bottom Point (BP) lands on specified position with a tolerance of ±1 m radius.
3. MP rotation of ±2°-3.5° from intended orientation before touchdown.
4. Safe and controlled operation at any stage.
5. Ability to perform reverse operation if needed.
6. The solution should be suitable for typical HLVs.

Nice to fulfil:

1. Lowering in higher sea states.
2. Easy transition from previous phase (upending).
3. Easy transition to next phase (piling).
4. Least complexity/cost of tool.
5. Limited modifications to vessel, crane and Lifting Tool.
6. Least amount of effort needed to perform the operation.
7. Least possible space required for the tool.

2

2.2. PROBLEM AND SOLUTION FORMATION

To pursue the establishment of the aforementioned requirements, problems need to be defined based on the requirements. By solving the proposed problems, the requirements are then achieved. The problems and sub problems that were defined in the functional design are presented below.

- Control vertical displacement/position on MP's lowering/lifting operation.
- Prevent excessive loads on crane.
  - Horizontal loads on sheave:
    - Side-lead and Off-lead angles from crane.
    - Side-lead and Off-lead angles from MP.
  - Vertical loads:
    - Wire loads/ Dynamic Amplification Factor (DAF).
    - Overturning moment.
  - Impact of MP with crane part.
  - Relative rotation between MP and crane higher than tolerance.
- Prevent excessive loads on lifting tool.
  - Axial forces (w.r.t. the pin that the hook is connected).
  - Radial forces.
  - Upend forces.
- Control positioning and orientation of pile bottom with respect to landing spot.
  - Control translation at pile bottom.
    - Vessel motions.
    - Static loads on MP.
    - Dynamic loads on MP.
  - Excessive rotation of MP.
- Transition from/to upend phase.
  - Detach from upend tool, i.e. bottom beam.
  - Lifting radius of crane.
  - Feasibility of reverse operation.
- Transition to piling phase.
  - Over constrained pile.
  - Detach from previous phase.

Table 2.1: Problems and sub problems relevance

	Problems						
	Control vertical displacement /position on MP's lowering/ lifting operation	Prevent excessive loads on crane	Prevent excessive loads on lifting tool	Control positioning and orientation of pile bottom w.r.t. landing spot	Transition from/to upend phase	Transition to piling phase	Attachment of tool in different types of vessels (1)
Sub problems	----------------	Horizontal loads on sheave: Side-lead, Off-lead (From MP; From crane)	Axial forces	Control translation at pile bottom (Vessel; Static; Dynamic)	Detach from upend tool, i.e. bottom beam	Over constrained pile	Attachment mechanism
Sub problems	----------------	Vertical loads: (Wire/ DAF; Moment)	Radial forces	Excessive rotation of MP	Lifting radius of crane	Detach from previous phase	Connection points
Sub problems	----------------	Impact of MP with crane part	Upend forces	--------------------------------	Feasibility of reverse operation	Connection of MP to MCPG	Permanent or temporary mechanism
Sub problems	----------------	Relative rotation between MP and crane higher than tolerance	-----------	--------------------------------	------------	--------------	--------------

Relevance Indicator

Dark blue: Highest importance

- Connection of MP to MCPG.

- Attachment of tool in different types of vessels.
  - Attachment mechanism.
  - Connection points.
  - Permanent or temporary mechanism.

In Table 2.1, one can visualize the problems' and sub problems' relevance. The reader can notice that not all of the problems are included in the table. Those problems and most of their sub problems are assumed to be non-existent in this research due to time limitation and the scope of the thesis. This does not mean at any case that those problems are to be taken lightly. At this Table, the relevance priority is indicated as well. This does not mean that in general the following relevance applies.

Table 2.2: Possible solutions for each sub problem

Problem	Sub problem		Sub solution #1	Sub solution #2	Sub solution #3	Sub solution #4	Sub solution #5
Control vertical disp./ position	------------------		Use MP guidance [Crane]	Control MP's weight [buoyancy modules]	Do not control [Upend MP when it lands to seabed]		
Prevent excessive loads on crane	Horizontal loads on sheave: Side-lead, Off-lead from MP		Limit MP rotations [Apply force to counteract the rotation, MCPG]	Limit MP rotations w.r.t. vessel [Double layer Pile Gripper]	Limit MP translations [Fixed clearance between vessel and MP]	Limit MP relative motions w.r.t. crane [Increase wire's length]	Mitigate loads on MP [Strategic vessel positioning to shield MP]
	Horizontal loads on sheave: Side-lead, Off-lead from crane		Limit vessel rotations [Double mooring system and place crane mid-ship]	Limit rotations and translations [Motion Compensating crane]	Cancel relative motions [MP and crane tip are fixed w.r.t. each other]	Limit MP relative motions w.r.t. crane [Increase wire's length]	Not limiting [This sub problem is not the bottleneck of the operation]
	Vertical loads Wire/DAF		Limit MP vertical motions [Heave compensating lowering tool]	Mitigate MP vertical loads Reduce MP mass [Buoyancy modules]	Not limiting [This sub problem is not the bottleneck of the operation]		
	Vertical loads Moment		Mitigate MP relative rotations w.r.t. crane [Increase wire's length]	Limit MP rotations [Apply force to counteract the rotation, MCPG]	Limit MP rotations at two points [Double layer gripper]	Minimize relative motions between crane and MP [Attach MP on vessel, zero clearance]	Not limiting [This sub problem is not the bottleneck of the operation]
	Impact of MP with crane part		Clearance between vessel and MP is fixed [Fixed passive gripper]	Clearance between vessel and MP is fixed [Bumpers at critical positions]	Limit MP rotations [Apply force to counteract the rotation, MCPG]	Zero clearance between vessel and MP [Attach MP on vessel]	Not limiting [This sub problem is not the bottleneck of the operation]
	Relative rotation between MP and crane tip higher than tolerance		Constrain MP axial rotations [Orientation rollers]	Mitigate effect of axial rotations of MP on crane [Swivel in crane block]	Mitigate loads on MP [Strategic vessel positioning to shield MP]	Not limiting [This sub problem is not the bottleneck of the operation]	
Control positioning and orientation of pile bottom w.r.t. landing spot	Control translation at pile bottom	Vessel (Drift)	Limit vessel motions [DP vessel]	Constrain vessel motions [JUB]	Limit influence of vessel motions on MP [Motion compensating crane or pile gripper]		
		Static (Current, Wind)	Limit MP translations [MCPG]	Constrain MP rotations [Double layer gripper]	React for static forces [Fixed passive gripper]	Compensate for MP motions [DP vessel]	Predict static forces [Based on prediction, integrate static on dynamic loads]
		Dynamic (Waves)	Limit MP rotations and translations [MCPG or double layer gripper]	Limit MP translations [Fixed Passive gripper]	Mitigate motions [Mooring system on MP]	Mitigate loads on MP [Strategic vessel positioning to shield MP]	Not limiting [This sub problem is not the bottleneck of the operation]
	Excessive rotation of MP (Yaw)		Constrain MP axial rotations [Orientation rollers]	Correct orientation of MP after operation [DP vessel]	Compensate for MP rotations [Rotate MP in seafastening]		
Prevent over constrain at touchdown			Not over constrained	Compliant system	Release constrain before touchdown		

2.3. POSSIBLE DESIGN STRATEGIES

After all the relevant problems and sub-problems are fully defined, different solutions for each subcategory needs to be derived. The author with the help of TWD came up with numerous solutions that could solve each problem. In Table 2.2, one can see the possible solutions for each of the sub problems. This will serve as a first approach to design possible strategies that might be able to control the MP throughout lowering. The different solutions that are presented in the table are not in order of preference.

By the time that all the different solutions are fully defined, a consideration of how to combine them into possible design strategies rises. Thus, after a repetitive process of possible combinations between sub-problems and sub-solutions, four different design strategies are the most governing and those will be further investigated in the generated model. The four different concepts can be visualized in Table 2.3 which with different colors the path of sub-solutions for each concept is given and in Table 2.4 an alternative representation is shown to the reader for simplicity reasons.

Table 2.3: Possible solution combinations

Problem	Sub problem	Sub solution #1	Sub solution #2	Sub solution #3	Sub solution #4	Sub solution #5
Control vertical disp./ position	-------------------	Use MP guidance [Crane]	Control MP's weight [buoyancy modules]	Do not control [Upend MP when it lands to seabed]		
Prevent excessive loads on crane	Horizontal loads on sheave: Side-lead, Off-lead from MP	Limit MP rotations [Apply force to counteract the rotation, MCPG]	Limit MP rotations w.r.t. vessel [Double layer Pile Gripper]	Limit MP translations [Fixed clearance between vessel and MP]	Limit MP relative motions w.r.t. crane [Increase wire's length]	Mitigate loads on MP [Strategic vessel positioning to shield MP]
	Horizontal loads on sheave: Side-lead, Off-lead from crane	Limit vessel rotations [Double mooring system and place crane mid-ship]	Limit rotations and translations [Motion Compensating crane]	Cancel relative motions [MP and crane tip are fixed w.r.t. each other]	Limit MP relative motions w.r.t. crane [Increase wire's length]	Not limiting [This sub problem is not the bottleneck of the operation]
	Vertical loads Wire/DAF	Limit MP vertical motions [Heave compensating lowering tool]	Mitigate MP vertical loads Reduce MP mass [Buoyancy modules]	Not limiting [This sub problem is not the bottleneck of the operation]		
	Vertical loads Moment	Mitigate MP relative rotations w.r.t. crane [Increase wire's length]	Limit MP rotations [Apply force to counteract the rotation, MCPG]	Limit MP rotations at two points [Double layer gripper]	Minimize relative motions between crane and MP [Attach MP on vessel, zero clearance]	Not limiting [This sub problem is not the bottleneck of the operation]
	Impact of MP with crane part	Clearance between vessel and MP is fixed [Fixed passive gripper]	Clearance between vessel and MP is fixed [Bumpers at critical positions]	Limit MP rotations [Apply force to counteract the rotation, MCPG]	Zero clearance between vessel and MP [Attach MP on vessel]	Not limiting [This sub problem is not the bottleneck of the operation]
	Relative rotation between MP and crane tip higher than tolerance	Constrain MP axial rotations [Orientation rollers]	Mitigate effect of axial rotations of MP on crane [Swivel in crane block]	Mitigate loads on MP [Strategic vessel positioning to shield MP]	Not limiting [This sub problem is not the bottleneck of the operation]	
Control positioning and orientation of pile bottom w.r.t. landing spot	Control translation at pile bottom: Vessel (Drift)	Limit vessel motions [DP vessel]	Constrain vessel motions [JUB]	Limit influence of vessel motions on MP [Motion compensating crane or pile gripper]		
	Control translation at pile bottom: Static (Current, Wind)	Limit MP translations [MCPG]	Constrain MP rotations [Double layer gripper]	React for static forces [Fixed passive gripper]	Compensate for MP motions [DP vessel]	Predict static forces [Based on prediction, integrate static on dynamic loads]
	Control translation at pile bottom: Dynamic (Waves)	Limit MP rotations and translations [MCPG or double layer gripper]	Limit MP translations [Fixed Passive gripper]	Mitigate motions [Mooring system on MP]	Mitigate loads on MP [Strategic vessel positioning to shield MP]	Not limiting [This sub problem is not the bottleneck of the operation]
	Excessive rotation of MP (Yaw)	Constrain MP axial rotations [Orientation rollers]	Correct orientation of MP after operation [DP vessel]	Compensate for MP rotations [Rotate MP in seafastening]		
Prevent over constrain at touchdown		Not over constrained	Compliant system	Release constrain before touchdown		

Concept #1
Loose/ Passive

Concept #2
Fixed/ Passive

Concept #3
Hybrid/ Active

Concept #4
Mooring MP

Table 2.4: Possible solution combinations-Alternative representation

Problem	Sub problem	Concept #1	Concept #2	Concept #3	Concept #4
Control vertical disp./	-------------------	Use MP guidance [Crane]	Use MP guidance [Crane]	Use MP guidance [Crane]	Use MP guidance [Crane]
Prevent excessive loads on crane	Horizontal loads on sheave: Side-lead, Off-lead from MP	Limit MP relative motions w.r.t. crane [Increase wire's length]	Limit MP rotations w.r.t. vessel [Double layer Pile Gripper]	Limit MP rotations [Apply force to counteract the rotation, MCPG]	Limit MP rotations [Apply force to counteract the rotation, MCPG]
	Horizontal loads on sheave: Side-lead, Off-lead from crane	Limit MP relative motions w.r.t. crane [Increase wire's length] Not limiting [This sub problem is not the bottleneck of the operation]	Cancel relative motions [MP and crane tip are fixed w.r.t. each other]	Cancel relative motions [MP and crane tip are fixed w.r.t. each other]	Cancel relative motions [MP and crane tip are fixed w.r.t. each other]
	Vertical loads Wire/DAF	Not limiting [This sub problem is not the bottleneck of the operation]	Not limiting [This sub problem is not the bottleneck of the operation]	Not limiting [This sub problem is not the bottleneck of the operation]	Not limiting [This sub problem is not the bottleneck of the operation]
	Vertical loads Moment	Mitigate MP relative rotations w.r.t. crane [Increase wire's length] Not limiting [This sub problem is not the bottleneck of the operation]	Limit MP rotations at two points [Double layer gripper]	Limit MP rotations [Apply force to counteract the rotation, MCPG]	Limit MP rotations [Apply force to counteract the rotation, MCPG]
	Impact of MP with crane part	Clearance between vessel and MP is fixed [Bumpers at critical positions]	Clearance between vessel and MP is fixed [Fixed passive gripper]	Limit MP rotations [Apply force to counteract the rotation, MCPG]	Limit MP rotations [Apply force to counteract the rotation, MCPG]
	Relative rotation between MP and crane tip higher than tolerance	Mitigate effect of axial rotations of MP on crane [Swivel in crane block] Mitigate loads on MP [Strategic vessel positioning to shield MP] Not limiting [This sub problem is not the bottleneck of the operation]	Mitigate effect of axial rotations of MP on crane [Swivel in crane block] Not limiting [This sub problem is not the bottleneck of the operation]	Mitigate effect of axial rotations of MP on crane [Swivel in crane block Not limiting [This sub problem is not the bottleneck of the operation]	Mitigate effect of axial rotations of MP on crane [Swivel in crane block Not limiting [This sub problem is not the bottleneck of the operation]
Control positioning and orientation of pile bottom w.r.t. landing spot	Control translation at pile bottom: Vessel (Drift)	Limit vessel motions [DP vessel]	Limit vessel motions [DP vessel]	Limit vessel motions [DP vessel] Limit influence of vessel motions on MP [Motion compensating crane or pile gripper]	Limit vessel motions [DP vessel] Limit influence of vessel motions on MP [Motion compensating crane or pile gripper]
	Control translation at pile bottom: Static (Current, Wind)	Compensate for MP motions [DP vessel]	Constrain MP rotations [Double layer gripper] React for static forces [Fixed passive gripper] Compensate for MP motions [DP vessel]	Limit MP translations [MCPG] Compensate for MP motions [DP vessel]	Limit MP translations [MCPG] Compensate for MP motions [DP vessel]
	Control translation at pile bottom: Dynamic (Waves)	Not limiting [This sub problem is not the bottleneck of the operation]	Limit MP rotations and translations [MCPG or double layer gripper]	Limit MP rotations and translations [MCPG or double layer gripper]	Mitigate motions [Mooring system on MP]
	Excessive rotation of MP (Yaw)	Correct orientation of MP after operation [DP vessel] Compensate for MP rotations [Rotate MP in seafastening]	Constrain MP axial rotations [Orientation rollers] Correct orientation of MP after operation [DP vessel]	Constrain MP axial rotations [Orientation rollers] Correct orientation of MP after operation [DP vessel]	Correct orientation of MP after operation [DP vessel]
Prevent over constrain at touchdown		Not over constrained	Compliant system Release constrain before touchdown	Not over constrained	Not over constrained

The four different concepts that are finally derived from the functional design, are briefly explained in the following paragraphs. In Figure 2.2, the first concept is depicted. That is the concept of free hanging MP. The question was rose about what motions and forces should we expect if the MP is freely hanging from the crane while it is lowered. Will the fluctuations lay in the defined tolerances? If not, how much compensation is needed throughout the lowering phase of the MP erection process.

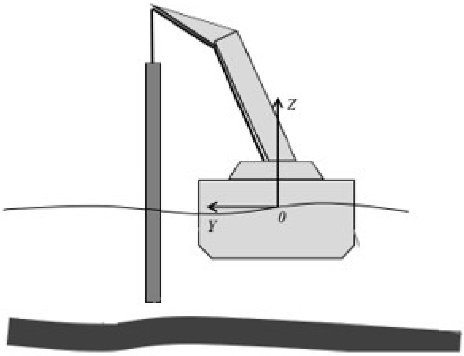

Figure 2.2: Design Strategy No.1: Free hanging MP

Secondly, as can be seen in Figure 2.3, the concept of a a fixed gripper is presented. The fixed gripper suggests a passive compensation of the motions that the MP will have and the strategy is integrated approximately at deck height. The author will perform different simulations to assess the strategy and evaluate whether it complies with the aforementioned requirements.

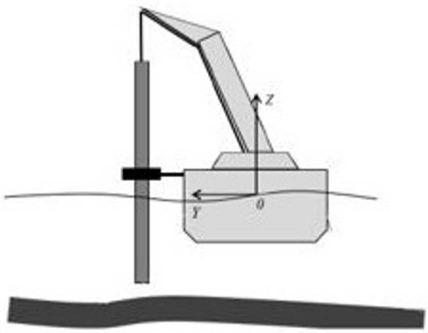

Figure 2.3: Design Strategy No.2: Fixed/Passive gripper

In addition, the company's concept will be tested. As one can see in Figure 2.4, the design strategy of MCPG is chosen as the third possible design strategy. In a latter stage, the active gripper is shown in detail and its system is well modelled to match a realistic design since this concept will be the one that the company will use to compensate for the piling phase of the MP installation regardless of which design strategy is chosen to control the lowering operation of the entire process.

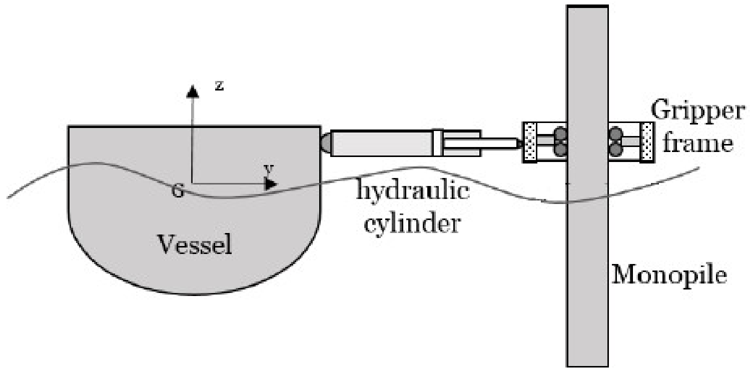

Figure 2.4: Design Strategy No.3: Active compensating gripper (MCPG)

Finally, the last possible design strategy is the mooring/double layered gripper. This can either be fixed gripper, meaning that between the two grippers there will be a fixed distance (picture on the right of Figure 2.5) and the second variation of this design strategy is a mooring double gripper on which the first gripper will be fixed in space and the second gripper will follow the BP of the MP throughout the lowering phase (picture on the left).

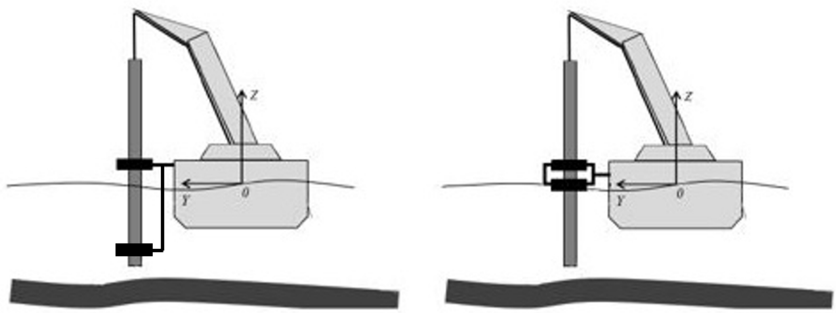

Figure 2.5: Design Strategy No.4: Mooring/Double gripper

3

ENVIRONMENTAL CONDITIONS

The important thing is not to stop questioning.
Curiosity has its own reason for existence.
One cannot help but be in awe
when he contemplates the mysteries of eternity,
of life, of the marvelous structure of reality.
It is enough if one tries merely to comprehend
a little of this mystery each day.

Albert Einstein

This chapter will illustrate the environmental conditions that take place in the offshore sector during the installation phase. The structures that are used in this sector are designed in such way, that can withstand various loads but the ones that are considered in this research are wind, current and wave loads. This chapter will illustrate how those loads are modeled in the simulation analysis as well as the assumptions and conventions that are established for the environmental conditions.

3

3.1. GLOBAL AND LOCAL CONVENTIONS

3.1.1. AXES AND MOTIONS DEFINITIONS

Firstly, a convention for the axes should be established for further understanding of the research that was made. The different conventions for coordinate systems are needed in order to define the forces, motions and any other vectors that might be needed in further steps of the analysis. In this thesis, three different axes systems are introduced and those are discussed further below.

Since in the lowering operation of a MP from a floating vessel nothing is fixed for the entire process time, no real point on any structure can be considered as the origin for Fixed Reference Axes (FRA). Thus, a FRA system is established in the mean water surface level and it is depicted in Figure 3.1. The FRA is a right handed fixed axis system, the Z-axis is directed vertically upward and the axis origin (O) placed at the mean water Free Surface (FS). All the coordinates that will be considered as FRA coordinates, will be notated with upper case letters.

In the above mentioned Figure, a second axes system is shown as well. This is the Local Structure Axes (LSA) which is a fixed body axes system that it has the axes origin on the Center of Gravity (COG) of the structure. Such axes system is needed for the convenience of describing the rigid body motions. Initially, the vessel's LSA is at the same point as FRA. Furthermore, such LSA exists for the MP with its COG as the origin of the axes.All the coordinates that will be considered as LSA coordinates, will be notated with lower case letters.

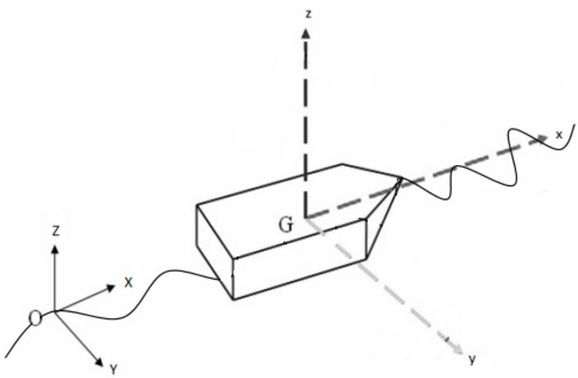

Figure 3.1: Axes conventions

3.1.2. AXES TRANSFORMATION AND EULER ROTATIONS

Since any rigid body in water has a dynamic behavior, it is required to describe the individual rotations of that body with the aid of Euler angles. The Euler angles are in general a very efficient way to keep track of a point of the body in space. Initially, Equation 3.1 describes the procedure to track a point from LSA to FRA, where r are the FRA coordinates of the point, r' the LSA coordinates and R the orthogonal rotation matrix. The three angles are typically named as ϕ, θ, ψ and are used to describe the orientation of any rigid body. In principle, three rotations are required to fully define the rotation matrix that will be used.

3

$$r = Rr' \tag{3.1}$$

The first rotation is performed by an angle ψ about $z - axis$ and named as R_ψ which can be described in Equation 3.4. The next rotation in sequence is by an angle θ about $y' - axis$. This rotation is notated as R_θ and described by the matrix in Equation 3.3. Finally, the third rotation is by an angle ϕ about $X - axis$. It is notated as R_ϕ rotation and Equation 3.2 corresponds to it. All the sequential rotations and their corresponding axes systems are depicted in Figure 3.2. The concluded axes (X,Y,Z) are the ones depicted in red color.

$$R_\phi = \begin{bmatrix} 1 & 0 & 0 \\ 0 & \cos\phi & -\sin\phi \\ 0 & \sin\phi & \cos\phi \end{bmatrix} \tag{3.2}$$

$$R_\theta = \begin{bmatrix} \cos\theta & 0 & \sin\theta \\ 0 & 1 & 0 \\ -\sin\theta & 0 & \cos\theta \end{bmatrix} \tag{3.3}$$

$$R_\psi = \begin{bmatrix} \cos\psi & -\sin\psi & 0 \\ \sin\psi & \cos\psi & 0 \\ 0 & 0 & 1 \end{bmatrix} \tag{3.4}$$

Finally, the rotation matrix is the product of the three individual successive matrices, $R = R_\psi \times R_\theta \times R_\phi$ and the resulting rotation matrix is presented in Equation 3.5. The purpose of the rotation matrix is to give the ability to the user to define a point from the LSA to the FRA and vice versa by using the inverse transformation of the rotation matrix ($R^{-1} = R^T$) which yields Equation 3.6.

$$R = R_\psi R_\theta R_\phi = \begin{bmatrix} \cos\theta\cos\psi & \sin\phi\sin\theta\cos\psi - \cos\phi\sin\psi & \cos\phi\sin\theta\cos\psi + \sin\phi\sin\psi \\ \cos\theta\sin\psi & \sin\phi\sin\theta\sin\psi + \cos\phi\cos\psi & \cos\phi\sin\theta\sin\psi - \sin\phi\cos\psi \\ -\sin\theta & \sin\phi\cos\theta & \cos\phi\cos\theta \end{bmatrix} \tag{3.5}$$

$$r' = R^{-1}r = R^T r \tag{3.6}$$

In Equation 3.7 one can see the expression for a point with coordinates $(x, y, z)^T$ in LSA and the transition to a point in FRA with coordinates $(X, Y, Z)^T$, where $(X_{cg}, Y_{cg}, Z_{cg})^T$ are the coordinates of the COG in FRA.

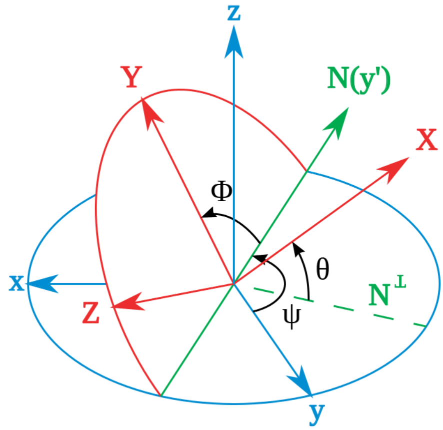

Figure 3.2: Euler transformation sequence

$$\begin{bmatrix} X \\ Y \\ Z \end{bmatrix} = \begin{bmatrix} X_{cg} \\ Y_{cg} \\ Z_{cg} \end{bmatrix} + R \begin{bmatrix} x \\ y \\ z \end{bmatrix} \tag{3.7}$$

For determining the angular velocity components, the time derivative of Equation 3.1 needs to be evaluated. Furthermore, by substituting Equation 3.6, leads to Equation 3.8 where $\dot{r}'$ is canceled since the LSA coordinates are constant. Hence, the resulting matrix $\dot{R}R^T$ can be identified as antisymmetric since R is orthogonal and the differentiation of $RR^T = I$ yields $\dot{R}R^T + (\dot{R}R^T)^T = O$.

$$\dot{r} = \dot{R}R^T r \tag{3.8}$$

The antisymmetric matrix described before will be named $\tilde{\omega}$. This matrix is defined in Equation 3.9 and describes the cross product of the components of the angular velocity vector $\vec{\omega} = (\omega_x, \omega_y, \omega_z)$, where Equation 3.10 represents their relation.

$$\tilde{\omega} = \begin{pmatrix} 0 & -\omega_z & \omega_y \\ \omega_z & 0 & -\omega_x \\ -\omega_y & \omega_x & 0 \end{pmatrix} \tag{3.9}$$

$$\dot{r} = \tilde{\omega} r = \omega \times r \tag{3.10}$$

The angular velocity is the summation of the three individual angular velocities that are established in sequence in order to obtain the final rotation, $\vec{\omega} = \vec{\omega}_\phi + \vec{\omega}_\theta + \vec{\omega}_\psi$. Those individual angular velocity vectors are represented in Equation 3.11. Finally, after the expansion of those components, the angular velocity vector is depicted in Equation 3.12.

$$\vec{\omega}_\psi = \dot{\psi}\vec{e}_z, \quad \vec{\omega}_\theta = \dot{\theta}\vec{e}_{y'}, \quad \vec{\omega}_\phi = \dot{\phi}\vec{e}_X \tag{3.11}$$

$$\omega = \begin{pmatrix} \omega_x \\ \omega_y \\ \omega_z \end{pmatrix} = \begin{pmatrix} 1 & 0 & -\sin\theta \\ 0 & \cos\phi & \cos\theta\sin\phi \\ 0 & -\sin\phi & \cos\theta\cos\phi \end{pmatrix} \begin{pmatrix} \dot{\phi} \\ \dot{\theta} \\ \dot{\psi} \end{pmatrix}, \quad \omega = A\dot{u} \tag{3.12}$$

The last step in the axis transformation subsection is to define a way to derive the angular velocity vector from the FRA to the LSA coordinates and this can be done using Equation 3.13

$$\omega' = R^T A\dot{u} = B\dot{u} \tag{3.13}$$

3

3.2. ENVIRONMENTAL LOADS

3.2.1. WIND LOADS

The first environmental loads that are described in this chapter are the ones that are caused from wind. Those loads in general are time dependent because wind fluctuations are the principle contributor to the wind load. In this thesis, the fluctuations are not taken into account. A uni-formal and steady wind profile is considered. In order to determine the wind force, firstly the wind pressure needs to be defined

$$q = \frac{1}{2}\rho_a U_{T,Z} \tag{3.14}$$

As it was before mentioned, q is the basic wind pressure or suction. ρ_a is the mass density of air and $U_{T,Z}$ is the wind velocity which is averaged over a time interval (T) at a specific height (Z) above sea water level.

The wind force acting on a structural member, normal to its axis is

$$F_w = C_s q S \sin\alpha \tag{3.15}$$

Where C_s is the shape coefficient that is determined based on Table 3.1 for different components based on Reynolds number. S is the area that is projected normal to the force direction acting on the member. Finally, α is the angle between the direction of the wind profile and the axis of the exposed member. It is assumed that $\alpha = 90°$ for the entire simulation of the operation.

Component	**Shape coefficients, C_s**
Flat walls of buildings	1.5
Overall projected area of structure	1.0
Beams	1.5
Smooth cylinder $R_e > 5 \times 10^5$	0.65
Smooth cylinder $R_e \leq 5 \times 10^5$	1.2
Rough cylinder, all R_e	1.05
Covered with ice cylinder, all R_e	1.2

Table 3.1: Shape coefficient, C_s, for perpendicular wind approach angles

3.2.2. CURRENT LOADS

The next environmental loads that will be considered in this research are the current loads. Current is of major impact and it is necessary to be evaluated for any simulations since it contributes to drift motions, large steady excursions, drag and lift forces. There are various categories of currents,

3

- Wind generated currents
- Tidal currents
- Circulational currents
- Loop and eddy currents
- Soliton currents
- Longshore currents

The currents that will be considered in this thesis are the wind generated and tidal currents since those are the most common currents applicable. The total current velocity is

$$V_c(z) = V_{c,wind}(z) + V_{c,tide}(z) \tag{3.16}$$

The wind current velocity follows the profile

$$V_{c,wind}(z) = V_{c,wind}(0) \times (\frac{d_0 + z}{d_0}) \quad for - d_0 \leq z \leq 0 \tag{3.17}$$

or

$$V_{c,wind}(z) = V_{c,wind}(0) \quad for - d_0 < z < 0 \tag{3.18}$$

The profile that gives the highest loads should be used in the specific application. Whereas, the variation of tidal current can be described as follow

$$V_{c,tide}(z) = V_{c,tide}(0) \times (\frac{d + z}{d})^{\alpha} \tag{3.19}$$

The wind generated current can be assumed that it is insignificant at a distance below the water level

$$V_{c,wind} = 0 \quad for\, z < -d_0$$

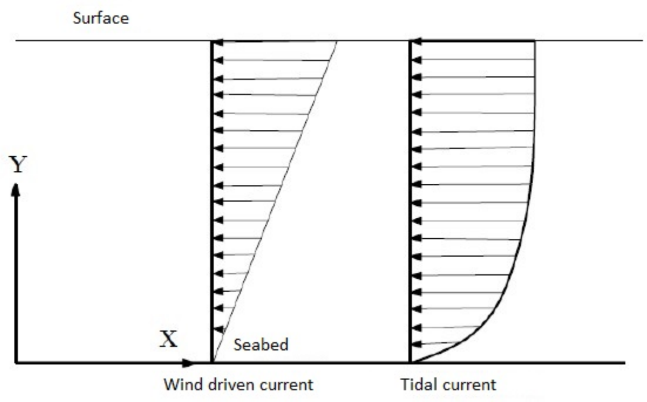

Figure 3.3: Wind and tidal current profiles

Where $V_c(z)$ is the total current velocity at z, z is the distance from water level (taken as positive upwards). $V_{c,wind}(0)$ and $V_{c,tide}(0)$ is the wind generated and tidal current velocity at the still water level respectively. The water depth up to still water level is depicted as d (taken as positive), $d_0 = 50m$ the reference depth and finally $\alpha = \frac{1}{7}$ an empirical exponent. In Figure 3.3, the different profiles for wind and tidal currents are depicted. If there are no data available, then the following formula can be used for the wind generated current velocity at the still water level

$$V_{c,wind}(0) = k \times U_{1hr,10m} \tag{3.20}$$

Where $U_{1hr,10m}$ is the 1 hour sustained wind speed at 10 meters above sea level and $k = 0.015 - 0.03$. Furthermore, the variation in water depth due to waves should be considered. There are two methods to stretch the current up to wave surface

- Linear Stretching:

$$z_s = (d + \eta) \times (1 + \frac{z}{d}) - d \quad for - d \leq z_s \leq \eta \tag{3.21}$$

- Non-linear Stretching:

$$z_s = z + \eta \times \frac{\sinh[k_{nl} \times (z + d)]}{\sinh(k_{nl} \times d)} \quad for - d \leq z_s \leq \eta \tag{3.22}$$

Where η is the water surface elevation, z_s is the stretched vertical coordinate and k_{nl} is the wave number (non-linear) that corresponds to the wave length λ_{nl}. In Figure 3.4, one can visualize the differences in the two different stretching methods. For this research the linear stretching is considered since it produces accurate estimations of hydrodynamic loads. DNV [2010]

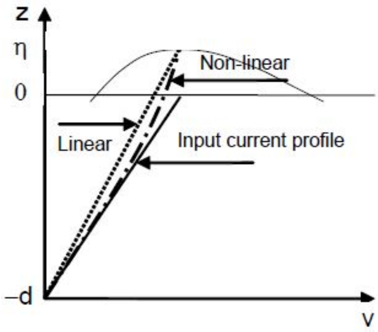

Figure 3.4: Linear and non-linear stretching of current profile up to wave surface

3.2.3. WAVE LOADS

In this subsection, the wave loads will be described. A more extensive elaboration will be presented since wave loads are the most important parameter in the analysis that will be made due to their dynamic character. In principle, waves can be generated from various reasons. Firstly, from a floating structure that is moving, by wind and sea water surface interaction, from tides, earthquakes and due to motion in partially filled tanks. Waves that are generated from wind will be further considered. Those waves can be categorized as such:

- **Sea**
  Those waves are triggered from the local wind field. In general, sea waves are characterized as very irregular, short-crested and in various deviating directions from the main wind field.
- **Swell**
  Swell waves are the ones that deviated from the local wind. Those waves are more regular, with long crests and with a more predictable wave height. They can propagate for great distances without any wind field.

The waves in general can also be classified based on their characteristics (wave length) and the environment characteristics (water depth) as follow,

- **Deep water waves:** Those waves are not influenced from the sea floor, $\frac{h}{\lambda} > \frac{1}{2}$
- **Shallow water waves:** Greatly influenced from the sea floor, $\frac{h}{\lambda} < \frac{1}{20}$

Where h is the water depth (m) and λ the wave length (m). A harmonic wave can is shown in Figure 3.5. The picture on the left,(a), represents a wave stopped at a random point in time. One might consider that as a picture taken in time. The picture on the right (b) represents a time trace of a wave. Time varies while displacement is still. The highest point of the wave is called 'crest' and the lowest one is called 'trough'. Where ζ_α is the wave amplitude (m), $H = 2\zeta_\alpha$ is the wave height which is measured vertically from crest to trough and T is the wave period (s).

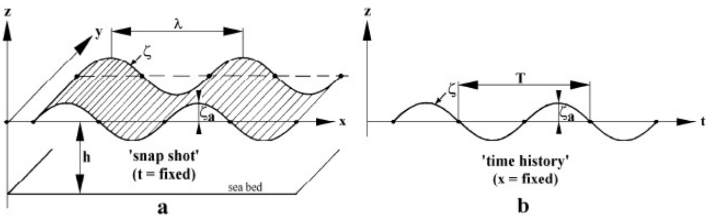

Figure 3.5: Harmonic wave definitions Journèe and Massie [2001]

The wind generated waves in general are random and irregular when characteristics such as wave length and wave height are considered. The best approach to generate a random sea state is to superpose various regular waves with different characteristics. The differences in regular and irregular waves with random propagation, direction, length and height can be visualized in Figure 3.6.

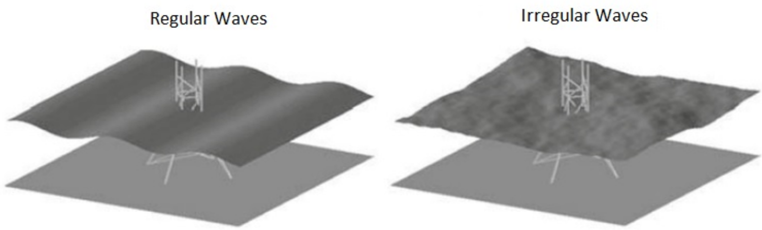

Figure 3.6: Illustration of the difference in the appearance of the sea surface Journèe and Massie [2001]

In Figure 3.7, the different wave theories that can be used for analysis are given based on the dimensionless wave steepness $(\frac{H}{g \times T^2})$ and the dimensionless relative depth $(\frac{h}{g \times T^2})$, where g is the gravitational acceleration $(\frac{m}{s^2})$. Based on the area of operation in this figure, a decision to use linear Airy wave theory was made since this method satisfies the demands of the research.

Linear Airy wave theory

Firstly, the wave elevation (m) is presented in Equation 3.23. Where θ the phase of the wave (rad) and $\theta = \kappa x - \omega t$, ω is the angular frequency $(\frac{rad}{s})$ and κ is the wave number $(\frac{rad}{m})$. Angular frequency's relation to wave period is given in Equation 3.24, whereas the relation between wave number and wave length is shown in Equation 3.25.

$$\zeta(x, t) = \zeta_{\alpha} \cos\theta \tag{3.23}$$

$$\omega = \frac{2\pi}{T} \tag{3.24}$$

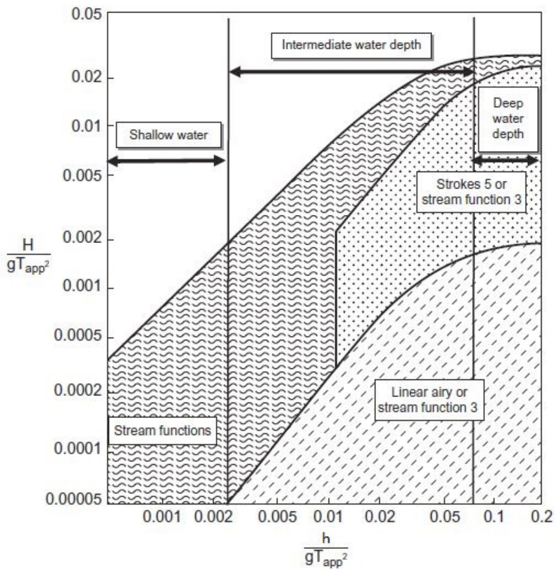

Figure 3.7: Regions of applying wave theories

$$\kappa = \frac{2\pi}{\lambda} \tag{3.25}$$

In addition, the dispersion relation is presented in Equation 3.26. All the different equations that are presented in this section, will be used to determine the wave parameters in order to create a realistic random sea state.

$$\omega^2 = g\kappa \tanh(\kappa h) = \frac{2\pi g}{\lambda} \tanh(\frac{2\pi h}{\lambda}) \tag{3.26}$$

In order to evaluate the forces on a submerged body, the particle velocities needs to be evaluated first. Thus, the velocity potential is given in Equation 3.27. The partial derivative of the velocity potential with respect to horizontal direction (x), results to the horizontal particle velocity, Equation 3.28. Similarly, a partial derivative of velocity potential with respect to vertical direction (z), results to the vertical particle velocity shown in Equation 3.29.
The second partial derivative of velocity potential with respect to horizontal and vertical directions, results to particle accelerations shown in Equations 3.30 and 3.31 respectively.

$$\phi = \frac{\pi H}{\kappa T} \frac{\cosh[\kappa(h+z)]}{\sinh \kappa h} \cdot \sin(\kappa x - \omega t) = \frac{\zeta_\alpha g}{\omega} \frac{\cosh \kappa(h+z)}{\cosh \kappa h} \cdot \sin\theta \tag{3.27}$$

$$u = \frac{\partial \phi}{\partial x} = \zeta_\alpha \cdot \omega \cdot \frac{\cosh[\kappa(h+z)]}{\sinh \kappa h} \cdot \cos\theta \tag{3.28}$$

$$w = \frac{\partial \phi}{\partial z} = \zeta_\alpha \cdot \omega \cdot \frac{\sinh[\kappa(h+z)]}{\sinh \kappa h} \cdot \sin\theta \tag{3.29}$$

$$\dot{u} = \frac{\partial^2 \phi}{\partial x^2} = \zeta_\alpha \cdot \omega^2 \cdot \frac{\cosh[\kappa(h+z)]}{\sinh \kappa h} \cdot \sin\theta \tag{3.30}$$

$$\dot{w} = \frac{\partial^2 \phi}{\partial z^2} = -\zeta_\alpha \cdot \omega^2 \cdot \frac{\sinh[\kappa(h+z)]}{\sinh \kappa h} \cdot \cos\theta \tag{3.31}$$

3

Profile extension methods

When a design or analysis is established that takes into account the wave height and the water level, more often than not a profile extension method should be considered since the wave crest in reality will be higher than the sinusoidal wave amplitude. The most common profile extension methods are discussed briefly below.

- **Constant extension**
  This is the simplest method that can be performed. Conventional linear theory is established for all water depths below still water level. Sequentially, the horizontal particle velocity that is derived in still water level is used as a constant for any value of z higher than zero.

- **Extrapolation**
  This profile extension method uses the same linear theory that is used for water depths below still water level for $z > 0$ as well, with a positive sign. This extrapolation method though, results to exaggerated velocities with respect to the actual ones. Thus, this is method is considered over conservative.

- **Wheeler Profile Stretching**
  The final method that is presented is also the most acceptable one. The Wheeler profile stretching in principle uses a dynamic approach based on z. The crossing of z-axis from positive to negative values is changing based on the water surface elevation. This results to a substitution of z with z' that takes into account the water elevation level. This profile extension method is used in this thesis as well.

$$z' = qz + h(q-1) \quad where: q = \frac{h}{h+\varsigma} \tag{3.32}$$

Where z' is a computational vertical coordinate (m): $-h \le z' \le 0$, z is the actual vertical coordinate (m): $-h \le z \le \varsigma$, q is a dimensionless ratio, ς is the elevation of the actual water surface (m), measured along the z-axis and finally h is the water depth (m). In Figure 3.8, the differences of those three profile stretching methods can be visualized.
After the regular waves are discussed, the need to create realistic sea state is the driving factor to elaborate on irregular waves. Those waves have random and varying wave length, phase, wave amplitude and direction of propagation. One must understand that an irregular sea can be achieved by superposing numerous regular waves with different characteristics as can be seen in Figure 3.9.

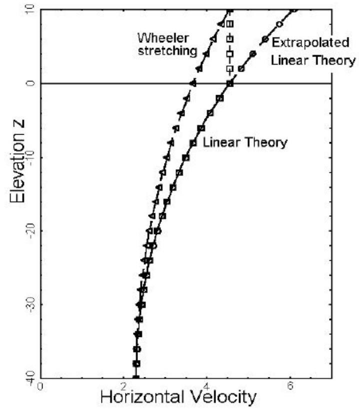

Figure 3.8: Comparison of horizontal water velocities Journèe and Massie [2001]

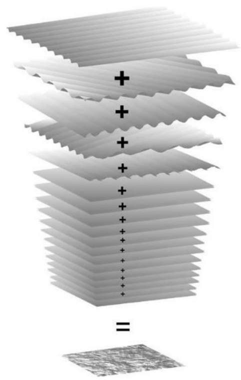

Figure 3.9: Superposition of many regular waves that conclude to an irregular sea

In order to conclude to the defined random sea sate, emphasis will be given to wave energy spectra. Firstly, a time record of wave series (1) is decomposed to many regular waves with Fourier series analysis. This analysis will yield numerous regular waves (2) with a set of wave amplitude and a phase, both for a specific angular velocity. The phases are discarded and wave amplitudes are used in order to structure the energy wave spectrum (3) through the expression in Equation 3.33 where $\Delta\omega$ is the frequency step. Two different empirical wave spectra will be discussed further below. After the energy wave spectrum is created, one can simply generate new regular waves (4) by deriving the wave amplitude using Equation 3.34. Adding random phases to the regular waves that were just generated will result to a "new"irregular sea (5) that will be the result of their superposition. All the before mentioned steps can be visualized in Figure 3.10.

$$S_\zeta(\omega_n)\cdot\Delta\omega = \sum_{\omega_n}^{\omega_n+\Delta\omega} \frac{1}{2}\zeta_{a_n}^2(\omega) \tag{3.33}$$

$$\zeta_a = \sqrt{2S_\zeta(\omega)\Delta\omega} \tag{3.34}$$

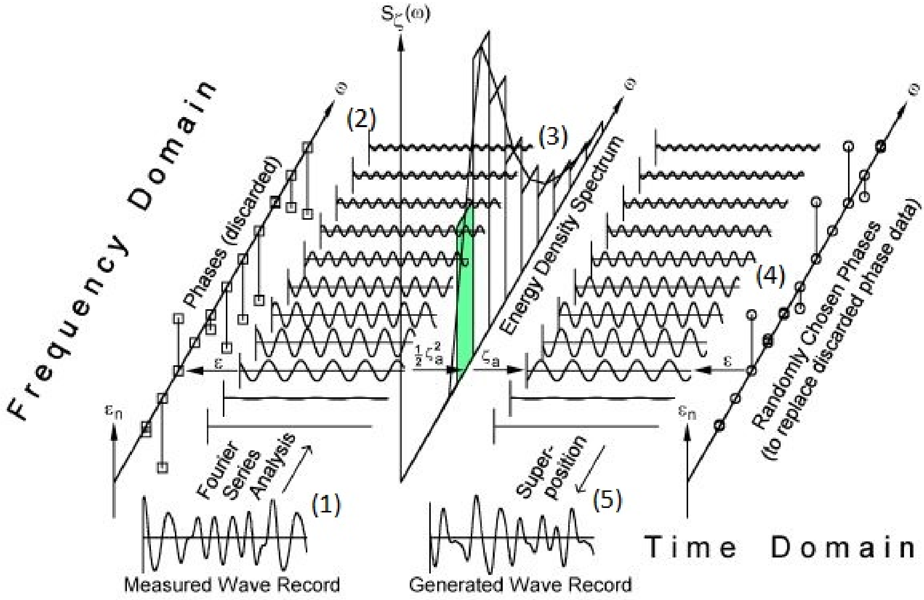

Figure 3.10: Wave record analysis and regeneration Journèe and Massie [2001]

In order to proceed to steps (4) and (5) of the procedure displayed in Figure 3.34, one needs either a measured wave record or a formulation of energy wave spectrum. Two different wave spectra are presented below. Firstly, the Pierson-Moskowitz spectrum is presented in Equation 3.35 which is suited for a fully developed sea; when the sea is created from a steady wind blown for for several days and over hundreds of miles.

$$S_{PM}(\omega) = \frac{5}{16} H_S^2 \omega_P^4 \cdot \omega^{-5} \exp\left(-\frac{5}{4}\left(\frac{\omega}{\omega_P}\right)^{-4}\right) \tag{3.35}$$

The second wave spectrum that will be presented, is the one that will be used over the entire research. This is the Joint North Sea Wave Project (JONSWAP) wave spectrum which is presented in Equation 3.36. This spectrum is a modification of the Pierson-Moskowitz which suggests that the waves do continue to grow while time or distance increased, thus a developing sea state in a fetch limited situation.

$$S_J(\omega) = A_\gamma S_{PM}(\omega) \cdot \gamma^{\exp\left(-0.5\left(\frac{\omega-\omega_P}{\sigma\omega_P}\right)^2\right)} \tag{3.36}$$

$$\sigma = \begin{cases} \sigma_a = 0.07 & for\, \omega \leq \omega_p \\ \sigma_b = 0.09 & for\, \omega > \omega_p \end{cases}$$

$$A_\gamma = 1 - 0.287 \ln(\gamma)$$

Where $S_{PM}(\omega)$ is the Pierson-Moskowitz spectrum, H_S the significant wave height (m), ω_P is the angular spectral peak frequency (rad/s), A_γ is a normalizing factor, γ a dimensionless peak shape parameter and σ the spectral width parameter. The only parameters that needs to be defined from the user are the significant wave height and the angular spectral peak frequency. The dimensionless peak shape parameter is set to 3.3 which is an average value suggested from DNV. Finally, in Equation 3.37 the superposition of all the individual regular waves takes place in order to reproduce the required random wave elevation; where ϵ is the phase angle (rad).

$$\zeta(t) = \sum_{n=1}^{N} \zeta_{a_n} \cos(\theta + \epsilon_n) \tag{3.37}$$

The generated wave spectrum is shown in Figure 3.11, where JONSWAP method was chosen, significant wave height of $2.5m$ and a peak period of $7sec$. Furthermore, in Figure 3.12, the representation of a random sea state is depicted where 300 wave components are superposed to result to the random generated sea state with the aforementioned characteristics.

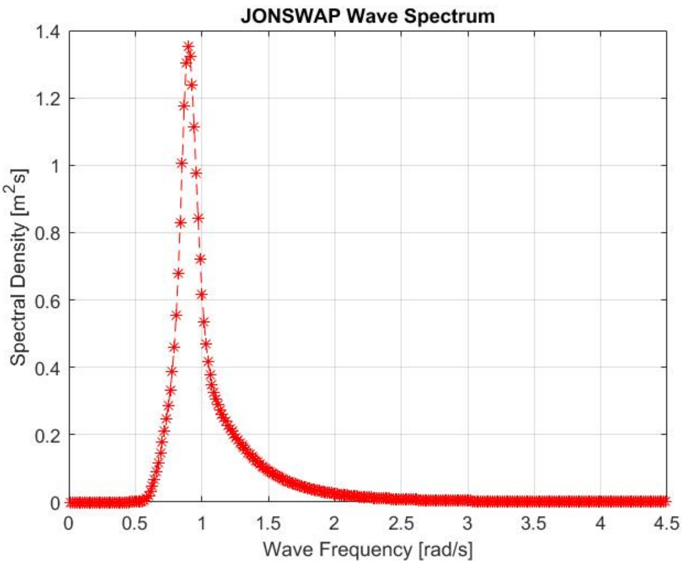

Figure 3.11: JONSWAP wave spectrum with $H_S = 2.5m$ and $T_P = 7sec$

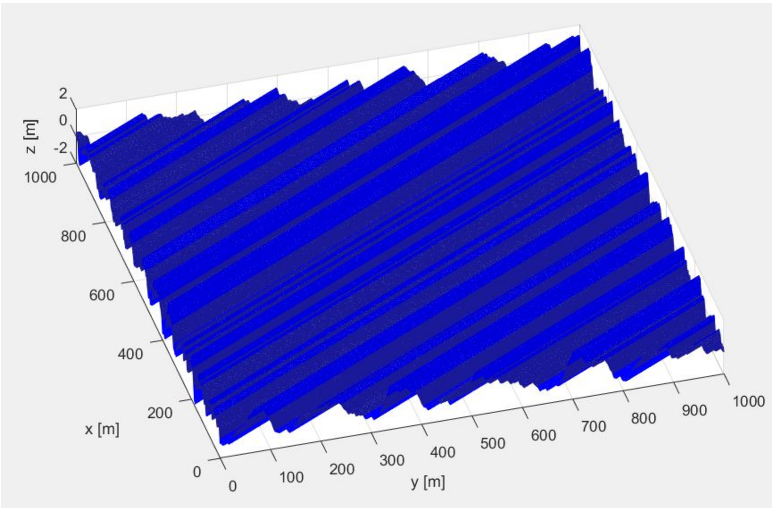

Figure 3.12: Random sea state realization with 300 wave components

4
MONOPILE MODEL

Have no fear of perfection; you'll never reach it.
Nothing in life is to be feared;
it is only to be understood.

Marie Curie

In this chapter, the generated model of MP is presented, including all involved parts and induced motions from the environment, crane and gripper(s). The methods that were used to define the forces, necessary coefficients and parameters are also discussed in this chapter. Finally, the software that were used and the procedure that was followed to determine the motions and forces for the above mentioned models is analysed.

4.1. VARIABLE DEFINITION AND NAMING

The entire system has many parameters as one can imagine. In order to make the analysis as comprehensive as possible and to comply with the analysis that TWD already has for the piling phase of the MP installation process, a need for a variable convention presents for the convenience of both readers and author. In order to derive the EOM of MP, several points need to be defined in both LSA and FRA as shown in Figure 4.1.

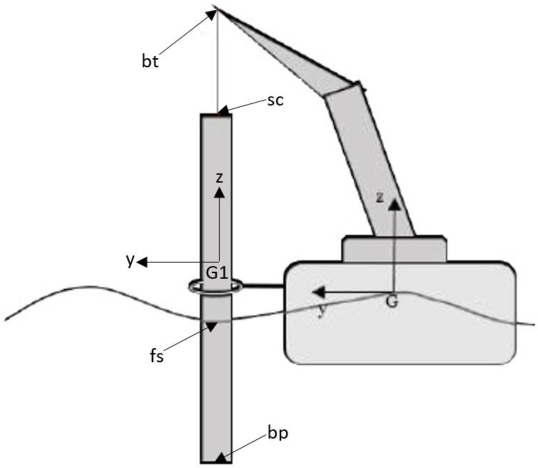

Figure 4.1: General layout

As one can see, there are two sets of axes. Those are the LSA of each component individually. Those axes have the origin at the same point as the COG. Moreover, the reader should have noticed that the FRA is not presented in the above mentioned figure. This is due to the fact that the vessel's axes system is at the same place as the FRA axes initially (for $t = 0$s). Below, the author defines all the important points that are shown in the figure, in LSA and FRA as well.

- COG: It is normally defined as the origin of LSA.

  Position is $CG = \left[x_{cg}, y_{cg}, z_{cg}\right]^T = [0,0,0]^T$ in LSA and $CG = \left[X_{cg}, Y_{cg}, Z_{cg}\right]^T$ in FRA. The initial position in FRA is $[X_0, Y_0, Z_0]^T$.

- Boom Tip (BT): The boom is considered as one part of crane that is mounted on the vessel, but not located in the LSA of MP.

  Position is $bt = \left[x_{bt}, y_{bt}, z_{bt}\right]^T$ in LSA and $BT = [X_{bt}, Y_{bt}, Z_{bt}]^T$in FRA.

- Sling connector (SC): It is located on the top of the MP or lifting tool. The lifting tool is considered to be a part of the MP in the analysis.

  Position is $sc = \left[x_{sc}, y_{sc}, z_{sc}\right]^T$ in LSA, and $SC = [X_{sc}, Y_{sc}, Z_{sc}]^T$ in FRA respectively. This two coordinates follow the relation expressed in Equation 3.7.

- FS point: It is defined as the center of the cross-water surface.

  Position is $fs = [x_{fs}, y_{fs}, z_{fs}]^T$ in LSA and $FS = [X_{fs}, Y_{fs}, Z_{fs}]^T$ in FRA. It changes with the wave propagation and MP motions.

- Bottom point: It is the point at the center of the lower end of the MP.

  Position is $bp = [x_{bp}, y_{bp}, z_{bp}]^T$ in LSA and $BP = [X_{bp}, Y_{bp}, Z_{bp}]^T$ in FRA.

4.2. MONOPILE MODEL

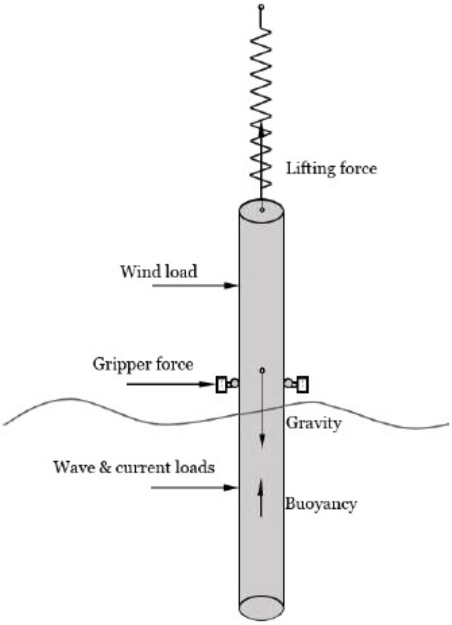

Figure 4.2: Forces acting on MP during lowering operation

As one can see in Figure 4.2, the forces that are considered in this analysis are the hydrodynamic forces (Wave and Current), the wind force, the gravitational and hydrostatic (Buoyancy) forces, the crane's wire lifting force (in this analysis the crane wire is modelled as a spring) and finally the gripper forces (if applicable). In order to construct the EOM for the MP, those forces needs to be defined for the current model. For the reader's convenience, firstly the method that was used to derive the EoM will be discussed in this section.

4.2.1. LAGRANGIAN MECHANICS

Instead of using Newtonian mechanics for the lowering analysis, Lagrangian mechanics will be used for several reasons.

- Firstly, the previous analysis that TWD created was based in Lagrangian mechanics as well and in order to comply with the previous model, those mechanics will be used in the lowering model as well.
- Furthermore, by using Newtonian mechanics, one is nearly bound to use a rectangular coordinate system whereas by using Lagrangian mechanics, the use of a generalized coordinate system is easily accessible. By generalized coordinates the reader should understand that various options exist, such as radial distances or angles.
- In addition, when the Newtonian mechanics are being used, the user should consider all of the constraint forces that exist in the system where by using Lagrangian mechanics most of the time those constraint forces can be avoided.

All of the aforementioned reasons might still not convince the reader about the use of Lagrangian mechanics but as the system gets more complex or tends to be a more realistic version of a physical problem, those advantages become of great importance. Initially, the definition of Lagrangian should be presented. The difference between kinetic and potential energy is named Lagrangian as one can see in Equation 4.1, where T is the kinetic and V the potential energy. The kinetic energy of the system is presented in Equation 4.2, where M is the total mass matrix and v the velocity matrix.

$$L = T - V \tag{4.1}$$

$$T = \frac{1}{2} M v^2 \tag{4.2}$$

The mass matrix is

$$M' = \begin{bmatrix} M & 0 & 0 & 0 & 0 & 0 \\ 0 & M & 0 & 0 & 0 & 0 \\ 0 & 0 & M & 0 & 0 & 0 \\ 0 & 0 & 0 & I_{xx} & 0 & 0 \\ 0 & 0 & 0 & 0 & I_{yy} & 0 \\ 0 & 0 & 0 & 0 & 0 & I_{zz} \end{bmatrix} \tag{4.3}$$

The velocity matrix (from Equation 3.12) is

$$v' = \begin{bmatrix} \dot{X} \\ \dot{Y} \\ \dot{Z} \\ \omega_x \\ \omega_y \\ \omega_z \end{bmatrix} = \begin{bmatrix} \dot{X} \\ \dot{Y} \\ \dot{Z} \\ \dot{\phi} - \sin\theta \cdot \dot{\psi} \\ \cos\phi \cdot \dot{\theta} + \cos\theta \sin\phi \cdot \dot{\psi} \\ -\sin\phi \cdot \dot{\theta} + \cos\theta \cos\phi \cdot \dot{\psi} \end{bmatrix} \tag{4.4}$$

The kinetic energy is

$$T = \frac{1}{2} v'^T \cdot M' v' \tag{4.5}$$

The potential energy consists of two contributions.

- Potential energy due to weight: $V_1 = MgZ_{cg}$
- Potential energy due to spring (crane wire): $V_2 = \frac{1}{2}\kappa_{cr}\Delta L_{wr}^2$

$$\Delta L_{wr} = L'_{wr} - L_{wr}$$

$$L'_{wr} = \sqrt{(X_{sc} - X_{bt})^2 + (Y_{sc} - Y_{bt})^2 + (Z_{sc} - Z_{bt})^2}$$

where k_{cr} is the crane stiffness, and ΔL_{wr} is the elongation of the crane wire. The crane stiffness can be calculated according to the following equation:

$$\frac{1}{k_{cr}} = \frac{l}{EA} + \frac{1}{k_0} \tag{4.6}$$

Where, E is Young's modulus, A is the cross-sectional area of the wire rope, $\frac{1}{k_0}$ is the crane flexibility and l is the total rope length. The empirical formula to estimate the crane stiffness is $k_0 = SWL \cdot 32.5 \left(\frac{kN}{m}\right)$ and $SWL(t)$ is the safe working load. Thus, the total potential energy is

$$V = MgZ_{cg} + \frac{1}{2}\kappa_{cr}\Delta L_{wr}^2 \tag{4.7}$$

Hence, the Euler-Lagrange equation that produces the system's EoM is presented in Equation 4.8, where $q, \dot{q}$ are the displacements and velocities respectively, F^{nc} are the non-conservative forces acting on the system and j is the examined degree of freedom $(j = X, Y, Z, \phi, \theta, \psi)$.

$$\frac{d}{dt}\left(\frac{\partial L}{\partial \dot{q}_j}\right) - \frac{\partial L}{\partial q_j} = F^{nc} \tag{4.8}$$

$$\frac{d}{dt}\left(\frac{\partial T}{\partial \dot{q}_j}\right) - \frac{\partial T}{\partial q_j} - \frac{d}{dt}\left(\frac{\partial V}{\partial \dot{q}_j}\right) + \frac{\partial V}{\partial q_j} = F^{nc} \tag{4.9}$$

4.2.2. MONOPILE'S EQUATIONS OF MOTION

By integrating all the above mentioned components in the Euler-Lagrange equation, the resulted EoM for the six degrees of freedom are derived and presented in Equation 4.10, where M is the newly derived mass matrix from Equation 4.5 and F^c are the conservative forces.

$$M\ddot{q} = F^c + F^{nc} \tag{4.10}$$

$$M = \begin{bmatrix} M & 0 & 0 & 0 & 0 & 0 \\ 0 & M & 0 & 0 & 0 & 0 \\ 0 & 0 & M & 0 & 0 & 0 \\ 0 & 0 & 0 & I_{xx} & 0 & -\sin\theta \cdot I_{xx} \\ 0 & 0 & 0 & 0 & \cos^2\phi \cdot I_{yy} + \sin^2\phi \cdot I_{zz} & \cos\theta \sin\phi \cos\phi \cdot (I_{yy} - I_{zz}) \\ 0 & 0 & 0 & -\sin\theta \cdot I_{xx} & \cos\theta \sin\phi \cos\phi \cdot (I_{yy} - I_{zz}) & \sin^2\theta \cdot I_{xx} + \cos^2\theta \sin^2\phi \cdot I_{yy} + \cos^2\theta \cos^2\phi \cdot I_{zz} \end{bmatrix} \tag{4.11}$$

Acceleration matrix is

$$\ddot{q} = [\ddot{X}, \ddot{Y}, \ddot{Z}, \ddot{\phi}, \ddot{\theta}, \ddot{\psi}]^T \tag{4.12}$$

Conservative forces are

$$F^c = F^{gravity} + F^{spring} \tag{4.13}$$

Finally, non-conservative forces are

4

$$F^{nc} = F^{buoyancy} + F^{hydro} + F^{wind} + F^{gripper} \tag{4.14}$$

4.2.3. FORCES DERIVATION

4.2.3.1. CONSERVATIVE FORCES

- **Gravity forces** are

$$F^{gravity} = [0, 0, Mg, 0, 0, 0]^T \tag{4.15}$$

- **Spring forces** are

$$F^{cr} = \left[F_x^{cr}, F_y^{cr}, F_z^{cr}, \left[F_x^{cr}, F_y^{cr}, F_z^{cr}\right] \cdot \frac{\partial R \cdot sc}{\partial \phi}, \left[F_x^{cr}, F_y^{cr}, F_z^{cr}\right] \cdot \frac{\partial R \cdot sc}{\partial \theta}, \left[F_x^{cr}, F_y^{cr}, F_z^{cr}\right] \cdot \frac{\partial R \cdot sc}{\partial \psi}\right]^T \tag{4.16}$$

where $\left[F_x^{cr}, F_y^{cr}, F_z^{cr}\right] = \left[-k_{cr}\Delta_{wr} \cdot \frac{X_{sc} - X_{bt}}{L'_{wr}}, -k_{cr}\Delta_{wr} \cdot \frac{Y_{sc} - Y_{bt}}{L'_{wr}}, -k_{cr}\Delta_{wr} \cdot \frac{Z_{sc} - Z_{bt}}{L'_{wr}}\right]$

4.2.3.2. NON-CONSERVATIVE FORCES

Hydrostatic force

The buoyancy force is a dynamic term since the submerged level varies through time and wave fluctuations as one can see in Equation 4.17. Meanwhile, in Equation 4.18, one can see the formula to evaluate the area that is to be taken in consideration when buoyancy force is calculated. Where, ρ_w is the water density, A_{cs} the cross sectional area, L_{sub} the submerged length of the MP, D_o, D_i the outer and inner diameter of the MP respectively and t the MP thickness.

$$F_z^{bu} = \rho_w g \nabla = \rho_w g A_{cs} L_{sub} \tag{4.17}$$

$$A_{cs} = \frac{1}{4}\pi(D_o^2 - D_i^2) = \frac{1}{4}\pi\left(D_o^2 - (D_o - 2t)^2\right) \tag{4.18}$$

Center of buoyancy is $cob = \left[x_{cb}, y_{cb}, z_{cb}\right]^T$. Then buoyancy matrix (forces and moments) is,

$$F^{bu} = \left[0, 0, F_z^{bu}, [0, 0, F_z^{bu}] \cdot \frac{\partial R \cdot cob}{\partial \phi}, [0, 0, F_z^{bu}] \cdot \frac{\partial R \cdot cob}{\partial \theta}, [0, 0, F_z^{bu}] \cdot \frac{\partial R \cdot cob}{\partial \psi}\right]^T \tag{4.19}$$

Hydrodynamic forces

In order to evaluate the hydrodynamic forces that act on a slender structure such as the MP, a division of the MP in small strips is necessary, allowing the user to evaluate the forces that act on each strip and eventually to sum up the numerous strips to estimate the total hydrodynamic force that acts on the MP. That force that is applicable on each strip can be decomposed to the following,

- Normal force
- Lift force
- Tangential force

and those force components can be visualized in Figure 4.3 where α is the angle of attack, V the water particles velocity, f_N the normal force, f_T the tangential force and f_L the lift force. The lift force is mainly due to the unsymmetrical cross-sectional, wake effect and vortex shedding, thus neglected in this analysis.

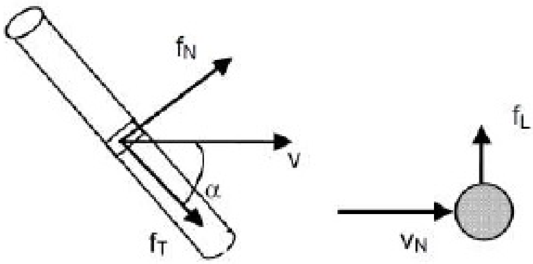

Figure 4.3: Force components acting on a strip of the MP

If the structure is small enough to allow the wave particles to move without disturbance, then the Morison's load formula can be used to evaluate the forces acting on the MP. This load formula is suitable to evaluate a drag and inertia force component of the hydrodynamic force. In the current simulation analysis the hydrodynamic forces are due to waves and current. Thus, the individual velocities for the water particles due to waves and current have to be evaluated-and this is achieved from Equations 3.28 through 3.31 for wave velocities and accelerations and Equation 3.16 for current velocity-and in extension to sum those components up whilst their direction (heading) is the same for both environmental conditions.

- **Normal Force**

The normal force can be decomposed to a force acting on the strip while the MP is fixed and the environmental conditions are varying and a part that the water is still and the MP is moving. Those components are integrated together in Equation 4.20.

$$f_N = f_{inertia} + f_{drag} = -\rho_w C_{An} A_{ocs} \ddot{r}_n + \rho_w (1 + C_{An}) A_{ocs} \dot{v}_n + \frac{1}{2} \rho_w C_{Dn} D_o v_{rn} |v_{rn}| \tag{4.20}$$

Where ρ_w is the water density, C_{An} is the added mass coefficient, A_{ocs} is the outer cross-sectional area, $\ddot{r}_n$ is the acceleration on the contact point of MP normal to axis, $\dot{v}_n$ is the fluid particle acceleration vector, C_{Dn} is the drag coefficient, D_o is the MP diameter and v_{rn} is the relative velocity vector which is the difference between the MP's and water velocity.

4

In order to have a correct force value, one should consider the fluctuation in fluid particle velocities and the MP motions. Hence, Equation 4.21 takes into consideration the before mentioned, where z_{fs}, z_{bp} are the local z-coordinates of FS and BT respectively, $i - N$ denotes each individual strip and δz the unit length of the strip.

$$F_N = \int_{z_{bp}}^{z_{fs}} -\rho_w C_{An} A_{ocs} \ddot{r}_n dz + \sum_{i}^{N} \left(\rho_w (1 + C_{An}) A \dot{v}_{n_i} + \frac{1}{2} \rho_w C_{Dn} D_o v_{rn_i} |v_{rn_i}| \right) \delta z \tag{4.21}$$

- **Tangential force**

According to regulations, the tangential force in a cylinder is small in comparison with the normal force since it is mainly caused by skin friction. Although, when it comes to slender cylinders with a significant length and relative tangential velocity, the tangential force cannot be discarded. The tangential force for a unit strip of the structure is depicted in Equation 4.22, where C_{D_t} is the tangential drag coefficient and v_r the magnitude of the relative velocity.

$$f_r = \frac{1}{2} \rho_w C_{D_t} D_o v_r^2 \tag{4.22}$$

The tangential drag coefficient can also be noted as $C_{D_t} = \pi C_{D_f} \cos(\alpha)$, where C_{Df} is the skin friction coefficient and $C_{Df} = 0.016$ is set as a default value. The tangential force can be simplified as the form which is proportional to the square of the tangential relative velocity $v_{rt} = v_r \cos(\alpha)$. The Equation 4.23 shows the final formula to identify the tangential for for the MP.

$$F_T = \int_{z_{bp}}^{z_{fs}} \frac{1}{2}\rho_w C_{Df}\pi D_o v_{rt}|v_{rt}|dz = \sum_i^N \frac{1}{2}\rho_w C_{Df}\pi D_o v_{rt_i}|v_{rt_i}|\delta z \tag{4.23}$$

Thus, the total forces and moments that are evaluated at each step of the simulation are presented below, where $v_{rni} = \sqrt{v_{rxi}^2 + v_{ryi}^2}$, $v_{rti} = v_{rzi}$.

$$\begin{aligned}
F_{Nx} =& \int_{z_{bp}}^{z_{fs}} -\rho_w C_A A_{ocs}\ddot{r}_x dz + \sum_i^N \left(\rho_w(1+C_A)A\dot{v}_{xi} + \frac{1}{2}\rho_w C_D D_o v_{rxi}|v_{rni}|\right)\delta z \\
F_{Ny} =& \int_{z_{bp}}^{z_{fs}} -\rho_w C_A A_{ocs}\ddot{r}_y dz + \sum_i^N \left(\rho_w(1+C_A)A\dot{v}_{yi} + \frac{1}{2}\rho_w C_D D_o v_{ryi}|v_{rni}|\right)\delta z \\
F_{Nz} =& \sum_i^N \frac{1}{2}\rho_w C_{Df}\pi D_o v_{rti}|v_{rti}|\delta z \\
M_{Nx} =& \int_{z_{bp}}^{z_{fs}} \rho_w C_A A_{ocs}\ddot{r}_y \cdot z dz + \sum_i^N -\left(\rho_w(1+C_A)A\dot{v}_{yi} + \frac{1}{2}\rho_w C_D D_o v_{ryi}|v_{rni}|\right)\cdot z\delta z \\
M_{Ny} =& \int_{z_{bp}}^{z_{fs}} -\rho_w C_A A_{ocs}\ddot{r}_x \cdot z dz + \sum_i^N \left(\rho_w(1+C_A)A\dot{v}_{xi} + \frac{1}{2}\rho_w C_D D_o v_{rxi}|v_{rni}|\right)\cdot z\delta z \\
M_{Nz} =& 0
\end{aligned} \tag{4.24}$$

Wind force

The same load formula that was used for Morison's drag force will be used for the wind force as well and it is depicted in Equation 4.25. Where, ρ_a is the air density, C_{Dw} is the wind drag coefficient, and v_{rn}^{wind} is the relative velocity between MP and wind. The wind drag coefficient C_{Dw} is affected by the effective shape coefficient C_e.

$$F_N^{wind} = \int_{z_{fs}}^{z_{sc}} \frac{1}{2}\rho_a C_{Dw} D_o v_{rn}^{wind}|v_{rn}^{wind}|dz = \sum_i^N \left(\frac{1}{2}\rho_a C_{Dw} D_o v_{rn_i}^{wind}|v_{rn_i}^{wind}|\right)\delta z \tag{4.25}$$

4.2.4. MONOPILE SIMULATION

In this section, the model that was created with the use of Matlab Simulink will be presented. Furthermore, results regarding displacements, forces and moments will be shown and analyzed. The author needs to explain the process that was followed in order to construct the full model. Since the procedure is not straightforward such as to include all the parts that are involved, at a first stage the MP is modeled as a free hanging body from the crane's BT which is introduced at first as a fixed point in the system. A part of the MP is already submerged in water (approximately 5 meters). The initial simulation was based on a quasi-static analysis, meaning that the MP is not lowered at all through the water but remains at the same level instead, to be subjected to the forces involved.

In addition, once the initial phase of the model that was described before is evaluated and verified, the author continued with adding a dynamically moving crane BT point in the model. By using a HLV's motion RAO, the time history of COG motions is derived and by using the position transformations that were explained in chapter 3, the motions for the crane BT is derived assuming a fixed crane (connection between vessel and crane BT). Thus, simulations and verification takes place for that model as well.

Once the model is verified, the entire process becomes dynamic. The MP is dynamically lowered through the water, increasing in such way the submerged level. By taking into consideration various lowering speeds that were provided from the company (based on actual crane winch speeds), the model is created in such way that the user can choose what lowering speed to use in a particular simulation.

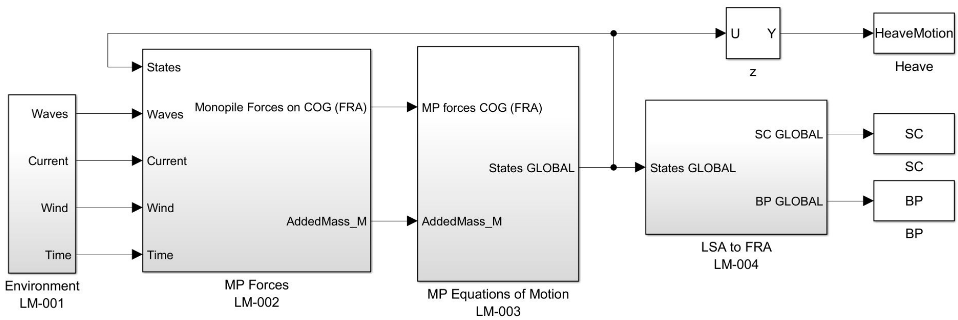

Figure 4.4: MP model overview

Firstly, the MP model overview is presented in Figure 4.4 that is the initial phase of modeling. To begin with, the environment conditions are introduced in the model, including the generated random sea state, the current and wind parameters. Those inputs are used to generate the random environment that the MP will be subjected to.

The block LM-002 includes all the forces that are taken into consideration in the current analysis and that block can be visualized in Figure 4.5. The inputs for this block are the instant positions and velocities of the MP, the environmental conditions and the running time of the simulation. The outputs are the MP forces calculated in FRA and the added mass matrix.

One can distinguish three different block types in the MP forces block. The sub-block LM-002-1 includes the distinguish between static or dynamic simulation analysis that the user prefers to establish. The sub-block LM-002-2 is set up in such way in order to allow the user to switch between a fixed or a moving crane BT for different simulations. The sub-blocks LM-002-3 up to LM-002-9 are created to evaluate the forces that act on the MP at the very instant of the simulation.

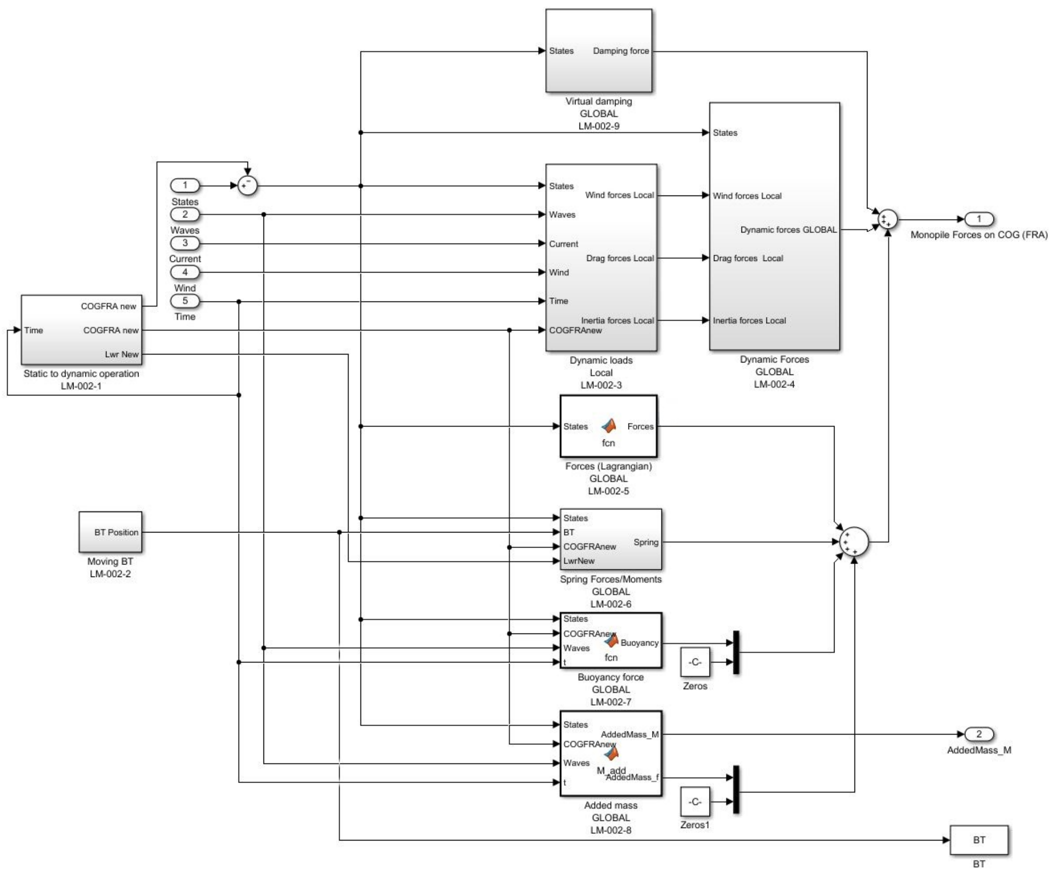

Figure 4.5: MP forces simulation block

Following, in the block LM-003 that is depicted in Figure 4.6, the motions are derived. The inputs to this block are the outputs of MP forces block (global forces acting at the COG and added mass matrix). After the total mass matrix is evaluated, a simple matrix derivation takes place and provides the velocities and accelerations of the MP. By integrating those values, the positions and velocities are derived and are used as the output of that block.

The last block of the MP model is the LM-004 that is used to translate the positions and velocities from global axes to local and vice versa based on what the user requires to derive. This block is depicted in Figure 4.7 and the purpose of its presence in this report is to aid the reader to understand and comprehend the theory of axes transformation that was discussed in chapter 3.

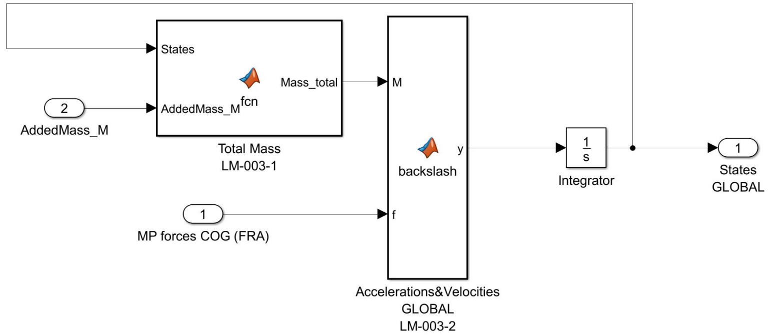

Figure 4.6: Equations of motion block

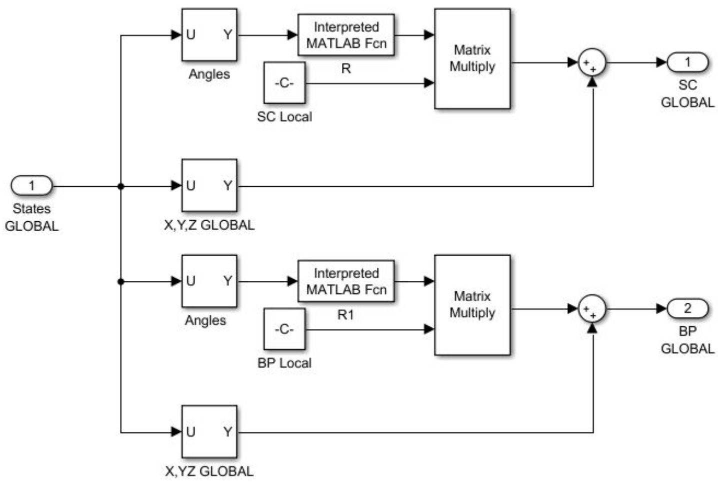

Figure 4.7: Translations transformations from local to global axes

4.2.5. MODEL PARAMETERS

In this subsection, some of the main parameters that were used for the MP modeling will be presented. Firstly, in Table 4.1 one can see the coordinates of the BT of the crane in FRA as well as the initial length and stiffness of the cable.

Variable	Value	Units
$\mathbf{X_{pos}}$	11.4	m
$\mathbf{Y_{pos}}$	-28	m
$\mathbf{Z_{pos}}$	100	m
Wire's Initial Length	41.6	m
Wire's stiffness	20000	kN/m

Table 4.1: Crane variables

Following, the MP parameters are depicted below. One comment that has to be made is regarding the parameter of Initial Submerged Length of the MP. As it was discussed in a previous chapter, the MP installation process is divided in several phases. The one preceding the lowering phase that is examined in this thesis, is the upending phase of the MP in a vertical position. Here, the assumption is made that when the lowering phase begins, the MP is already submerged in some level as a result of the previous phase (upending). In this case, the submerged length is set as $5m$ below sea water level. All of the MP parameters can be seen in Table 4.2.

Parameter	Value	Units
Diameter	8.5	m
Length	68.4	m
Thickness	0.066	m
Mass	1057	t
Lifting Tool Mass	84.56	t
Initial Submerged Length	5	m
$\mathbf{I_{xx}}$	527190	$t.m^2$
$\mathbf{I_{yy}}$	527190	$t.m^2$
$\mathbf{I_{zz}}$	18798	$t.m^2$

Table 4.2: Monopile Parameters

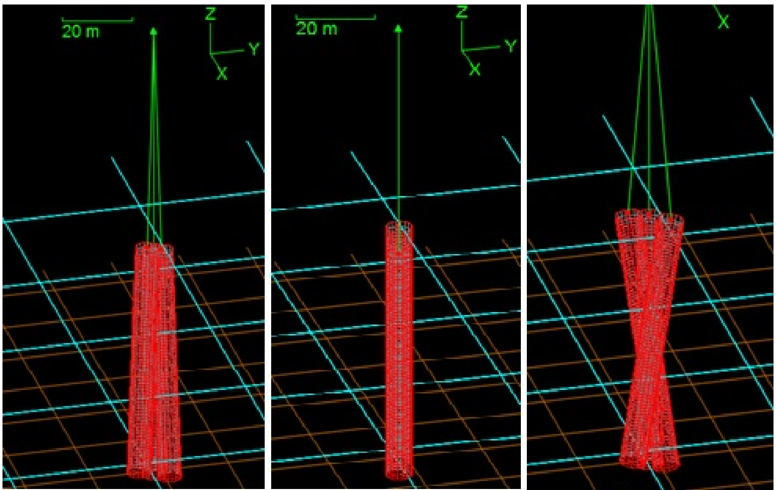

Mode 1
Surge&Sway

Mode 2
Heave

Mode 3
Roll&Pitch

Figure 4.8: Different modes of free-hanging monopile

After the model is created, the need to examine at what submerged level the highest motions and forces rise. By identifying that submerged level of the MP (critical depth), the author will be able to check if at that level the forces and motions are acceptable based on the existing limitations and tolerances. If the answer is that both the forces and motions are within acceptable tolerances, then any other submerged level will be acceptable as well since at the critical depth the highest loads and motions exist. In order to identify the critical depth, firstly the natural frequencies and periods have to calculated. Based on those parameters, the most critical mode of the MP will be derived. Eventually, various simulations will take place for different submerged levels and the critical mode will be examined. The submerged level that produces the biggest critical mode motions is the critical depth of the MP.

Parameter	Surge	Sway	Heave	Roll	Pitch
Natural Period [sec]	17.236	17.236	2.067	4.708	4.708
Natural Frequency [rad/sec]	0.365	0.365	3.040	1.335	1.335

Table 4.3: Eigenfrequencies and Eigenperiods of free hanging monopile

The natural frequencies and periods are calculated and presented in Table 4.3 for all the degrees of freedom that are examined. The different modes of the free hanging MP can be visualized in Figure 4.8. The wave period is closest to the roll and pitch natural period of the MP, thus those two degrees of freedom will be examined for different submerged levels of the MP.

5

Vessel model and Dynamic Positioning

Study hard what interests you the most
in the most undisciplined, irreverent
and original manner possible.

Richard Feynman

This chapter initially illustrates the vessel model that was included in the research that the company provided. Since the vessel model is considered as a black box for the author, a brief explanation will be presented for the reader in order to understand the purpose that it has in the complete model and to introduce the inputs/ outputs of it. Furthermore, the DP that was created for the vessel in order to hold the required position and heading is explained in this chapter.

5.1. VESSEL CONVENTIONS

The first step to introduce the vessel model is to make the reader aware of the conventions that were used for this section. As it was stated in a previous chapter, since different sections are involved (MP, vessel, Global Reference, Gripper), a distinction between the vessel's local axes and FRA is made. As one can visualize in Figure 5.1, the LSA that is vessel bound is placed at the vessel's COG and the orientation of the axes initially parallel to the FRA.

In addition, as was stated in a previous chapter, a convention for the states takes place. The states with capital letters refers to vessel's states represented in the FRA $[X_v, Y_v, Z_v, \Phi_v, \Theta_v, \Psi_v]$, where the subscript v is used for referencing vessel motions since the same convention is used for MP motions.

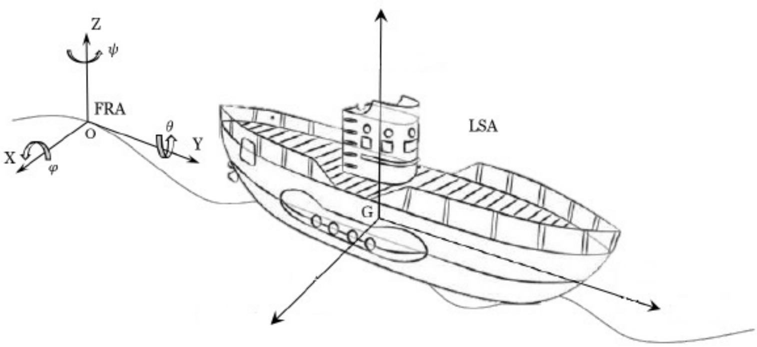

Figure 5.1: Vessel Conventions

Furthermore, in Figure 5.2 the vessel motions are presented to the reader. The vessel has six degrees of freedom and the convention for naming as well as positive/ negative directions are given in the list below:

- **Surge (x):** Positive direction towards the bow.
- **Sway (y):** Positive direction towards portside.
- **Heave (z):** Positive direction upwards.
- **Roll (ϕ):** Positive direction with starboard side down.
- **Pitch (θ):** Positive direction with bow side down.
- **Yaw (ψ):** Positive direction with bow rotating towards portside.

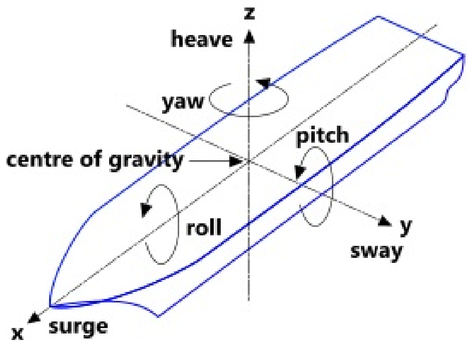

Figure 5.2: Motion conventions

5.2. VESSEL MODEL

5

In order to create the vessel model, the first step is to consider Newton's 2^{nd} law as can be visualized in Equation 5.1. Since a complex model is required in order to match reality as much as possible, all the phenomena that take place in the problem will be decomposed to simpler problems. Each of those problems will be explained and analyzed further below. The decoupling will be based on waves and motions. After the analysis of each mode, the different concepts are superposed to create the final vessel's EoM. The different modes that will be analysed are presented in Table 5.1.

$$m\ddot{x} = \sum F \tag{5.1}$$

Mode	Waves	Motions
M1	NO	NO
M2	NO	YES
M3	YES	NO
Superposition	YES	YES

Table 5.1: Modes decomposition

From the above mentioned decomposition of different modes, the right hand side of Equation 5.1 will be evaluated. In other words, the forces that are exerted on the vessel will be determined. In Figure 5.3 one can see the superposition of the different modes. This figure illustrates firstly the wave motions while the structure is still and the second part is the opposite, the structure is moving while the surrounding fluid is still.
To begin with, mode M1 will be analysed. This mode implies that neither the waves nor the resulting vessel motions are considered. Thus, since the vessel is just floating in water the following forces are experienced (considering the z axis or heave motion):

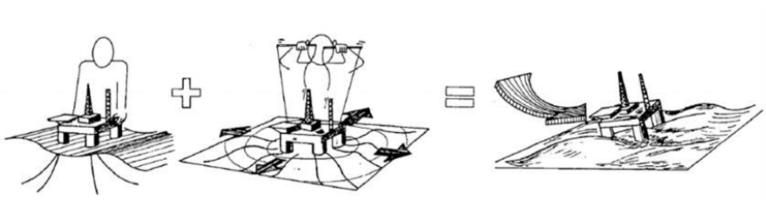

Figure 5.3: Wave loads superposition Journèe and Massie [2001]

- Gravitation force: $-mg$
- Buoyancy force: $\rho g \nabla$,where$\nabla$is the dispaced volume of the vessel

Those forces that are exerted on the vessel, cancel out by Archimides'law of course and hence the total force of M1 is zero. Furthermore, mode M2 will be considered. This mode suggests to consider only the motions from waves but not the waves themselves. Those forces are:

5

- The hydrostatic reaction force, which is the force that the vessel feels when it is moving with an infinitely low speed and can be depicted in Equation 5.2.

$$F_s = -c \cdot x \quad \text{,where } c \text{ is the restoring matrix that contains the coefficients for all vessel motions} \tag{5.2}$$

- Hydrodynamic reaction force which is the force acting as a "correction" for the previous force since the motion is not infinite slow. It is called radiation force and can be visualized in Equation 5.3, where α is the added mass matrix, b is the damping matrix for all motions and $\dot{x}, \ddot{x}$ the velocity and acceleration matrix which includes all motions.

$$F_r = -\alpha \cdot \ddot{x} - b \cdot \dot{x} \tag{5.3}$$

Finally, mode M3 is presented which suggests that the forces that the vessel experiences from regular waves are considered and ignore the vessel's motions. This force is called wave exciting force and its components are analysed below:

- Froude-Krilov (F_w) force which is the force that the vessel feels due to the pressure of water and it is not affected from the presence of the vessel.
- Diffraction force (F_d) which is again a "correction" on the previous force since the fluid is actually disturbed from the vessel.

Hence, by substituting all of the above mentioned forces in Newton's 2^{nd} law which is depicted in Equation 5.1, the derivation of vessel's equation of motion is achieved and it is depicted in Equation 5.4.

$$(M+\alpha)\cdot\ddot{x}+b\cdot\dot{x}+c\cdot x=F_w+F_d \tag{5.4}$$

When the forces and EOM were theoretically derived, a practical simulation took place using MATLAB/Simulink software. As one can visualize in Figure 5.4, the first block (far left) is created to generated the vessel forces based on states, environmental conditions and vessel properties. In addition, forces and moment from the DP model are driven as input to this sub-block in order to derive the total forces and moment that act on the vessel at all the different process times that the simulation is executed.

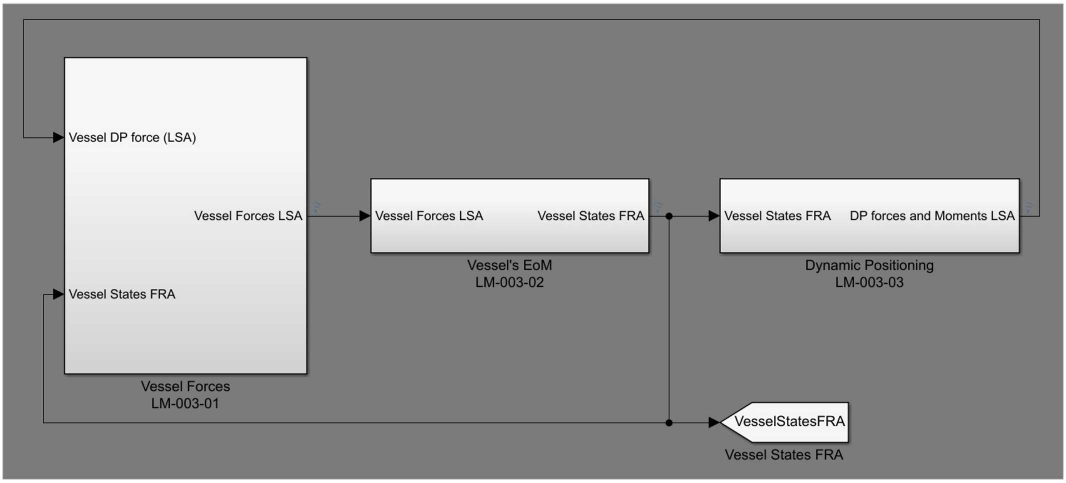

Figure 5.4: Vessel model generated in MATLAB/Simulink

The forces that are calculated from the above mentioned sub-block are used as input to the "Vessel's EoM" sub-block (presented in the middle of Figure 5.4) that holds the instantaneous mass and added-mass matrices and from that sub-block the states (velocities and positions) in all degrees of freedom are derived.
In addition, the far right sub-block in the aforementioned Figure, depicts the DP model that will be further elaborated in the following section of this chapter.

5.3. DYNAMIC POSITIONING

As it was discussed in the first steps of the thesis, there is a need to switch from JUB to floating vessel for installing an OWT for numerous reasons. In order to achieve this alteration in the process, the vessel requires DP to maintain the requested position and orientation throughout the operation. This section will introduce the DP that floating vessel requires in order to successfully perform the MP installation process. Many definitions are given through the years for DP and all of them fluctuate around the same meaning. The author deemed the International Maritime Organization (IMO) definition as the most proper one to describe its application and it is presented below.

"Dynamically positioned vessel (DP vessel) means a unit or a vessel which automatically maintains its position (fixed location or predetermined track) exclusively by means of thruster force."

5.3.1. PURPOSE OF DP

It is well established that throughout the years, technology evolved dramatically. Marine and offshore activities dates back to the decade of 20's where the first steps to offshore drilling were executed. As those activities were performed in very shallow waters near shore, the need for a solution such as DP was not yet developed. This was not always the case though, since the development and technology paced in very fast rate. During the decade of 40's the first drilling platforms that could operate in depths of lower than 10 meters were constructed.

Figure 5.5: Dynamic Positioning applications

Of course, the solutions for such operation profiles (regarding allowable depth) were quickly saturated since the demand for operating in higher depths was essential. This is the reason that in the decade of 50's, the first Jack-Up Rigs were created. Although nowadays such barges can operate normally in water depths up to 120 meters, the need for a solution that could be more efficient, operate in higher depth and be more cost effective was established. Then the concept of DP was formed. The first DP vessel dates back to 1961 (Eureka vessel) and since then tremendous steps in the DP sector were achieved, making the concept more attractive when it can be considered as an alternative for the operation's convenience. In Figure 5.5, one can visualize some of the applications that DP is need for.

5.3.2. ANALYSIS OF DP SYSTEM

In the following subsection, a detailed explanation will take place regarding the complete control system and in a later stage the blocks will be extensively analysed based on alternative principles that can be used, different possibilities and introduce the ones that were used in this research and modeling. With the aid of DP, the vessel's operator can control surge, sway and yaw (horizontal plane) allowing in such way to perform offshore activities that in any other way (besides mooring) would be very difficult to achieve.

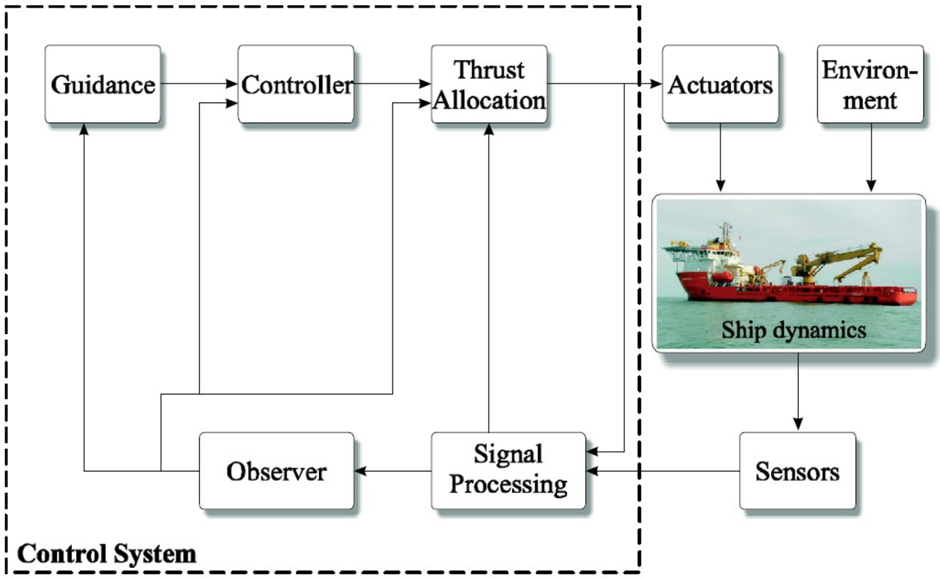

Figure 5.6: Overview of a control system build for vessels

As one can see from Figure 5.6, many parts come together in the overall control strategy. The ship experiences some forces and moment from the environment, such as waves, current and wind, that cause changes to the vessel states, most importantly translations, rotations, velocities and accelerations. Through sensors, numerous parameters are measured in order to convert and track the necessary states. The measured signals subsequently are fed in the signal processing operation that filters, observes and predicts the actual controlled states.
Through the user (operator), a requested position and heading is given to the system. The difference between the requested state and the observed one is used as an input to the controllers that will determine the magnitude of forces and moment that are needed in order to achieve the requested position and orientation. That magnitude is sequentially fed to the thrust allocation process that will determine how to distribute that signal to the individual thrusters and propellers. The outcome of thrust allocation then becomes the command for the actuators that will provide the required thrust to achieve the requested placement of the vessel.

5.3.3. REFERENCE SYSTEMS AND SENSORS

In order to maintain the position and orientation of a vessel, the different controlled states need to be measured. Those measurements come from the various position and heading reference systems that are installed on a vessel. Numerous systems exist that can aid the process of measuring the position and orientation and a list of the most used in vessels installed with DP system is presented below.

1. **Global Positioning System (GPS)**: The most common position reference system integrated in vessels is the GPS. This system in principle uses a quite complex technology to determine the position but the concept that it uses is simple. The GPS receiver that is installed on the vessel requests a signal from numerous satellites (normally 4). The satellites will send a signal at the exact same time all together (GPS satellites have an atomic clock since high precision and satellite interaction is necessary) to the GPS receiver. Then the GPS receiver knowing the exact time that the signal was transmitted from each satellite, it can measure the time that was required for the signal to reach the destination.

   The receiver also knows the exact position of each satellite at the time that the signal was sent and from there on its position is calculated. Of course though, the measurements might have errors caused by several factors and this is the reason that the Differential GPS (DGPS) is used in most cases. This system uses an extra base receiver to enhance its accuracy and provide better results to the DGPS receiver that is installed on board.

2. **Acoustic reference systems:** Such systems require both transponders and transducers to operate. The transducer is placed in the hull of the vessel and on the other hand the transponder is placed on the seabed. When the vessel needs to identify its location, a signal is sent from the transducer to the transponder which then it is triggered to reply. The overall time required is noted and by knowing the sound velocity in water, the distance can be determined.

3. **Other systems:** Numerous options exist to identify the position of the vessel such as inertial navigation, laser and radar systems but also different systems can be deployed in order to evaluate the vessel's heading. Most commonly used systems for heading reference are the gyroscopes that that actually used in the inertial navigation systems that can find the vessel's motions on all degrees of freedom with the aid of accelerometers.

5.3.4. Signal processing

As it was stated in the previous subsection, the measurements from the Position reference systems will have a noise. This noise can either be very big or significantly small in comparison with the system's accuracy and based on the sensor(s) that performed the measuring. Various ways exist that could aid the process of filtering the noise as well as the vessel's unwanted motions. The vessel's motions can be categorized in two parts, the Low Frequency (LF) motions that are due to wind, current and non-linear wave forces, and the Wave Frequency (WF) or High Frequency (HF) motions that are due to oscillatory wave components.

When considering DP, only the LF motions and forces are of interest since the effect of linear wave forces in sea states up to medium intensity is considerably small. Furthermore, in order to achieve normal operational conditions, power consumption and to avoid excessive wear of the actuators, it is strongly advised to compensate and control only the LF motions and not to react for each wave that reaches the vessel.

In Figure 5.7, one can see the differences between LF and WF motions as well as the total motions of those components. In order to filter the WF from the complete motions, three main filters are considered. Low pass and notch filters are two options for filtering, with quite simple implementation procedure but a significant problem is introduced in the system with the use of those filters, phase lag. The introduced phase lag results to high inaccuracies when relatively big systems and high gain controls are involved.

A good way to overcome this problem, is with an observer that can separate the WF motions from the LF ones. A Kalman filter though, not only operates as a LF filter. As it was mentioned before, significant noise disturbances occur in the sensor measurements. Kalman filter is also used to filter out those noises, predict and estimate the vessel's position and velocity based on previous measurements and the hydrodynamic model of the vessel.

Furthermore, the Kalman filter can be used for situations which the measurements are unavailable for a limited period of time. Such situations are described as dead reckoning and those instances might have a small effect or devastating impact depending on the operation, the magnitude of the problem and the DP class. Since Kalman filter is of great importance in a vessel's DP operation, an extensive analysis of its function will take place in the following pages.

5.3.5. Kalman filter

In order to design and tune a Kalman filter, the mathematical model of the vessel that hold LF and WF motions is needed. Initially the LF control plant will be introduced, followed by the bias model and finally the WF model. By doing so, the complete motions

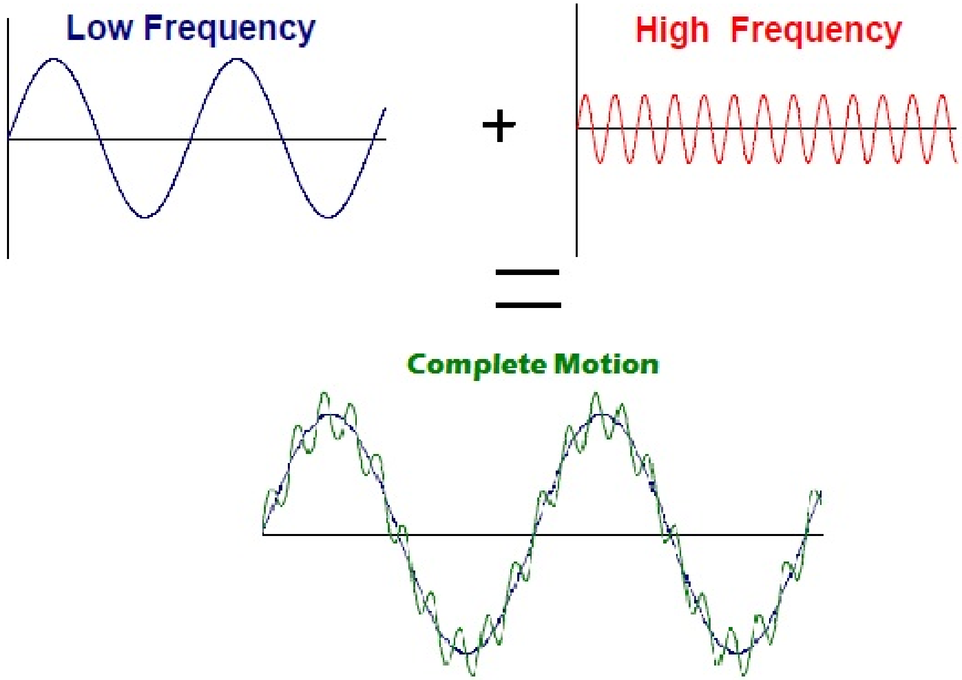

Figure 5.7: Low and high frequency components of vessel's motions

that are derived from the simulation can be categorized with the use of the Kalman filter, keep the ones that are of interest, predict and correct the motions and then compensate respectively based on the controllers that are used for DP.
As it was stated before, the controlled degrees of freedom with the use of DP are the horizontal plane ones (surge, sway and yaw). A note needs to be made now, that the position (x,y) and heading (ψ) that constitute the generalized position $\eta = [X, Y, \Psi]^T$ are referred to FRA, whilst $v = [\dot{x}_l, \dot{y}_l, \dot{\psi}_l]^T$ are the vessel's velocities in LSA. Thus,

$$\dot{\eta} = R(\psi)v \tag{5.5}$$

where $R(\psi)$ is the rotation matrix that was described in a previous chapter but for the reader's convenience, it is presented here once more.

$$R(\psi) = \begin{bmatrix} \cos(\psi) & -\sin(\psi) & 0 \\ \sin(\psi) & \cos(\psi) & 0 \\ 0 & 0 & 1 \end{bmatrix}$$

One can see that $R^T(\psi) = R^{-1}(\psi)$. The non-linear kinetic EOM can be described by

$$M\dot{v} + Dv + R^T(\psi)G\eta = \tau + R^T(\psi)b \tag{5.6}$$

where M is the mass matrix for surge, sway and yaw, M_v the vessel's mass, α the respective added mass for each degree of freedom and I_{zz} the moment of inertia about z-axis.

$$M = \begin{bmatrix} M_v + a_x & 0 & 0 \\ 0 & M_v + a_y & a_{y,\psi} \\ 0 & a_{\psi,y} & I_{zz} + a_\psi \end{bmatrix} \tag{5.7}$$

The damping matrix D is the summation of two parts, the skew symmetric Coriolis-centripetal matrix and the non-linear damping matrix that is defined as $D(v) = D_L + D_N(v)$. The first part can be ignored from the control design since the vessel's velocities are very small when DP is active. Regarding the second part of the damping matrix, that is build up from a linear (D_L) part and a non-linear ($D_N(v)$) part, it is proven that in low speed operations, the linear term of the matrix is the dominating, thus only that part will be considered.

$$D = \begin{bmatrix} b_x & 0 & 0 \\ 0 & b_y & 0 \\ 0 & 0 & b_\psi \end{bmatrix} \tag{5.8}$$

Where b is the linear damping terms for each degree of freedom. The stiffness matrix G is equal to zero, $G = 0_{3\times3}$, since no mooring exists in a vessel operating with DP. The vector τ is the control input of the system, $\tau = [\tau_x, \tau_y, \tau_\psi]^T$. Finally, b is the bias vector that will be discussed in the following section and $b \in \mathbb{R}^3$.
In a dynamic system that operates in the real world and not in an ideal environment, disturbances will always be present. Such disturbances in a vessel that operates with the use of DP can be categorized as second order LF disturbances and first order WF disturbances. The first category or bias model, can be described by the first order Markov process and it is shown in Equation 5.9

$$\dot{b} = -T_b^{-1} b + E_b w_b \tag{5.9}$$

where $b \in \mathbb{R}^{3\times1}$ is the vector of bias forces and moment, $T_b \in \mathbb{R}^{3\times3}$ a diagonal matrix of positive bias time constants, $E_b \in \mathbb{R}^{e\times3}$ a diagonal matrix scaling the amplitude of the noise and $w_b \in \mathbb{R}^{3\times1}$ is a zero-mean Gaussian white noise vector.
On the other hand, a model for the first order wave-induced WF disturbances is needed in order to complete the motions of the vessel as well as the disturbances acting on the total system. That model derived in frequency domain is given by the following equation for each direction (surge, sway and yaw).

$$\xi_{(s)} = \frac{\sigma_i s}{s^2 + 2\zeta_i \omega_{0i} s + \omega_{0i}^2} w_{\xi i(s)}, \quad i = 1,2,3 \tag{5.10}$$

Where $\omega_{0i} = \frac{2\pi}{T_i}$ is the dominating wave frequency, T_i is the wave period are in the range of 5 to 20 seconds in the North Sea for wind generated seas. ζ_i is the relative damping ratio, $w_{\xi i(s)}$ is a Gaussian white noise process (input) and σ_i a parameter related to the wave intensity.

Representing the model in state space realization,

$$
\begin{aligned}
\dot{\xi}_1^{(i)} &= \xi_2^{(i)} \\
\dot{\xi}_2^{(i)} &= -\omega_{0i}^2 \xi_1^{(i)} - 2\zeta_i \omega_{0i} \xi_2^{(i)} + \sigma_i w_{\xi i}
\end{aligned}
\tag{5.11}
$$

and with a more compact realization, the model can be written as

$$
\begin{aligned}
\dot{\xi}_\omega &= \begin{bmatrix} 0 & I \\ -\Omega^2 & -2Z\Omega \end{bmatrix} \xi_\omega + \begin{bmatrix} 0 \\ \Sigma \end{bmatrix} w_\xi \\
\eta_\omega &= \begin{bmatrix} 0 & I \end{bmatrix} \xi_\omega
\end{aligned}
\tag{5.12}
$$

where $\xi_w = [\xi_1, \xi_2]^T$, $0 \in \mathbb{R}^{3\times3}$ is a zero matrix, $\Omega = diag[\omega_{01}, \omega_{02}, \omega_{03}]$, $Z = diag[\zeta_1, \zeta_2, \zeta_3]$ and $\Sigma = diag[\sigma_1, \sigma_2, \sigma_3]$.
Concluding, the total vessel's control model can be derived by combining the three aforementioned parts and the result is shown below.

$$
\begin{aligned}
\dot{x} &= A(x)x + B\tau + Ew \\
y &= Cx + v
\end{aligned}
\tag{5.13}
$$

Where

$$
x = \begin{bmatrix} \eta \\ v \\ b \\ \xi_1 \\ \xi_2 \end{bmatrix}, \quad A(x) = \begin{bmatrix} 0 & R(\psi) & 0 & 0 & 0 \\ 0 & -M^{-1}D & M^{-1}R(\psi) & 0 & 0 \\ 0 & 0 & -T_b^{-1} & 0 & 0 \\ 0 & 0 & 0 & 0 & I \\ 0 & 0 & 0 & -\Omega^2 & -2Z\Omega \end{bmatrix}
$$

$$
B = \begin{bmatrix} 0 \\ M^{-1} \\ 0 \\ 0 \\ 0 \end{bmatrix}, \quad C = \begin{bmatrix} I & 0 & 0 & 0 & I \end{bmatrix}, \quad w = \begin{bmatrix} w_b \\ w_\xi \end{bmatrix}, \quad E = \begin{bmatrix} 0 & 0 \\ 0 & 0 \\ E_b & 0 \\ 0 & 0 \\ 0 & E_\omega \end{bmatrix}
$$

In order to set up a Kalman filter, the need to know about its functionality rises. The complete system can be categorized in two sections. The prediction process and the correction process. Both processes and the steps involved will be explained below.
Firstly, by considering the system dynamic model, Equation 5.14 is derived. This equation is used to make an estimation of the states that are of interest.

$$
x_k = A \cdot x_{k-1} + B \cdot u_k + w_{k-1} \tag{5.14}
$$

Where, x_k is the estimated state. This could be either the vessel's position, heading or velocities based on the assumption that the Kalman filter will be used for DP. A is a matrix that relates the state at a step that is exactly before the present time $(k-1)$ with the state at the present time (k). This matrix is derived from the mathematical model that was introduced before. This holds for B as well, which is a matrix that relates the control input (u_k) with the state (x_k). Finally, W_k is the process noise of the model. In DP cases this is assumed as constant and a normal distribution of zero mean and Q (the process noise covariance) is given, $p(w)\ N(0,Q)$.

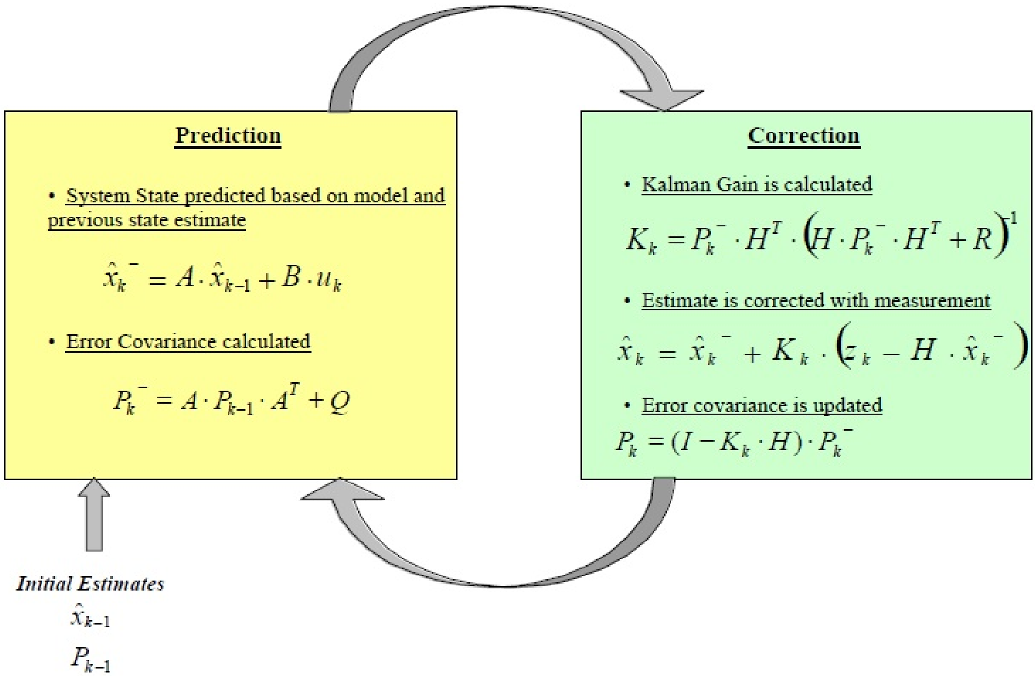

Figure 5.8: Kalman structure of prediction-correction process

Next, the position reference system or the sensors that were discussed earlier, will provide a measurement Z_k from the measurement model based on Equation 5.15 ,where H is a matrix that correlates the state to the measurement and acts as a description for the dependency of the state from the measurement. Furthermore, v_k is the measurement noise. It is assumed that this noise is independent from the process noise and following $p(v)\ N(0,R)$ where R is the measurement noise covariance that depicts the measurement's uncertainty.

$$z_k = H \cdot x_k + v_k \tag{5.15}$$

In addition, before explaining the prediction and correction steps of Kalman filter, two new variables need to be introduced. To begin with, $\hat{x}_k^-$, that is the *a priori estimate* at step k and it is based on the prior values of that state at previous time steps. The second variable to be introduced, is $\hat{x}_k$, that is the *a posteriori state estimate* that is estimated given measurement z_k. In Figure 5.8, the reader can see the steps of the prediction-correction process that the Kalman filter derives.

Then the prediction step takes place. As on can see in Equation 5.16, the Kalman filter based on the model and the current state, will evaluate the *a priori* estimate. Subsequently, the Kalman filter calculates the error covariance P_k^-, which is the uncertainty of the above mentioned prediction, and follows Equation 5.17.

$$\hat{x}_k^- = A \cdot \hat{x}_{k-1} + B \cdot u_k \tag{5.16}$$

$$P_k^- = A \cdot P_{k-1} \cdot A^T + Q \tag{5.17}$$

After the prediction is established, the correction step is calculated. In this step, the predicted state that was based on Position reference system measurement will be corrected through the *a posteriori* state estimate. In Equation 5.19, the correction takes place that relates the prediction step (first part of the equation) with the correction (second part). At this point, the Kalman gain K_k is calculated as well with Equation 5.18. The Kalman gain shows the weight of the new measurement as well as the weight of the model (amount of uncertainty).

$$K_k = P_k^- \cdot H^T \cdot (H \cdot P_k^- \cdot H^T + R)^{-1} \tag{5.18}$$

$$\hat{x}_k = \hat{x}_k^- + K_k \cdot (z_k - H \cdot \hat{x}_k^-) \tag{5.19}$$

In Figure 5.9, one can visualize the process of the prediction-correction that is performed through Kalman filter in a block diagram overview. [Cadet, 2003]

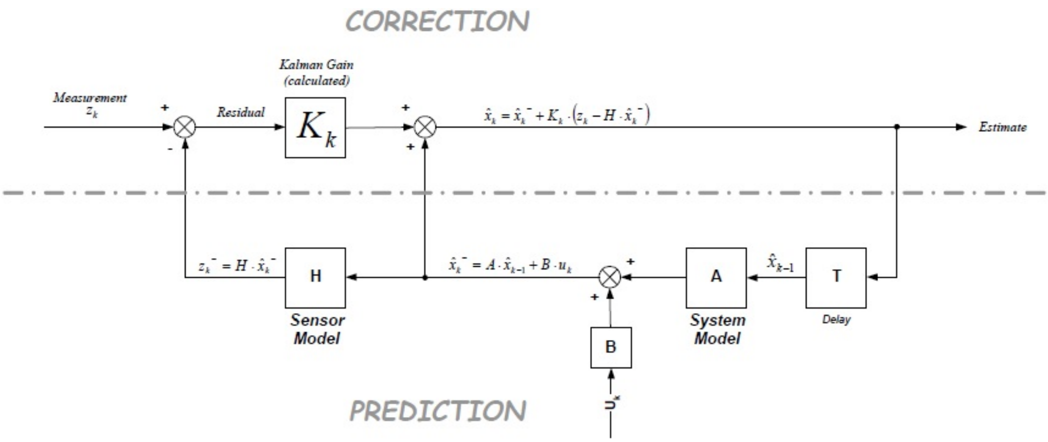

Figure 5.9: Block diagram for Prediction-Correction of Kalman filter

The effect of a Kalman filter is illustrated in Figure 5.10. As one can see, the first graph shows the total motions of the vessel for surge direction, where in the second graph only the LF motions are given, filtering out in such a way the WF motions that can be seen in the last figure. The vessel was subjected to a constant current speed of $0.5 m/s$, a wind speed of $10 m/s$ and mean wave drift loads with a universal heading of 150°.

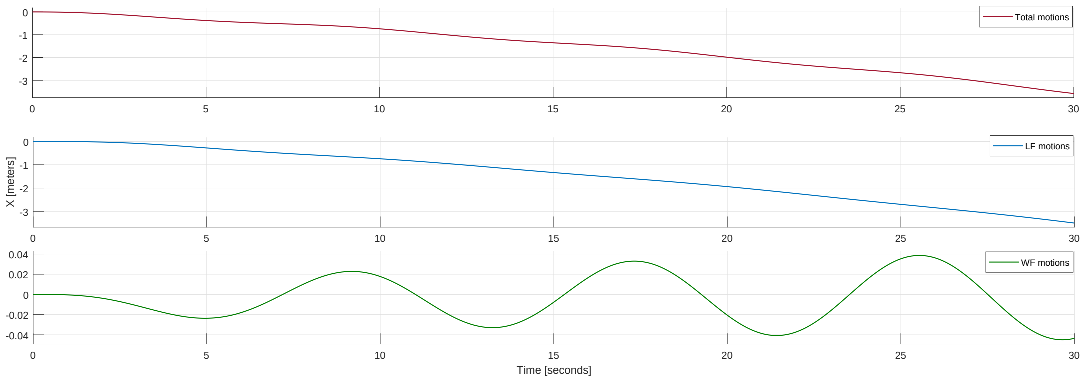

Figure 5.10: Total, LF and WF motions of the vessel

5.3.6. CONTROLLERS

As it was shown in Figure 5.6, after the position is measured, the signal is processed and the Observer performs the necessary actions, the actual position of the vessel is subtracted from the desired position, $r(t)$, deriving in such way the position error, $e(t)$. The most common controller that is applied nowadays is the PID controller. The author deemed that the easiest way to describe this controller is through the block diagram method, that for the particular situation can be seen in Figure 5.11.

The PID controller's name comes from the operators that consist it, where P stands for Proportional, I for Integral and D for Derivative. On its core, the controller's functionality is based on the derived error, to correct the measured state through the three processes that were introduced above and will be explained below.

The first component of the controller, is the Proportional gain. This gain can be considered as the ratio between the input (error) and the output response. Thus, as one can see from Equation 5.20, the input gets multiplied with the P gain. The purpose of this process is to increase the controlled response's speed. Though P gain is helpful up to a limit, careless tuning will result to oscillations of the process and might lead to instability if the gain is further increased.

$$P_{out} = K_p e(t) \tag{5.20}$$

The controller also has an Integral component, that is used to multiply the error and integrate it as it is shown in Equation 5.21. This part is suitable for eliminating the steady state error since its response keeps increasing if the error is not zero. When the error becomes zero, then this component does not affect the response.

$$I_{out} = K_i \cdot \int_0^t e(\tau) d\tau \tag{5.21}$$

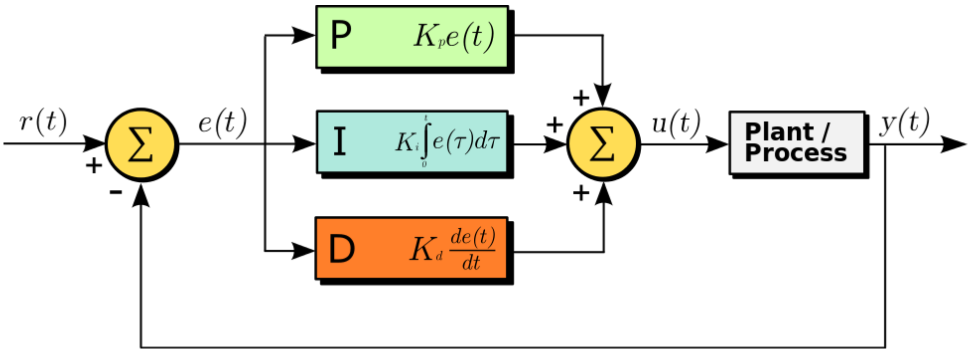

Figure 5.11: PID controller block diagram

Finally, the last component of the controller is the Derivative. Its response is relatable with the rate of change of the system's response and its formula can be seen in Equation 5.22. By altering the derivative gain, the overshoot is decreased, the control system can react more strongly or more smoothly to the error and in such way increase or decrease respectively the speed of the control system response.

$$D_{out} = K_d \frac{de(t)}{dt} \tag{5.22}$$

Combining all of the aforementioned components, Equation 5.23 results. Converting this equation with Laplace transform, the transfer function of the controller is derived and shown in Equation 5.24. As shown in Figure 5.11, the plant's transfer function is needed as well in order to have a complete control system for DP.

$$u(t) = K_p e(t) + K_i \cdot \int_0^t e(\tau)d\tau + K_d \frac{de(t)}{dt} \tag{5.23}$$

$$TF_{PID} = K_P + \frac{K_I}{s} + K_D s \tag{5.24}$$

Thus, Equation 5.4 that depicts the vessel EoM is transformed as well in the s-domain. A comment needs to be made at this point, since only surge, sway and yaw are the states that needs to be controlled, the stiffness parameters for those motions are zero and hence discarded from the transfer function that is shown in Equation 5.25.

$$TF_{vessel} = \frac{1}{(M+a)s^2 + Bs} \tag{5.25}$$

The open-loop transfer function then is the multiplication of the controller and the vessel's plant and it is depicted in Equation 5.26, where the closed loop transfer function is shown in Equation 5.27.

$$TF_{OL} = \frac{K_P + \frac{K_I}{s} + K_D s}{(M+a)s^2 + Bs} \tag{5.26}$$

$$TF_{CL} = \frac{K_P + \frac{K_I}{s} + K_D s}{1 + \frac{K_P + \frac{K_I}{s} + K_D s}{(M+a)s^2 + Bs}} \tag{5.27}$$

After the control system is introduced, the need to tune the controller gains rises. This can be done with various methods but two of the most popular ones are discussed.
Firstly, the Ziegler-Nichols method is introduced. The integral and derivative gains are set to zero and the proportional gain is increased until the response starts to oscillate. When the response reaches that point, the period that the oscillations have (P_c) is measured as well as the critical gain (K_c). Then the three gains can be derived from the Ziegler-Nichols table that is depicted below.

Control	**K$_P$**	**K$_I$**	**K$_D$**
P	$0.5K_c$	-	-
PI	$0.45K_c$	$0.54\frac{K_c}{P_c}$	-
PID	$0.6K_c$	$1.2\frac{K_c}{P_c}$	$\frac{3K_cP_c}{40}$

Table 5.2: Ziegler-Nichols control tuning method

The second method that is widely used for tuning a PID controller is the trial and error method which is similar with the Ziegler-Nichols method. After setting the I and D gains to zero, the P gain is increased until the response reaches steady oscillations. Then the I gain is increased until the steady state error is zero and the oscillations cease to exist. Finally, when both P and I gains are set, the D gain is increased until the response reaches the required overshoot and rapidity. Franklin et al. [2014]
In the DP modelling, the first method was used to determine the controller gains and an approximation of the rise time (required time for the signal to move from 10% to 90% of its steady state value) that a typical system of DP has. In Figure 5.12, one can see the control system response for a step pulse. The particular control system is for controlling the surge motion of the vessel. The response characteristics are shown in the figure as well.

5.3.7. THRUST ALLOCATION AND ACTUATORS

As it was shown in Figure 5.6, the DP control system is usually divided in two main parts. The first part generates the necessary forces and moment to overcome the error in position and heading using the controllers, while the second part is focused on optimally distributing those forces and moment to the actuators.
A combination of thrusters, rudders and propellers are the components that constitute the thrust allocation of a vessel and their operation is based on the command from the control system that is build in such way that takes into account the number, power and position of the aforementioned actuators. Unfortunately, the thesis is not considering thrust allocation due to time limitations as well as lack of information for the specific system.

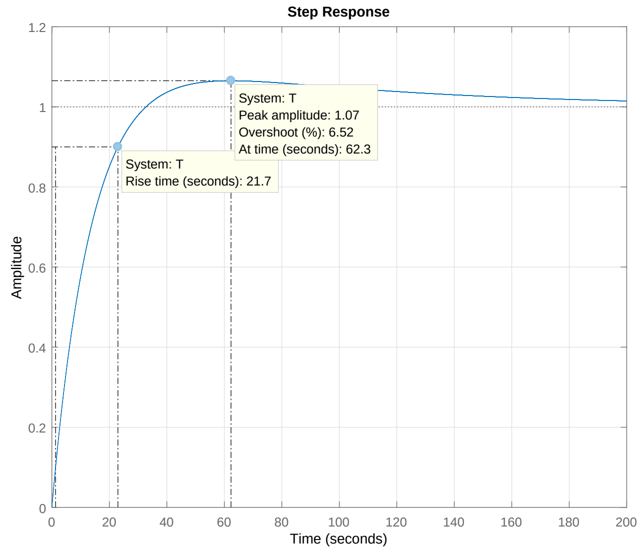

Figure 5.12: Control system response

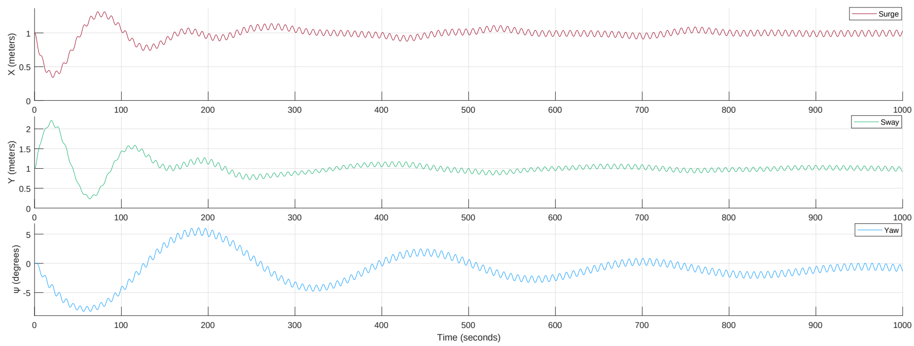

Figure 5.13: Vessel's COG motions in surge, sway and yaw

6

MONOPILE CONTROL STRATEGIES

Study hard what interests you the most
in the most undisciplined, irreverent
and original manner possible.

Richard Feynman

This chapter will present the results for all the possible design strategies that were established in the second chapter. After all the different contributing parts were modeled, the simulation and analysis took place. Then the results that were produced are discussed and finally the MCA is presented that concluded to the optimal design strategy that will be followed for the lowering operation of the MP from a floating vessel.

6.1. FREE FLOATING MONOPILE

To begin with, the concept of free floating MP is discussed. As it was mentioned in the previous chapter, this concept is considered and it is a part of the design strategies mostly because the author wanted to investigate the impact of a free hanging MP, what the motion envelope would look like, to what extend the gripper is needed. It is not considered as an actual solution for the operation since from experience and common sense, it is well established that this case can be easily discarded from the possible design strategies.

Before starting the analysis, one should understand the impact that a floating vessel has in such operation. The influence of the vessel on the lowering phase is transmitted through the connection points. Those are the crane's BT point that is connected to the MP through the crane wire and the second connection point is the gripper. Firstly, the translations of the crane's BT point are illustrated and in a latter stage the gripper's translations will be shown since in this case, the gripper is not applicable.

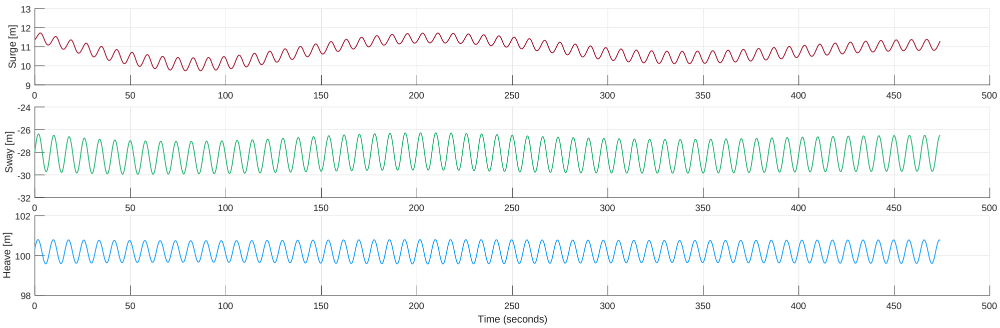

Figure 6.1: Boom tip point translations

From Figure 6.1, it is clearly shown that the floating vessel can significantly influence the operation since in surge translation, the vessel creates a disturbance in motion that varies from $9.7-11.8m$ approximately. This is a variation of 2 meters in surge direction, where in sway direction this variation of motion is almost double, varying from -26 - $-30m$ due to the heading of the environmental loads. The variation in heave motion is close to $1m$. Those variances are solid evidences that a floating vessel can influence a lot the installation process of a MP since those variances are transmitted in the MP motions from the crane wire.

In order to present the results for the case that no gripper is included, it was deemed as sufficient to illustrate the motions of the MP at the top point (SC) and the lowest point (BP) as well as the rotations of the MP. Firstly, the coordinates that the MP is required to be placed is given. Those coordinates will be the same for all different simulations and design strategies. In addition, those coordinates correspond to FRA to make the comparison among different design strategies easier and more understandable.

- $X = 11.4m$
- $Y = -28m$

In Figure 6.2, one can see the SC point translations. As it was expected, the motions of the SC point are influenced from the crane's BT motions. The motions in surge vary from 10-12.7m and in sway from -25.9 - $-29.6m$. Furthermore, one can see that the simulation is dynamic from the heave motion graph. The MP is lowered through time and the lowering speed that was chosen is $3\frac{m}{min}$ that is considered as an average speed for such operation. The SC point in heave starts from 63.4m and it stops at 35.4m. After lowering the MP for 28m, the operation stops 2m above the seabed for safety reasons. From the response of the SC point in heave translation, one can understand that the operation is dynamic.

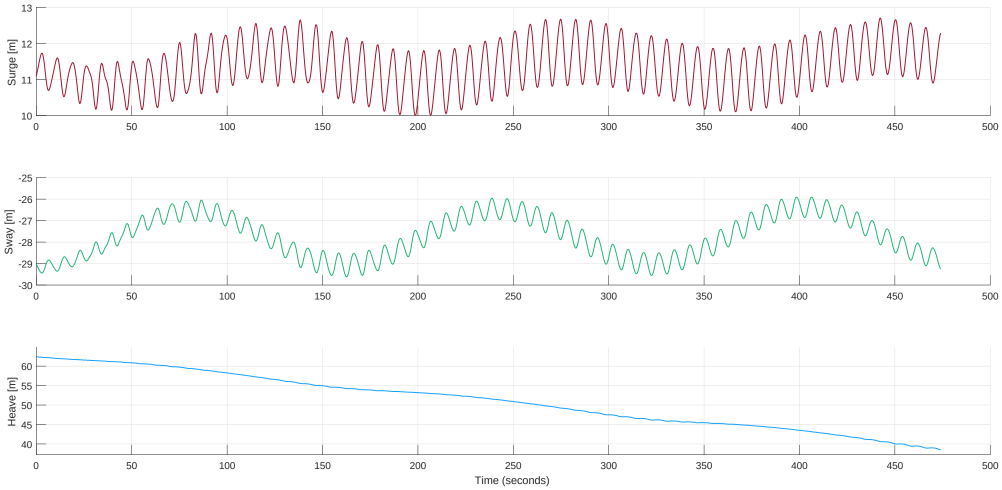

Figure 6.2: Sling connection point translations

As it was mentioned before, it is deemed sufficient for the reader's understanding to depict the motions of the top and bottom points of the MP since it is a rigid body and the rotations as well. In Figure 6.3, the reader can see the translations of the MP's BP. It is clearly shown that the variation of motions is much bigger at the bottom in comparison with the top of the MP. This is only logical since the BP is subjected to wave and current forces as well. The BP in surge direction moves from 7.5 up to 15m whilst the sway motions of that point vary from -23 to $-33m$ approximately. This is a clear indication of the necessity of the gripper in such operation.

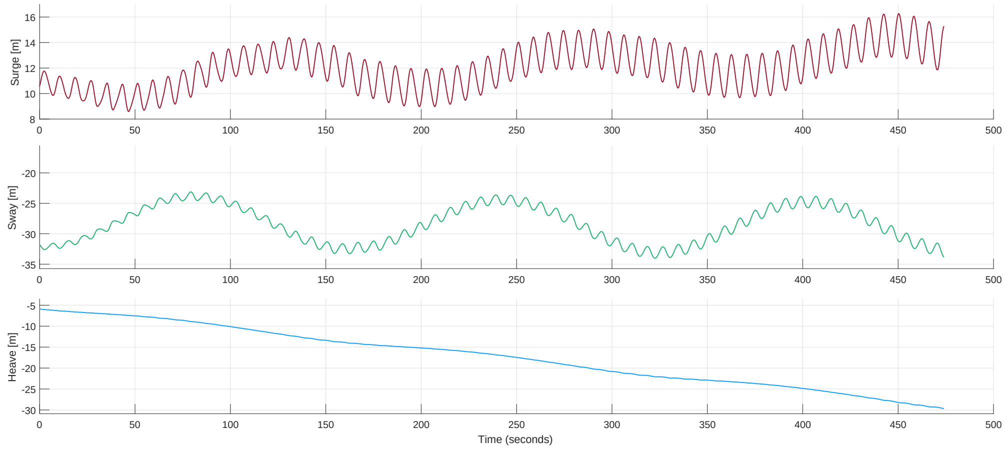

Figure 6.3: Bottom point translations

The last graph that will be shown for the case of free hanging MP is shown in Figure 6.4. In this graph the reader can see the MP rotations around the three axes, throughout the entire lowering operation. Since roll rotation is coupled with sway translations, it is only logical to have a fluctuation that is higher than the one in pitch rotation due to the heading of the environmental loads. Furthermore, yaw rotation is considered to be zero, due to symmetrical shape of the MP around z axis and because it causes singularities in the simulation. Even if that rotation would be considered, the result would be insignificant in comparison with the other rotations and translations.

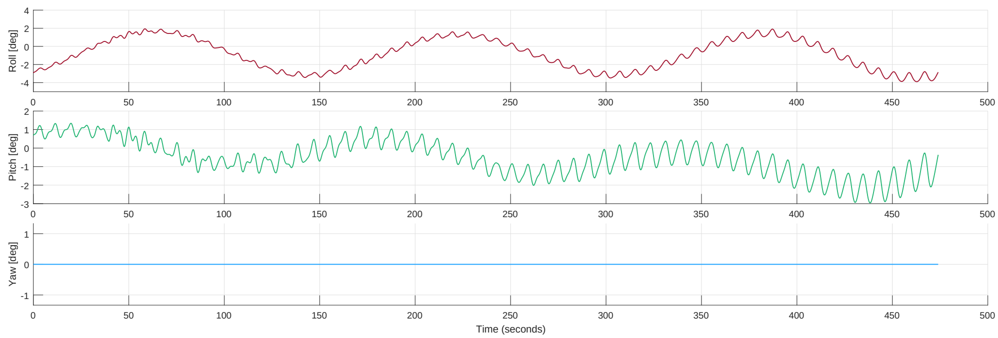

Figure 6.4: Monopile rotations

6.2. FIXED/PASSIVE GRIPPER

This next section will describe, present and analyze the fixed gripper concept that is mostly used in JUB since a fixed ground is in position. The concept of fixed gripper is in fact a straight forward solution for the operation if the motions from the environmental loads are kept in acceptable margins. In the following figure, one can grasp the concept of the fixed passive gripper.

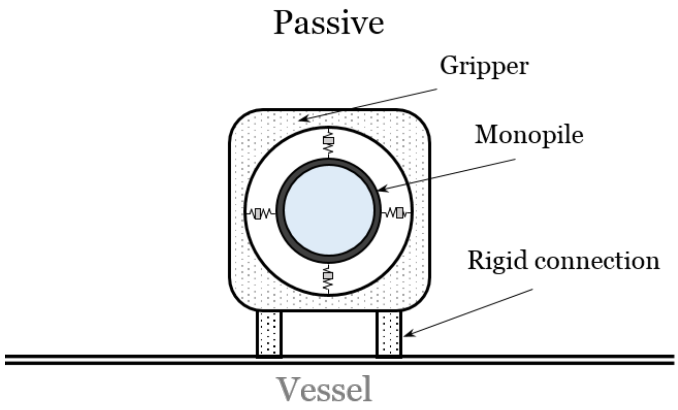

Figure 6.5: Schematic layout of a fixed passive gripper

The gripper is rigidly connected to the vessel and the MP is locked in the gripper. The connection between the MP and the gripper is assumed to be a spring-damper system in two directions, surge and sway. The generated model of the fixed gripper is in fact considered as one spring-damper in each direction, combining the stiffness and damping coefficients of both sides in one.

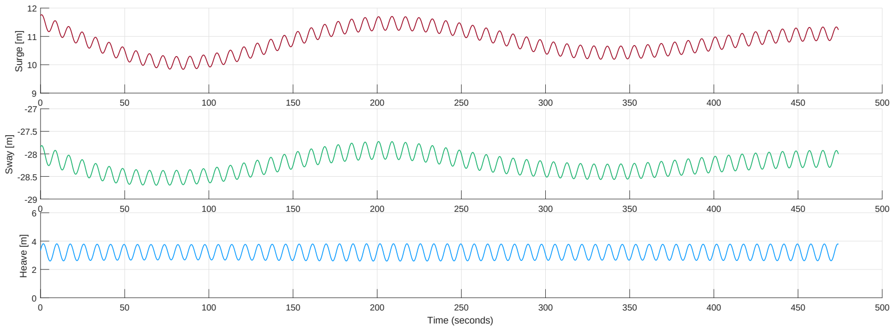

Figure 6.6: Fixed gripper translations due to vessel motions

In the concept of fixed gripper, it is only logical that the gripper motions will follow the vessel motions since a rigid connection between the two exists. That means that the motion envelope of the MP finds its limitation at the motions of the vessel. Even though the vessel motions at its COG are small, the integration of those motions at the point that the gripper is connected becomes quite significant. The gripper's translations are presented in Figure 6.6, where those motions are in FRA for the reader's convenience.
In Figure 6.7, the translations and rotations of the MP COG are shown. The fluctuations for all degrees of freedom are within acceptable levels. Furthermore, the reader should notice that the fluctuations become smaller throughout the operation. This is because the MP's submerged length increases through time and this implies that the motions are damped with the increase of the water submergence.

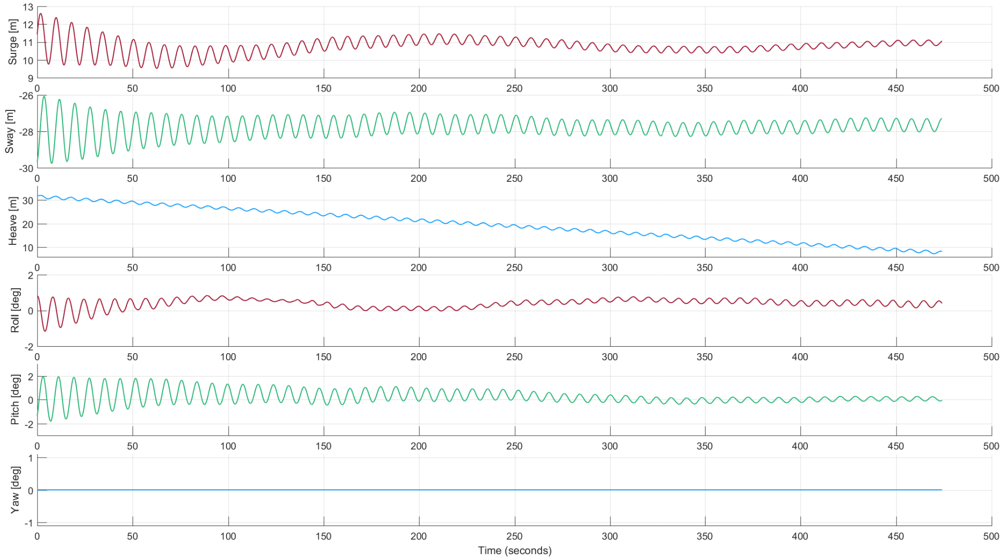

Figure 6.7: Monopile translations and rotations at center of gravity

In addition, it is clear that by using the gripper, the motions of the MP are drastically decreased and this can be understood when a comparison between this case and the results from the free floating MP is performed. Since this case has promising results, more results are shown for the reader's convenience and those results are discussed further below.

The following three figures show a more in depth response of the MP when it lowered through the water with the use of the gripper. As for the previous case, the top and bottom points of the MP are shown since those will have the highest fluctuations in surge and sway. By looking Figures 6.8 and 6.9, the reader will see that the motions in surge are fluctuating from $10-12m$ approximately whilst the fluctuations in sway initially vary from -26 to -30 and after 100 seconds, those fluctuations do not exceed $1m$. The reason for this distinction between the first 100 seconds of the lowering phase can be explained from the impact of the water that acts as damping for the MP once the critical depth is surpassed.

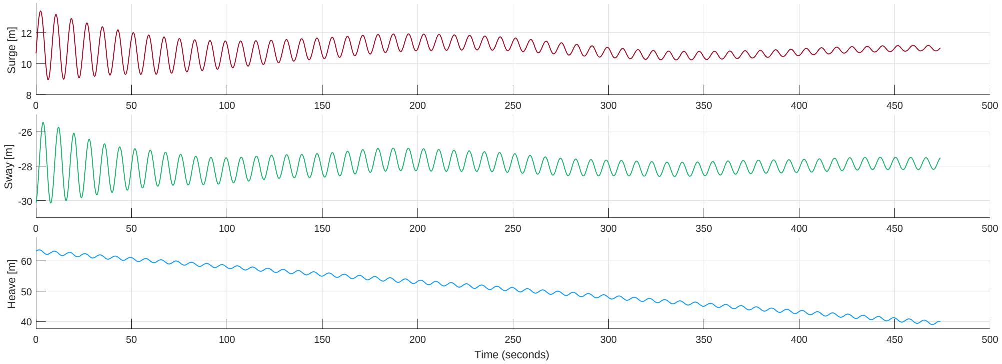

Figure 6.8: Sling connection point translations

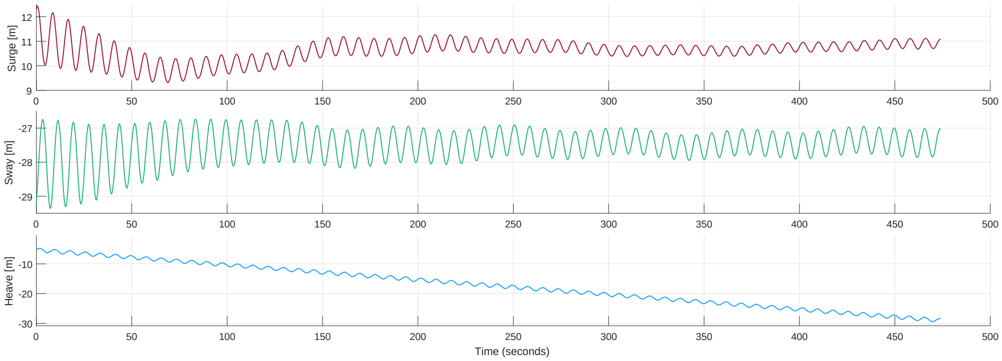

Figure 6.9: Bottom point translations

In order to evaluate the impact that the lowering phase has on the crane, three different metrics were deemed sufficient for monitoring. Firstly, the DAF is presented in the top graph of Figure 6.10.

The DAF in principle shows the ratio between the dynamic and static load in order to describe the amount of times that stresses should be multiplied to the deflections that come from the static loads when a dynamic load is present.

$$DAF = \frac{F_{total}}{Mg} \tag{6.1}$$

A rule of thumb for the maximum acceptable DAF value is 1.3. If the ratio surpasses this metric's maximum value, a bigger crane or alternative design strategy should be considered for safety purposes. It is clear that the DAF for the specific case lay on satisfactory levels and one should notice that this value is slowly decreased throughout the lowering operation. This is because the MP feels lighter through the operation since its submerged volume increases thus the buoyancy force increases too.

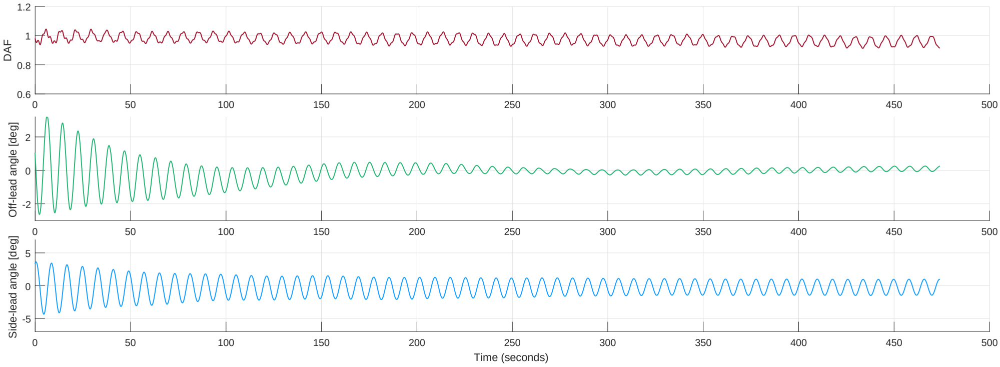

Figure 6.10: DAF, off-lead and side-lead angles

The other two metrics that are used to evaluate the MP's influence on the crane are the off-lead and side-lead angles. Those two angles are considering the crane wire orientation and its deviation from the vertical. Such angles occur when the lifted object is pushed/pulled away from the imaginary vertical line of the BT. Off-lead is the direction away from the crane whilst side-lead is the direction perpendicular to the crane boom orientation.

The acceptable angles for those metrics are considered to be ±3°. As can be seen in the aforementioned figure, both off-lead and side-lead angles are within acceptable limits even though side-lead angle in the initialization phase reaches the limit of acceptable deviation.

Finally, the total forces and moment that act on the MP's COG are shown in Figure 6.11. As it was stated before, the results show a consistency since the forces and moments reduce throughout the operation even though those values are within the acceptable margins for a typical operation of lowering a MP with the use of a fixed gripper.

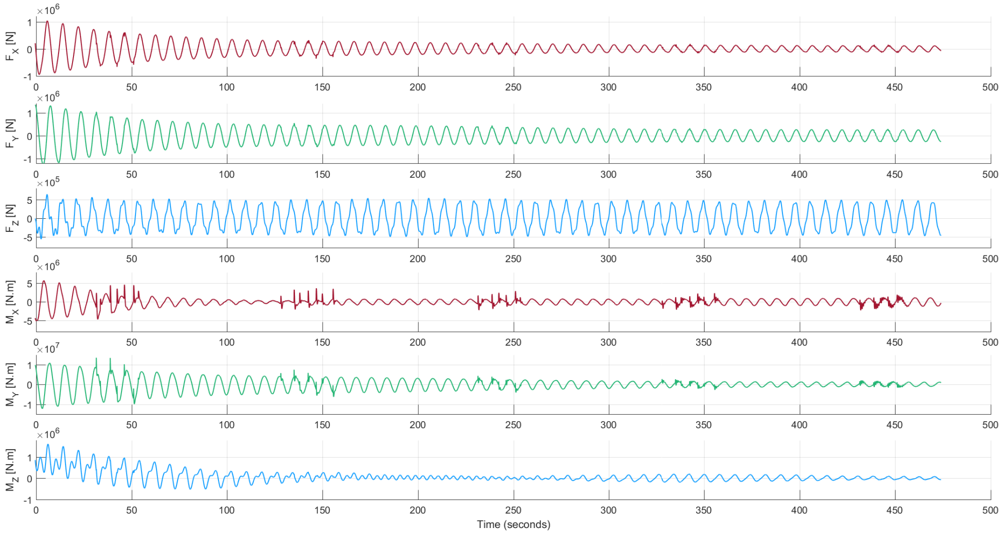

Figure 6.11: Total forces and moment acting on monopile's center of gravity

6.3. ACTIVE GRIPPER

The next concept to be discussed is the active compensating gripper configuration. In order to actively control the required state, an actuating system is needed. Such system consists of a power and a control part. Those parts interact together as one can see from Figure 6.12, where the control part gives an order to the power part and sequentially the latter part gives a feedback to the first part.

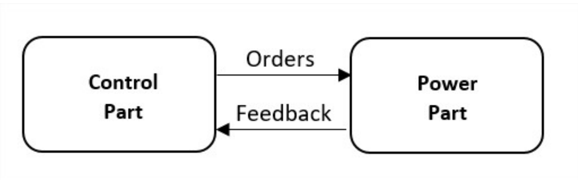

Figure 6.12: Actuation system overview

In principle, three different actuators can be considered. Those are the hydraulic, pneumatic and electrical actuators. After reviewing the alternatives for choosing an actuator, the author in collaboration with the the company decided that hydraulic actuator should be used. The main reason for this decision is that the hydraulic actuators are best suited for high-force applications. Furthermore, since high-precision of millimetres is a secondary goal and considering that a hydraulic actuating system can accommodate its parts (pumps and motors) in a considerable distance from the acting point and prevent the excess loss of power, the choice for such system was made.
In Table 6.1, one can see the trade-off between the three possible actuators that are considered for the active compensating gripper. The reason for the choice of hydraulic actuator is mostly the power to weight ratio as well as the company's knowledge-availability on the particular type of actuators. Furthermore, even though the speed, precision and efficiency aspects are important, they have a secondary role in the choice of actuator.

Actuator type	Speed	Precision	Power to weight ratio	Efficiency	Knowledge-Availability
Pneumatic	High	High	Medium	Medium-Low	No
Electric	High	High	Medium-Low	High	No
Hydraulic	Medium	Medium	High	Medium-Low	Yes

Table 6.1: Trade-off table of possible actuators

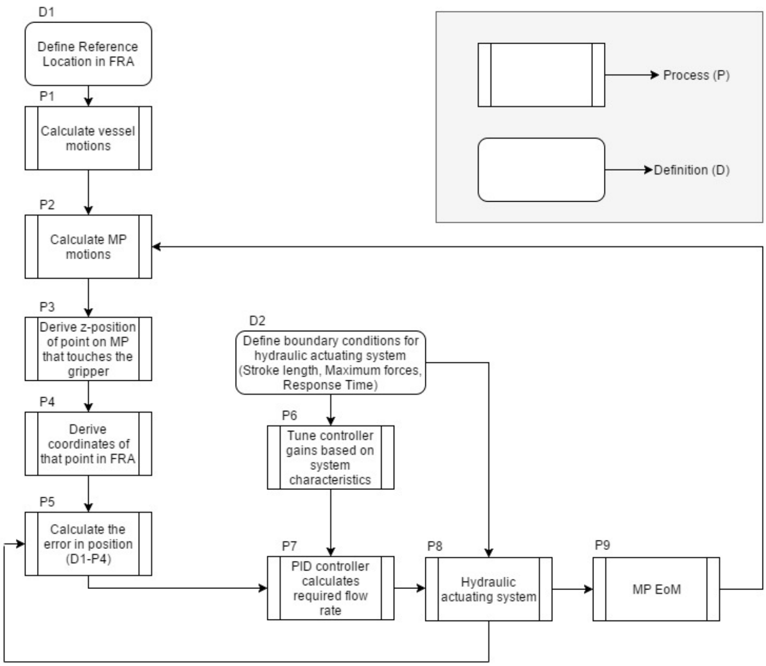

Figure 6.13: System layout for active compensating cylinder

In Figure 6.13 the complete control system for active gripper is shown. Firstly, the position that the MP needs to be placed is derived in FRA. The simulation model then, calculates the vessel motions as well as the MP motions. Sequentially, the vertical coordinate of the gripper-MP interface is derived from the MP motions and is converted to FRA. Then the horizontal coordinates of that point are subtracted from the referenced ones that were calculated in the first step of the process. Thus, by doing so the position error is derived.
Since an active compensation is needed, that error is fed in the PID controller that will calculate the required flow rate that the proportional valve will provide in order to compensate for the position error. The controller is tuned based on system characteristics for the hydraulic actuating system, such as rise time and overshoot that it provides. The required flow rate from the controller then is fed in the hydraulic actuation system that will be explained further in the next paragraphs.
The hydraulic actuation system then by giving a command to correct the position it provides a change of piston location. The flow rate then achieves a difference in pressure (higher or lower) to move the piston. By multiplying the pressure with the effective area of the piston, the required force is derived. The resulting force then is used as an input in the MP EoM.

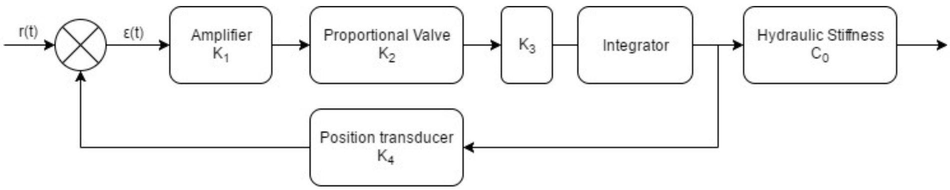

Figure 6.14: Hydraulic actuation system

The actual position of the gripper-MP interface is subtracted from the reference position r(t) to result in the position error. That error is amplified in order to be translated in valve signal (Volts). That signal then is used as the input in the proportional valve that will evaluate the flow rate ($\frac{m^3}{sec}$) that is required to compensate for the position error. The resulting flow rate sequentially is divided by the effective piston area ($k_3 = \frac{1}{A_{eff}}$) to derive the speed.
By integrating the speed, the new position is obtained that is then subtracted from the reference position to complete the closed-loop system. The difference in position then is multiplied with the hydraulic stiffness to result in the effective force that will be fed in the MP EoM. The aforementioned procedure is schematically depicted in Figure 6.14.
In order to continue to the simulation of the hydraulic actuating position control, firstly the required parameters need to be defined. Initially, the maximum allowable force in surge and sway was deemed to be $3000kN$. This assumption for such big force is derived from the safety measurements that the system will be designed for higher forces than the realistic ones to be able to compensate for scenarios higher than the assumed ones.

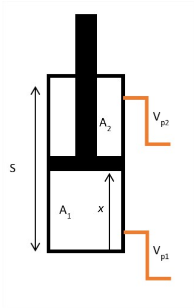

Figure 6.15: Double acting, single ended hydraulic cylinder

Then the cylinder stroke was assumed to be 3 meters (± 1.5 meters) in each direction, the maximum compensation velocity to be $0.25 \frac{m}{sec}$, the maximum achievable pressure 265 bar and the overall efficiency to be 0.91. All the aforementioned values are provided to the author from the company.

For the actuator, double acting, single-ended hydraulic cylinders were chosen since the both in surge and sway motions, compensating force should be acted in positive and negative directions for correcting MP and vessel motions. This type of cylinder can be seen in Figure 6.15 where S is the stroke of the cylinder, A_1 and A_2 are the effective areas of the piston and V_{p1} and V_{p2} are volume for the pipes that are connected to the cylinder. Since the cylinder is single-ended, it is only logical that the effective areas will be different because the rod is connected in one side of the piston. Albers [2010]

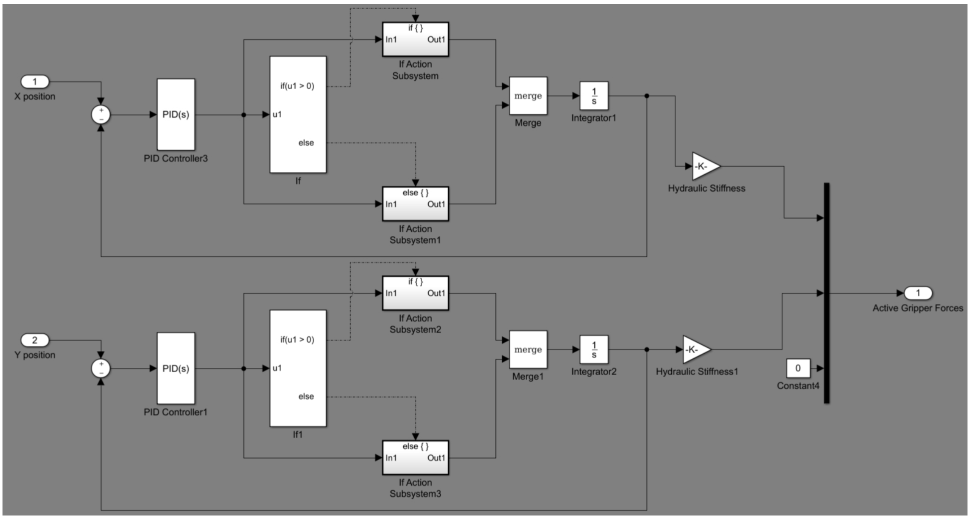

Figure 6.16: Simulink implementation of hydraulic actuating system

$$C_0 = \frac{E \cdot (\sqrt{A_1} + \sqrt{A_2})^2}{S + \frac{V_{p1}}{A_1} + \frac{V_{p2}}{A_2}} \tag{6.2}$$

Based on the initial assumptions, the areas were derived as well as the hydraulic stiffness. In principle, a hydraulic cylinder behaves as a spring with a stiffness C_0 due to the elasticity of the oil. That stiffness for the particular case of a double acting, single-ended cylinder is defined in Equation 6.2 where E is the fluid elasticity.
In Figure 6.16, the reader can visualize the way that the model for the active compensating gripper was created. After the position error is derived, the PID controller regulates the flow rate from the proportional valve. Then depending on the sign of the flow rate, it gets divided with appropriate effective piston area that is different for the upper area that the rod is connected and the area that is free of piston rod.
Sequentially, the resulting speed is integrated to give the new position of the piston. As it was discussed before, the new position is multiplied with the hydraulic stiffness since the cylinder oil acts as a spring to result in the forces that act on the MP at the interface between gripper and MP. Those resulting forces are added up with all the other forces to be the input in MP EoM.

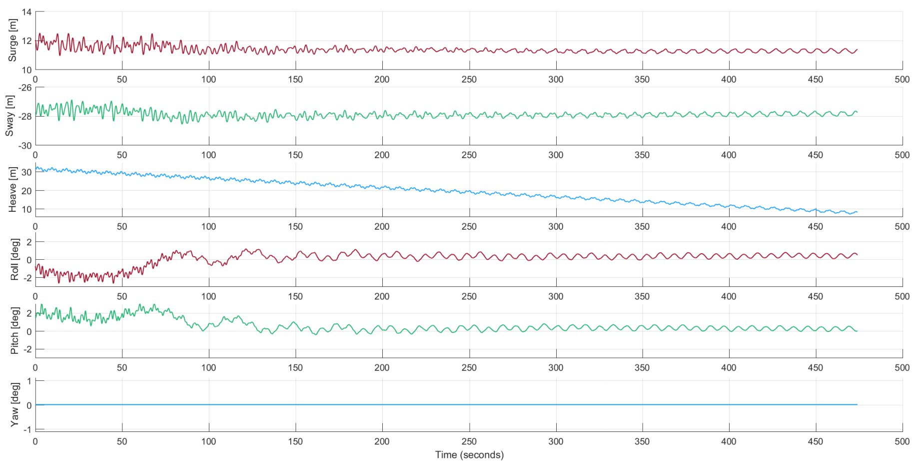

Figure 6.17: Translations and rotations at monopile's center of gravity

After the active gripper is introduced and analysed, the reader can see the results from the simulation for the particular case in the following figures. As can be seen in Figure 6.17, the translations and rotations of the MP at the COG are derived. With a first glance, one can notice that the motions are much better than the previous cases since the MP is not influenced any more from the vessel motions due to current and waves.

The MP rotations for both roll and pitch have fluctuations no more than 2° that are deemed as very promising since with such small rotations, the loads on the crane are within the acceptable margins.

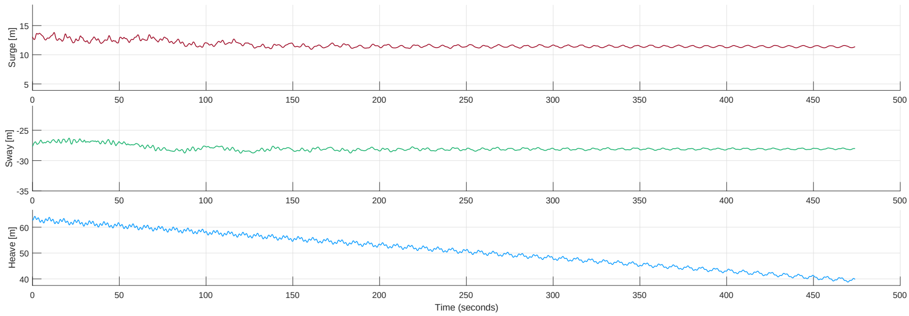

Figure 6.18: Sling connection translations

6

The MP translations at the COG were deliberately not discussed since Figures 6.18 and 6.19 show the SC and BP translations respectively that are much easier to comprehend since at that points the maximum translations occur. It is very clear that the translations for both points are not influenced from the slow-varying motions of the vessel considering that a stable fluctuation of approximately 1 meter is the result in surge for both points. The variation in motions for sway on the other hand are within 1.5 meters concluding in such way that this case has the most stable resulting motions of the MP throughout the entire lowering operation.

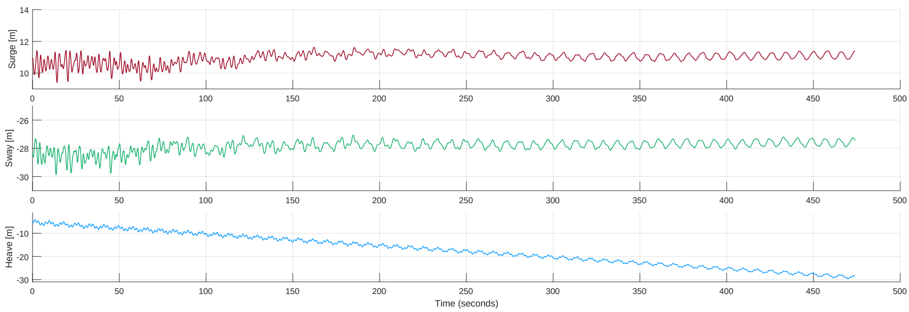

Figure 6.19: Bottom point translations

6.4. MOORING/DOUBLE GRIPPER

The final gripper configuration that was derived from the functional design in Chapter 2 is the mooring/double gripper. This configuration is build up for testing alternatives such as double fixed gripper and single fixed gripper in combination with a gripper that follows the BP of the MP. Various simulations for the alternative gripper solutions were performed considering different distance between grippers, different gripper stiffness and damping coefficients and different lowering speeds.

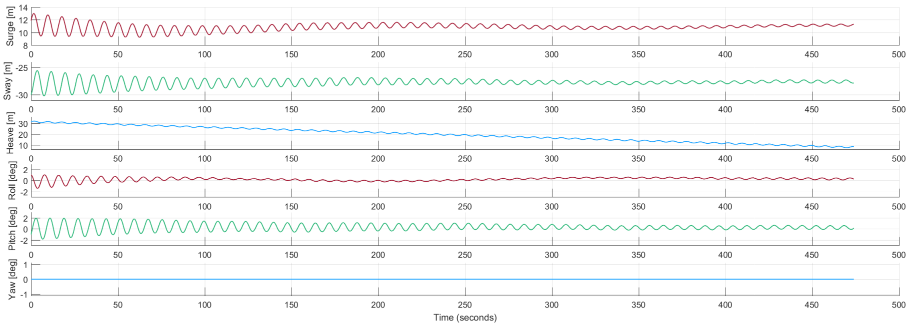

Figure 6.20: Translations and rotations at monopile's center of gravity for a mooring gripper

In Figure 6.20, the resulting translations and rotations for the MP COG are shown. The rotations of the MP for both roll and pitch vary between ±2°, where the translations of the MP are more understandable in the following figures that depict the SC point as well as the BP of the MP.

From those two figures, it is clear that the bottom part of the MP has smaller variation in motions both in surge and sway than the SC point. While the SC point has a variation in surge motion of approximately 3 meters, the same translation for the BP has a variation of 2 meters.

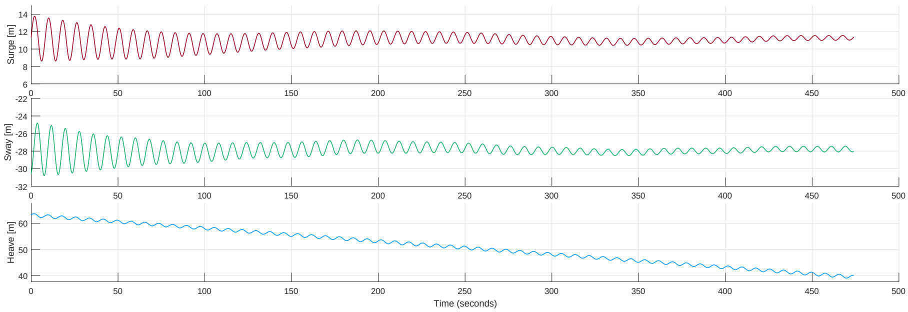

Figure 6.21: Translations at sling connection point for a mooring gripper

The same concept follows for sway motions as well, where the variation of motions for the top point is 4 meters approximately and on the other hand, the sway variation are between $3m$. This is only logical since the gripper(s) are closer to the BP rather than the top point of the MP, damping in such way the lower point motions more.

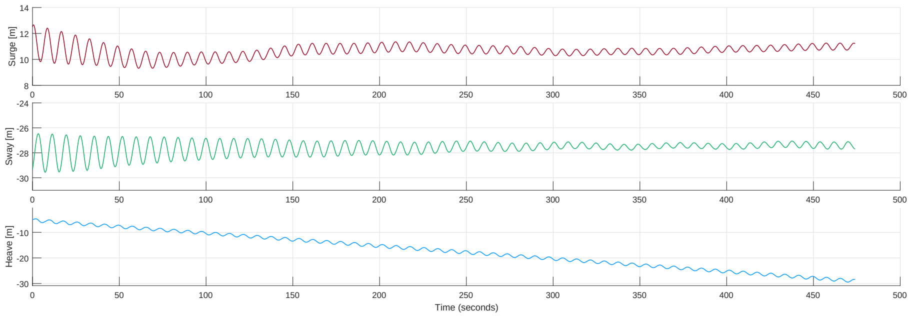

Figure 6.22: Translations at bottom point for a mooring gripper

As one can see from those figures, even though the results are within acceptable margins, such results can also be produced from a single passive gripper. Through the simulations with a single fixed gripper, the results show higher translations and rotations than the ones with double fixed or double hybrid gripper but the difference between the alternatives is not that significant.
The reason that all the different gripper solutions other than the active gripper have similar results, is that none of them compensates for the vessel motions which is the most significant part of the disturbances. That means that whatever solution for a gripper is presented, if it does not counteract for the forces that act on the MP through the vessel, the results will be similar to any other passive solution.

6.5. MULTI-CRITERIA ANALYSIS

The final part of this research, is to perform a MCA to identify which of the different concepts is the best suited for the lowering operation of the MP. Before explaining the procedure of MCA, the reader can visualize the Simulink model that the the author created for alternating between different gripper strategies in Figure 6.23. The user can easily switch between methods to visualize results for numerous simulations.
After all the parts of the simulation model are created and all the different design strategies are simulated, the MCA takes place to evaluate each one separately but compare the alternatives as well. In order to perform a MCA, firstly the goal of the entire process needs to be defined. That is the choice of a design strategy to control the MP throughout the entire lowering operation of the erection process.
Furthermore, the criteria for a MCA need to be defined. The following criteria were decided after trilateral discussions between the author, the company and the university. The criteria are further divided in sub-criteria in order to give a clearer impression of the important factors in such analysis and make sure that a correct strategy will be chosen

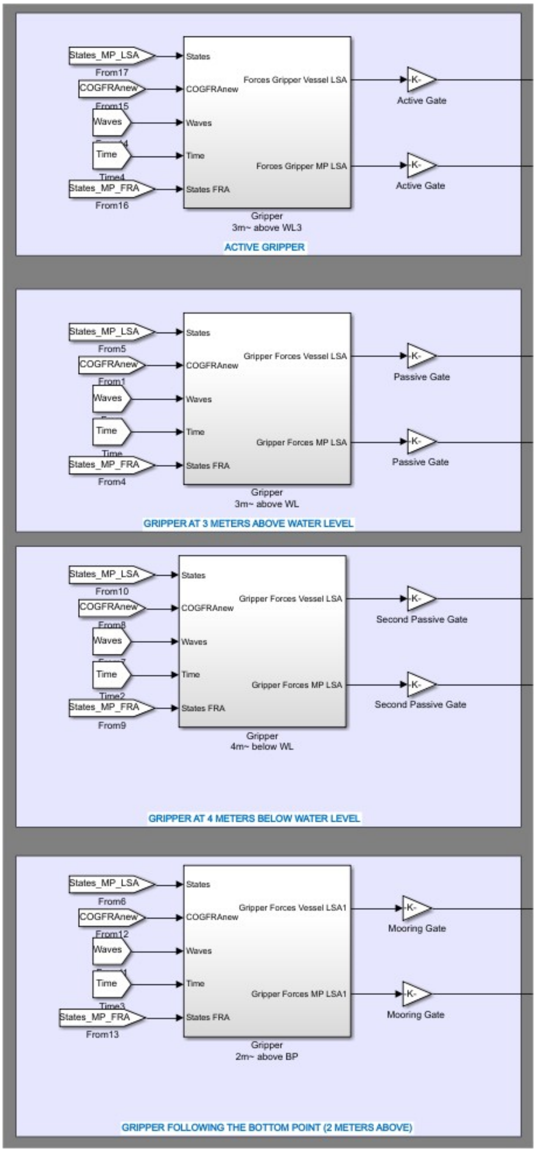

Figure 6.23: Simulink model for alternative gripper configurations

that took into consideration those factors. The criteria and sub-criteria are shown and explained below.

- **Safety**: This is the most important factor in such operation since the safety should be the top priority for any stakeholder that is involved. This criterion will be evaluated based on the response of the complete simulation for each strategy. The

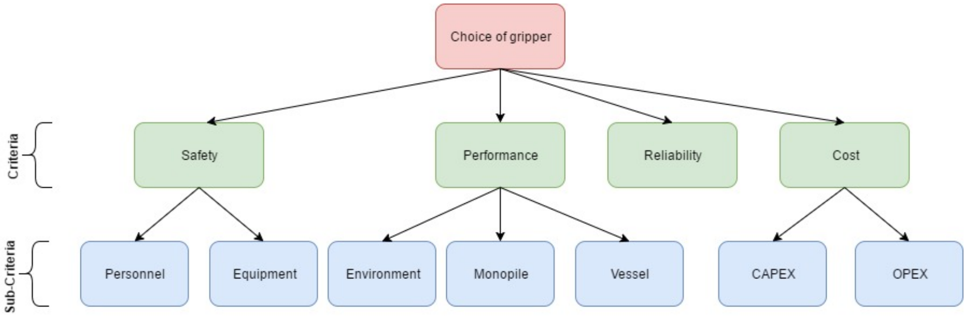

Figure 6.24: Criteria and sub-criteria for evaluation of design strategies

safety is further sub-categorized in safety of personnel and equipment. The weight factor of safety was chosen to be 30% since it is of great importance. Each sub-criterion has a weight factor as well. Personnel has an assigned weight factor of 60% and for equipment the weight factor is 40%. It needs to be mentioned that the weight factors of the sub-criteria should sum up 100% of each criterion and the summation of the weight factors of all criteria should result to the same total.

- **Performance**: The way that the design strategy performs throughout the operation is of great importance. This criterion demonstrates the ability of the design strategy to accomplish the required task in a manner that the requirements for the operation are met. The total performance criterion gains a weight factor of 30% as well and is sub-categorized in three parts. Firstly the environment sub-criterion, which means the response that the design strategy has in the environmental conditions such as the significant wave height and the peak period. Since this part is very important, a weight factor of 40% of the total performance percentage is assigned to it.

  The next sub-criterion is regarding the MP. This holds the information for performance of the design strategy for different MPs with a variation of lengths, diameters and weights. A weight factor of 35% is assigned to that sub-criterion. Lastly, the vessel integration is of great importance and is decided as a sub-criterion. This involves the ease of integrating the design strategy in a floating vessel. This metric is measured by the complexity of the individual design strategy since the more complex the design strategy is, the more man-hours, space and modifications will be needed to integrate it on the vessel. A weight factor of 25% is assigned to it.

- **Reliability**: A criterion that is very important for the attractiveness of any design strategy is the reliability of the system. This is the ability of the system to perform its intended function without degradation or failure. This is mostly based on the moving parts that the system consists of. Thus, the reliability is not divided in sub-categories but a weight factor of 25% is assigned to this criterion.

- **Costs**: The final criterion that is considered as important for the evaluation of the process is how much it costs to be installed on a vessel as well as what are the daily expenses after installation. Thus, two sub-criteria are defined to complete the costs metric. Firstly, the Capital Expenditures (CAPEX) which include the expenses that a company needs to undertake in order to obtain the system. This includes installation costs and modification costs for the existing vessels.

The second sub-criterion is the Operational Expenses (OPEX) which includes the day-to-day expenses such as inventory costs, maintenance and insurance. This is also a very important aspect of the criteria. The costs criteria has a weight factor of 15%, the CAPEX sub-criterion has 40% of the total whilst the OPEX has 60%. It needs to be mentioned that since the cost cannot be calculated in the current phase of the MCPG development, it is based on the amount of steel that are needed as well as the complexity of the design strategy.

In order to assess the strategies through a MCA, there is a need to perform numerous simulations with different inputs and parameters that will lead to a clear indication on each strategy's score. Since safety, reliability and cost cannot be quantified at the current phase of the analysis, only the performance metric is considered for the simulations. That criterion is divided in three categories: Environment, MP and Vessel.
For the assessment of each strategy regarding the environment sub-criterion, the author considered different environmental conditions, in order to evaluate how susceptible each strategy is during the variation of the environmental conditions. The requirements that were deemed as most important for this assessment are presented below.

- The MP motions at the BP just before the touchdown. The position difference between the highest and lowest motions of that point is derived and then compared with the maximum allowable tolerance of that point, which is 2 meters just before touchdown.

- The crane's off-lead and side-lead angles are the second metric. The absolute values of the maximum angles through the operation are derived and then compared with the maximum allowable angle that is 3 degrees.

Thus, for the environmental sub-criterion, one can see in Figure 6.25, the performance for different significant wave heights of all considerable strategies. On the left hand side of that figure, the surge deviation from the referenced is shown for the MP's BP, where on the right hand side, the sway motions are presented. It is clear that the MP's BP position is not the bottleneck for the analysis. This is only logical since once the MP is lowered, its motions gets damped as it was shown in previous sections. The waves do not influence significantly the specific response but it is once again clear that the active compensating gripper is the least sensitive from all the solutions even though all of the strategies lay on acceptable margins.
As for the previously discussed figure, numerous simulations were performed to assess the strategies' response regarding the off-lead and side-lead angles metric. The simulations had different significant wave heights as input, a wave peak period of 8 seconds and an environmental heading of 150 degrees. The values for this metric are derived at the initialization phase of the MP lowering since at that section the largest angles occur. The reason for that is the crane wire's length which is the smallest from the entire operation and the motions of the MP have the biggest fluctuations at that phase.

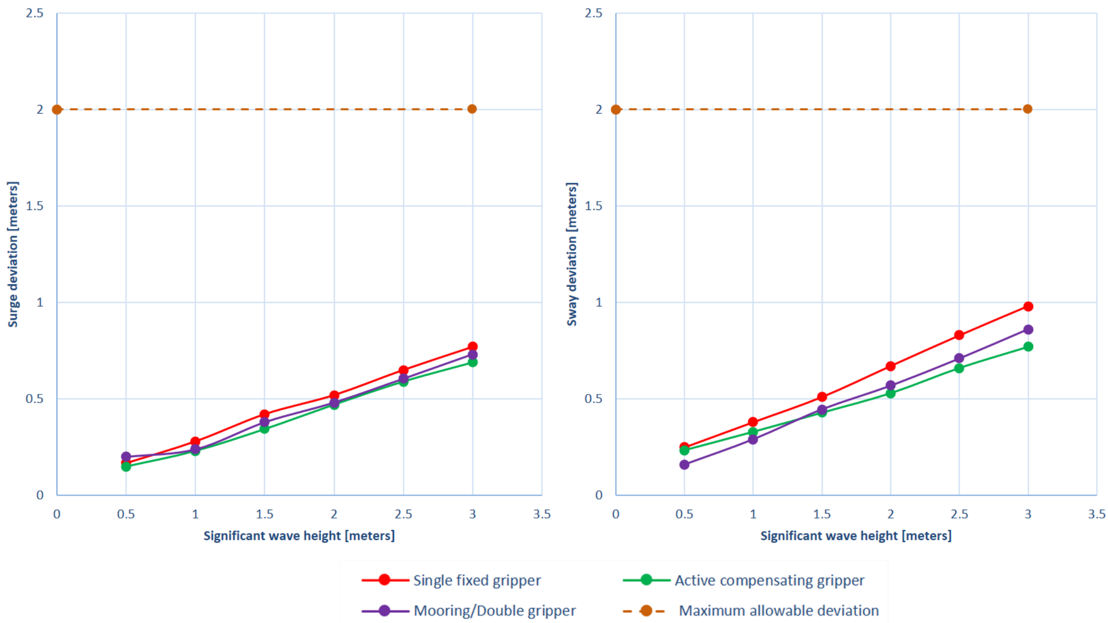

Figure 6.25: Performance of different strategies for horizontal translations of monopile's bottom point regarding significant wave height

The maximum allowable angle for both off-lead and side-lead is 3 degrees. From Figure 6.26 it is clear that the limitation to our operation for the variation of the significant wave height comes from those angles instead of the MP's BP motions near seabed. Another significant observation can be established from this performance analysis that the side-lead angles are higher than the off-lead angles and this is only logical due to the heading of the environmental loads. The single fixed gripper finds its limitation at approximately 2 meters of significant wave height, where the mooring/double strategy is limited at approximately 2.25 meters. On the other hand, the active compensating gripper even for a significant wave height of 3 meters is still operable.

Maybe the most significant remark for this performance analysis is that the single fixed and mooring/double gripper have approximately the same slope. That means the change of significant wave height influences the two strategies the same and this is only logical since both concepts are rigidly connected to the vessel. Nevertheless, the mooring/double strategy has more control of the MP through the changes since two constraints exist. In contrast, it is obvious that the active compensating gripper has a significantly smaller slope. This shows that the strategy is less influenced by the change of significant wave height than the other two concepts which is the expected result.

As it was discussed earlier, the second metric of the performance analysis is the environmental heading. For the evaluation of the strategies for their performance regarding the environmental heading, the author considered four different directions which are: $60°, 150°, 210°, 300°$. In Figure 6.27, one can see the conventions for the environmental

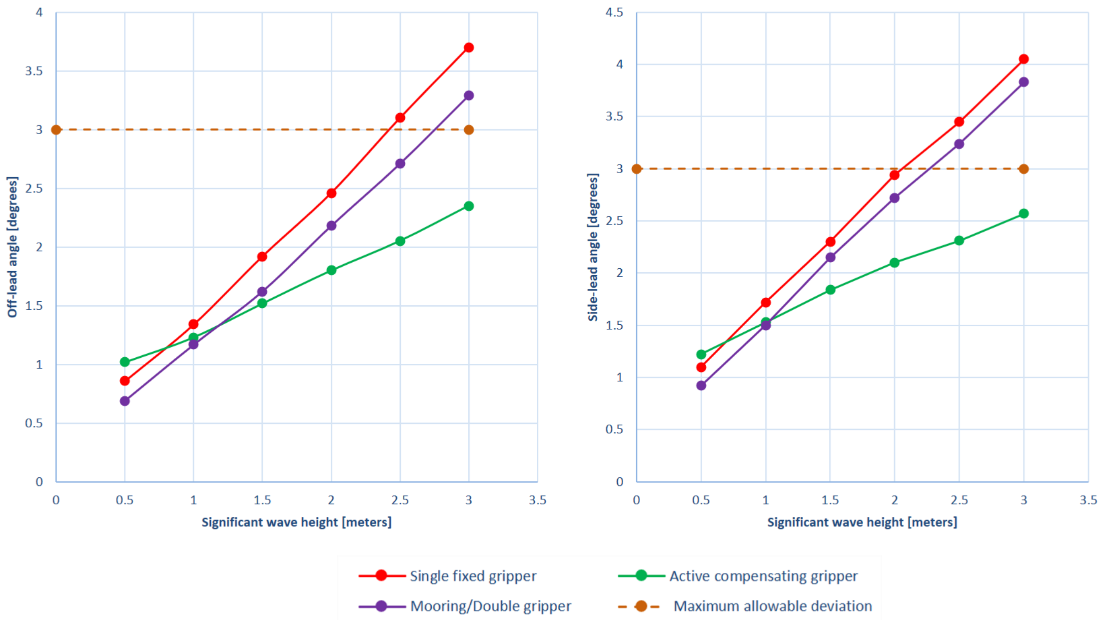

Figure 6.26: Performance analysis for off-lead and side-lead angles regarding significant wave height

headings. The same two requirements were considered for this metric as for the previous one. Firstly, one can see in Figure 6.28 the BP surge and sway highest deviation from reference position for the different environmental headings. From this performance analysis, few observations can be derived.

It is observed that the highest motion deviation occurs for all strategies at 300° and the lowest at 150°. This is only logical considering the placement of the vessel, gripper and MP. Furthermore, all of the strategies have responses that are within acceptable limits as it was expected since it is often the case that the limitation occurs from the off-lead and side-lead angles instead of the BP motions just before touchdown since those motions get damped by the time that the MP lowering is almost finished.

In addition, the second metrics which are the crane's off-lead and side-lead angles are shown in Figure 6.29. As it was expected, the crane angles are the governing factors for the operability of the strategies. For both metrics that were shown in this performance analysis, a significant wave height of 2.5 meters and a wave peak period of 8 seconds were considered. Both the single fixed and the mooring/double grippers surpass the maximum allowable angle deviation making the operation in such way unsafe thus not considered. It is also shown that their response follows the same path since the vessel motions that influence the MP's response are not compensated by any means.

Furthermore, the active compensating gripper is at all headings reliable and operable concluding to the remark that this strategy is less sensitive to the change of environmental heading. This remark is also supported from the fact that the steepness of the

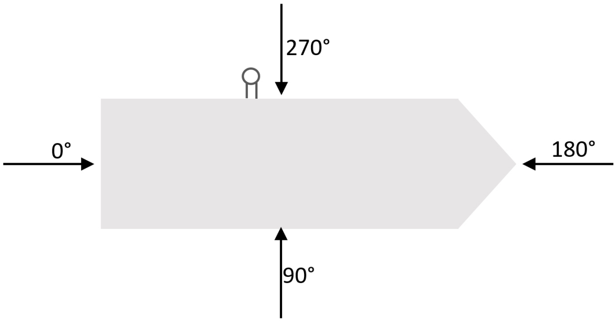

Figure 6.27: Convention of environmental headings

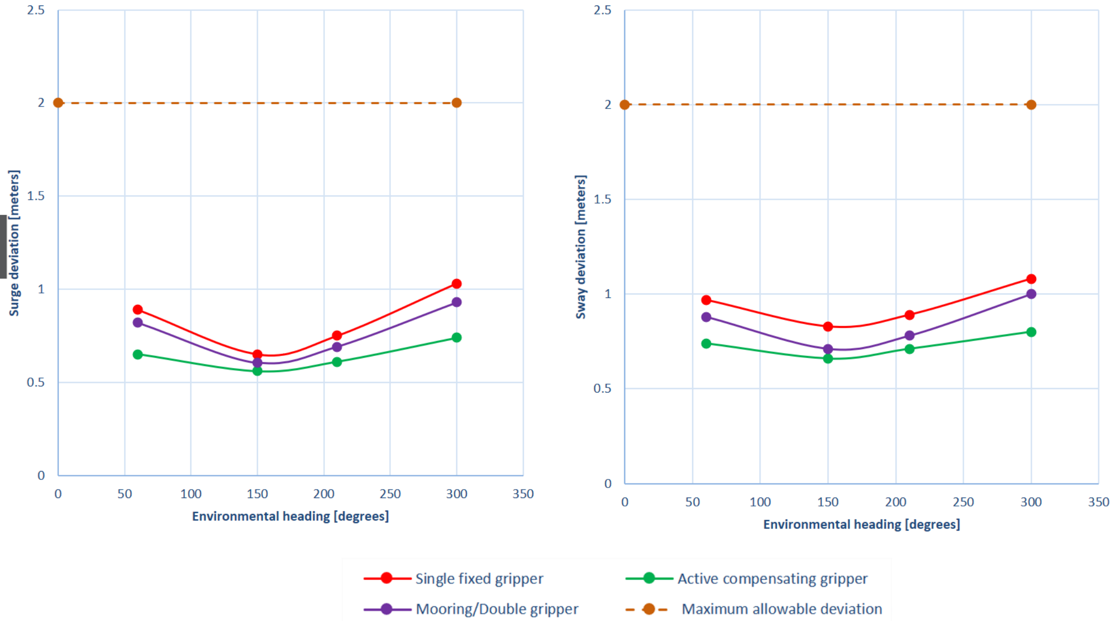

Figure 6.28: Performance analysis for horizontal translations of monopile's bottom point regarding environmental heading

strategy's response is significantly smaller than the previous two concepts. It needs to be mentioned that the vessel influences the operation in a way since the crane motions that are a result of vessel motions are not compensated from the gripper. That means that since the vessel motions are influenced from the environmental heading because of its projected area, the active compensating gripper is influenced, even though it is in a limited way, by the vessel motions implicitly.
In order to assess the MP sub-criterion, firstly the different MPs that are considered are presented in Table 6.2. The particular MPs were chosen to cover a variety of dimensions

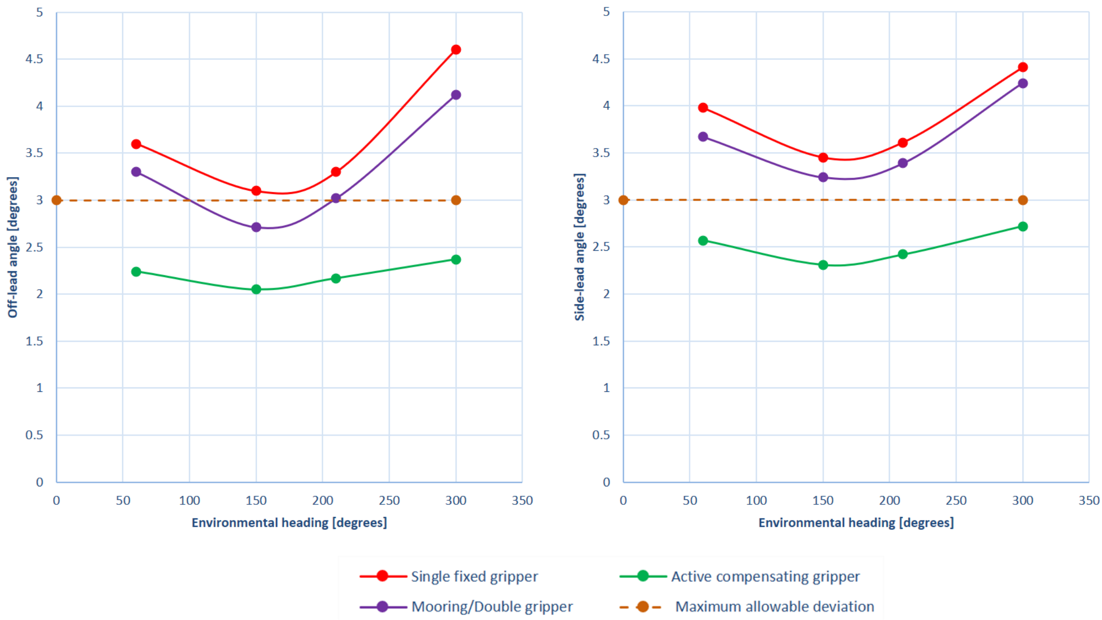

Figure 6.29: Performance analysis for off-lead and side-lead angles regarding regarding environmental heading

including both small and extreme cases to obtain a more realistic performance analysis. Since in the previous analyses it was proven that the BP's horizontal motions were not the critical ones but the off-lead and side-lead angles are, this analysis is performed only for those metrics.

Monopile	Length [m]	Weight [t]	Diameter [m]	Thickness	Water depth [m]
Nr. 1	68.4	1057	8.5	0.066	30.7
Nr. 2	84.8	1280	7.8	0.078	39.3
Nr. 3	102.6	1550	8.75	0.095	45
Nr. 4	50.2	667	7.1	0.069	22.5

Table 6.2: Considered monopiles for the assessment

For the particular metric, all of the aforementioned MPs are considered, a significant wave height of 2.5 meters, a wave peak period of 8 seconds and a heading for environmental loads of 150°. After establishing the performance analysis, it was clear that the most critical metric was the side-lead angle due to the environmental heading. For this reason, only this metric is shown in comparison with the variation of weights and lengths of the MPs. In Figure 6.30 one can see the results from this analysis.

As it was expected, the MP's weight has a significant impact on the response. While its weight increases, the side-lead angle deviation reduces. This is due to the fact that the inertia of the MP plays a significant role in the motions and makes the response to lay in smaller fluctuations. On the other hand, when the length of the MP increases, the

side-lead angle deviation increases too. This is also expected, since the moment arm is increased and the gripper(s) have an increase in their distance between their acting point and the SC point of the MP.
Another observation that can be derived from this figure, is the steepness of the grippers' response. While the single acting gripper and the mooring/double gripper have approximately the same response, the active compensating gripper has a response with less steepness than the other two concepts. That observation in extend implies that this strategy is less susceptible to changes in MP dimensions.

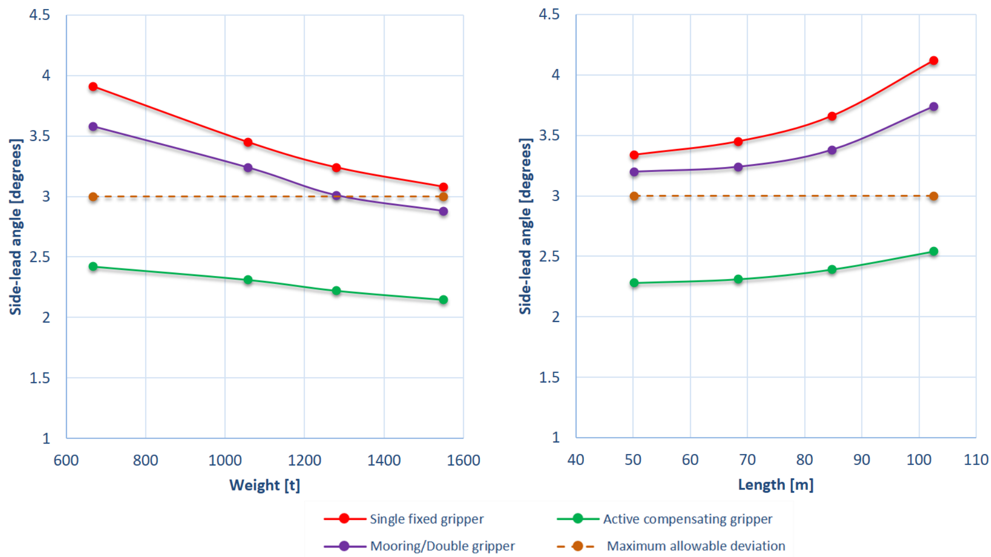

Figure 6.30: Performance analysis for off-lead and side-lead angles regarding monopile dimensions

After defining the criteria and sub-criteria that will be the foundation of the MCA, the weight factors were assigned. Next, the design strategies are evaluated based on those criteria, comparing the concepts amongst them and scoring them in a scale of 1 – 10, with 1 being a poor performance and 10 the best performance possible. The result of the MCA can be seen in Table 6.3, where all the aforementioned parts are presented.

Criteria	Sub-criteria	Weight factor		Free hanging MP	Fixed	Mooring/Double	Active
Safety	-	0.3	-	-	-	-	-
-	**Personnel**	-	0.6	5	9	9	9
-	**Equipment**	-	0.4	4	7	8	9
Performance	-	0.3	-	-	-	-	-
-	**Environment**	-	0.4	2	4	5	8
-	**Monopile**	-	0.35	3	7	7	8
-	**Vessel**	-	0.25	7	6	4	5
Reliability	-	0.25	-	9	8	7	7
Cost	-	0.15	-	-	-	-	-
-	**CAPEX**	-	0.4	9	7	4	5
-	**OPEX**	-	0.6	9	8	7	6
Score	-	1	-	**6.06**	**7.265**	**6.835**	**7.465**

Table 6.3: Score for different design concepts

Taking into consideration all the different simulations and criteria, the aforementioned analysis results to the winning strategy that is suggested to follow. The winning strategy is the active compensating gripper that has the ability to compensate for the MP motions and react on the vessel motions as well. The design strategy does not perform as well as the others in the costs criterion since the cost of a more advanced system is only logical to be more expensive than the simpler ones.

Furthermore, the concept of active gripper is ranked as moderately good in the reliability criterion as well. The reason for this score is that the concept has significantly more parts than the single fixed gripper and many more moving parts than the mooring/double gripper strategy. The reason that the mooring/double concept scores the same with the active gripper in the reliability criterion is due to the fact that two layers of rings are needed. This means that all parts, moving and not, are doubled.

Even though the active compensating gripper scores moderately in two categories, the concept compensates for the difference in the Performance criterion since it has a much more flexible operation than the remaining concepts. Finally, the gripper performs remarkably well in the safety criterion since by having such a small motion envelope it constraints in a big fraction the margin for hazard.

After the scoring is established for all the different strategies based on all criteria and sub-criteria that concluded to the wining strategy of active compensating gripper the author considered to perform a sensitivity analysis to evaluate how susceptible the weight factors that were assigned to the criteria are to change on their values. Since the safety, reliability and cost criteria are not evaluated based on quantified measurements but rather qualitative assessment, only the performance criterion is considered for the sensitivity analysis.

The aforementioned criterion is divided in the environment, MP and vessel sub-criteria. Those three different parts are assigned with numerous weight factors and by maintaining the score on all criteria fixed, the overall score of each strategy is reassessed and presented in Figure 6.31. Since the vessel sub-criterion is not as important for the performance as the environment and MP, it is considered that its weight factor can only vary from 10% to 40% while the other two sub-criteria are flexible to a weight factor between 10% to 90% if possible.

The purpose of this sensitivity analysis is to check whether the wining strategy is affected

6

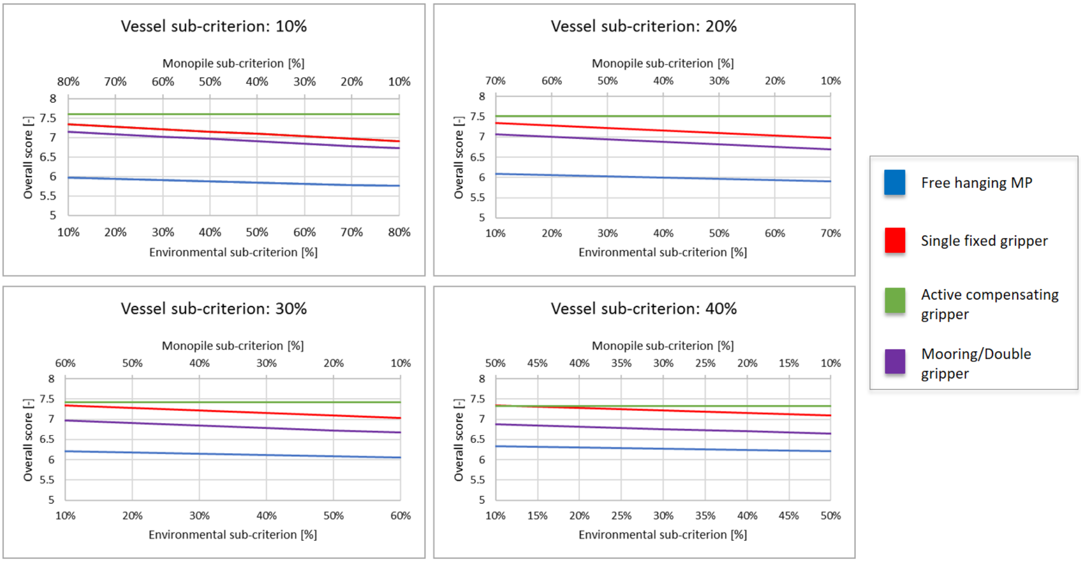

Figure 6.31: MCA weight factors sensitivity

by the change of the weight factors since uncertainty is involved. As one can see from this figure, the active compensating strategy is always the wining one except just one case. That case is when the vessel's weight factor is 40%, the MP's weight factor 50% and the environment weight factor just 10%. This case would be rarely to never considered since the weight factors are unwise distributed. By performing this sensitivity analysis, one can understand that the active compensating gripper that is the wining strategy will always be the chosen one regardless of the weight factor distribution if that distribution is sensibly divided to the sub-criteria. Another remark can be drawn from this sensitivity analysis that in some cases, the single fixed gripper can be considered but under very controllable and favourable circumstances.

7
CONCLUSIONS AND RECOMMENDATIONS

There is no real ending.
It's just the place where you stop the story.

Frank Herbert

This chapter concludes the entire research. After analysing all the different components, modelling all the parts of the scope and simulating the various control strategies, some conclusive remarks are presented that were the outcome of the entire project and not just the simulations part. In addition, some recommendations are presented to the reader for future references in such projects.

7.1. CONCLUSIONS

This thesis examined the lowering operation of a MP from a floating vessel through different design strategies. It integrated various different aspects in the analysis, in order to make it more realistic. Beginning with a functional design, the problems that will be encountered through the operation were derived and it concluded with the possible design strategies.
Next, the hydrodynamics part takes place, for the author to derive the required forces formulas to model the MP, environment and vessel. Since a floating vessel is preferred, a need for DP rises. Thus, a simplified system was developed to compensate for the horizontal motions of the vessel through filtering and controlling. In addition, the system integration part takes place, that models the possible design strategies in order to control the MP motions and compensate for induced vessel motions that were going to affect the MP behaviour.
Lastly a MCA is deployed, since a choice needs to be made between the design strategies that will conclude to the suggested winning strategy to be followed in such operations. In Figure 7.1, the reader can see the overall model that was created in MATLAB/Simulink, which includes all the aforementioned parts.

Figure 7.1: Model overview in Simulink

By finishing this research, multiple conclusions are derived. Those conclusions result from the overall analysis and modelling and not just from the outcome of the project. The conclusions from the research are presented below and since those resulting remarks are of great importance, several changes and alternatives can be considered for future research.

- The active compensating gripper can cope with different headings of the environmental loads as well as different peak wave periods but when it comes to significant wave heights, the concept is more sensitive since this parameter affects mostly the MP motions instead of the vessel motions.

- MP motions are reduced to a large extend with the use of the active compensating gripper when the vessel is a great influence in the MP's response.

- The active gripper is modelled with a PID controller, in order to regulate the flow rate that the proportional valve sends to the hydraulic cylinder. Since there are constantly fluctuations in the motions and the gripper-MP interface is continuously changing its position through the entire lowering operation, a PID controller with constant gains is not realistic and it can be misleading to an extend.

- Through the lowering operation, two connections exist through the vessel and the MP; the gripper and the crane's lift wire. In extension, there are two sources that influence the MP motions, the BT point of the crane and the gripper that is integrated to the vessel.

  As it was discussed in a previous stage of the thesis, the vessel's COG translations and rotations are not very significant but when those motions travel to the BT, the motions at that point become of great importance. Thus, it would be wise that a motion compensating crane can be researched to assess the impact that it could have in such operation since it might be a good alternative for controlling the lowering operation of the MP erection process.

- If the significant wave height is smaller than 2 meters, the environmental heading is favourable and the vessel induced motions are not of great influence, a fixed passive gripper might be an option to consider for the lowering operation. In order to consider the fixed passive gripper, extensive analysis should be made based on the area of operation and environmental loads.

- Even if a fixed gripper can be considered for the lowering phase, an active compensating strategy is absolutely essential to achieve a successful piling phase of the MP since the translation and rotation tolerances in that phase are significantly smaller than the ones in lowering.

- The gripper loses its influence throughout the lowering operation since the distance between the gripper and the MP's COG becomes smaller, resulting in such way to smaller moment arm, thus less influence from the gripper to correct the MP motions.

- Throughout the lowering operation, the MP motions become smaller since the submerged volume of the MP increases and the MP gets more damping from the water as the length from the BP of the MP to the waterline increases. Furthermore, it was discussed in Chapter 3, that the forces beneath the waterline decrease while the submergence level increases.

7.2. RECOMMENDATIONS

In order to conclude this thesis report, some recommendations are given that are derived from this analysis. Those recommendations are essential aspects that have to be examined if a realistic simulation of the MP installation process is required. The recommendations that the author can suggest are presented below.

- While performing the functional design process of the analysis, some of the problems were considered to be out of scope and thus not analysed. It is critical that those problems will be taken into consideration and checked in order to complete the lowering analysis and to result in more realistic conclusions.

- It is wise to consider different vessels and gripper positions to assess the sensitivity of location. Since such design will be integrated in various HLVs in the future, this sensitivity analysis is also an essential aspect that has to be considered.

- An extensive elaboration on the MCA is also strongly recommended. The different strategies have to be assessed and ranked based on the established criteria, subcriteria and weight factors. To achieve a realistic MCA, those parameters have to be defined with more accuracy. Furthermore, the score of each strategy on the MCA will need a revision that will be based on quantifying measurements instead of qualitative assessments and assumptions.

- In addition, a better design of the active compensating gripper and its hydraulic actuating system should be considered, that involves a more realistic representation of the parameters that are considered to achieve position control.

- Combining some of the conclusive remarks, a hybrid solution might be an option to consider. That is, to use an active compensating gripper for the first part of the lowering operation, that the motions are higher and for the second part to lock the hydraulic actuating system, transforming the gripper in such way to a fixed passive one.

  Since the gripper loses its influence and the motions become smaller throughout the lowering operation, this solution can be a considerable option for power management and more efficient system that will add value to the concept.

- It was mentioned before that a simplified and ideal DP system was deployed in the research. It would be of great importance to implement a more sophisticated control system including thrust allocation and power management system in order to assess the required power that will be needed in such operations and to get a better impression on a more realistic simulation of such operation.

References

Peter Albers. *Motion Control in Offshore and Dredging*. Springer Science & Business Media, 2010.

European Wind Energy Association et al. *Wind in our Sails-The coming of Europe's offshore wind energy industry*. EWEA, 2011.

Olivier Cadet. *Introduction to Kalman Filter and its Use in Dynamic Positioning Systems*. Dynamic positioning conference, 2003.

DNV. Dnv-rp-c205 environmental conditions and environmental loads. *Norway: DetNorskeVeritas*, 2010.

European Wind Energy Association (EWEA et al. The european offshore wind industry– key trends and statistics 2015, 2016.

Odd Faltinsen. *Sea loads on ships and offshore structures*, volume 1. Cambridge university press, 1993.

Gene F. Franklin et al. *Feedback control of dynamic systems*. Harlow : Pearson Education Limited, 2014.

Johan MJ Journèe and WW Massie. Offshore hydrodynamics. *Delft University of Technology*, 2001.

R Munnig Schmidt, Georg Schitter, and Adrian Rankers. *The Design of High Performance Mechatronics-: High-Tech Functionality by Multidisciplinary System Integration*. IOS Press, 2014.

JG Snijders. Wave filtering and thruster allocation for dynamic positioned ships. *Delft University of Technology*, 2005.

Asgeir J Sørensen. Marine control systems propulsion and motion control of ships and ocean structures lecture notes. 2012.

Michael S Triantafyllou and Franz S Hover. Maneuvering and control of marine vehicles. *Department of Ocean Engineering, Massachussets Institute of Technology, Cambridge, USA*, 2002.